

UNIVERSITÀ DEGLI STUDI DI MILANO

SCUOLA DI DOTTORATO IN
MEDICINA SPERIMENTALE E BIOTECNOLOGIE MEDICHE

DIPARTIMENTO
Biotecnologie Mediche e Medicina Traslazionale

Curriculum endocrinologico e metabolico

TESI DI DOTTORATO DI RICERCA

Zebrafish as model system to study the role of the *GLIS3* transcription factor in the pathogenesis of congenital hypothyroidism

Settore Med/13 - Endocrinologia

GIUDITTA RURALE

TUTOR: Prof. LUCA PERSANI

COORDINATORE DEL DOTTORATO: Prof. Massimo Locati

A.A.
2017-2018

a papà e mamma,

“L’uomo incontra Dio dietro ogni porta
che la scienza riesce ad aprire.”

Albert Einstein

RINGRAZIAMENTI

Di questi tre anni, la cosa più importante per me è stata imparare a non smettere mai di domandare. Più si resta stupiti e curiosi davanti alla realtà e ai risultati che essa ci offre e più diventa interessante conoscere e quindi lavorare.

Per questo, il ringraziamento più grande va al mio professore, Luca Persani, perché mi ha sempre dato l'opportunità di scommettere su questa curiosità, facendomi vedere che vale la pena andare fino in fondo per poter costruire qualcosa.

Ringrazio Federica per l'aiuto costante e fondamentale e per il suo desiderio di imparare a lavorare insieme e Paolo per il prezioso aiuto in ambito molecolare! Un grazie anche a tutti i miei colleghi per il supporto e il confronto importante.

Grazie alla mia famiglia che ha sempre scommesso su di me, a tutti i miei amici più cari, a Greta mia sorella e a Matteo per avermi cambiata nel modo più vero.

INDICE

ABSTRACT	8
INTRODUCTION	11
<i>I. THE THYROID GLAND: AN OVERVIEW</i>	<i>11</i>
<i>II. THYROID MORPHOGENESIS: A MULTISTEP PROCESS</i>	<i>16</i>
<i>A. Zebrafish thyroid gland: similarities and differences</i>	<i>18</i>
<i>III. GENETIC REGULATION OF THYROID DEVELOPMENT</i>	<i>19</i>
<i>IV. INTERACTION BETWEEN ENDODERM AND MESODERM</i>	<i>22</i>
<i>DURING THYROID DEVELOPMENT</i>	<i>22</i>
<i>A. Nodal pathway</i>	<i>22</i>
<i>B. Notch pathway</i>	<i>23</i>
<i>C. Sonic Hedgehog pathway</i>	<i>24</i>
<i>V. CONGENITAL HYPOTHYROIDISM (CH)</i>	<i>26</i>
<i>VI. THE TRANSCRIPTION FACTOR GLI-SIMILAR 3 (GLIS3)</i>	<i>28</i>
<i>VII. GLIS3 AND CONGENITAL HYPOTHYROIDISM</i>	<i>31</i>
<i>VIII. ANIMAL MODELS OF NDH</i>	<i>33</i>
<i>IX. ZEBRAFISH AS A MODEL TO STUDY THE ROLE OF GLIS3</i>	<i>35</i>
<i>DURING THYROID DEVELOPMENT</i>	<i>35</i>
<i>X. AIM OF THE PROJECT</i>	<i>36</i>
MATERIALS & METHODS	37

<i>I. ZEBRAFISH MAINTENANCE</i>	37
<i>II. REAL-TIME qRT-PCR</i>	37
<i>A. Total RNA extraction and cDNA synthesis</i>	38
<i>B. Real-Time PCR</i>	38
<i>III. SYNTHESIS OF PROBES FOR IN SITU HYBRIDISATION</i>	39
<i>A. Cloning and transformation reaction</i>	39
<i>B. Isolation of plasmid DNA</i>	40
<i>C. Probes labelling and synthesis</i>	41
<i>IV. WHOLE MOUNT IN SITU HYBRIDISATION (WISH)</i>	41
<i>V. LOSS-OF FUNCTION ANALYSIS</i>	41
<i>VI. RESCUE EXPERIMENTS</i>	43
<i>VII. IMMUNOFLUORESCENCE</i>	45
<i>VIII. IMMUNOCYTOCHEMISTRY</i>	45
<i>IX. CYCLOPAMINE TREATMENT</i>	46
<i>X. DAPT TREATMENT</i>	46
<i>XI. STATISTICAL ANALYSIS</i>	47
RESULTS	48
<hr/>	
<i>I. STRUCTURE AND CONSERVATION OF ZEBRAFISH GLIS3</i>	48
<i>II. EXPRESSION OF GLIS3 DURING ZEBRAFISH DEVELOPMENT</i>	50
<i>III. KNOCKDOWN EXPERIMENT WITH GLIS3 MORPHOLINO</i>	51
<i>ANTISENSE OLIGO</i>	51
<i>IV. EVALUATION OF THE PHENOTYPE OF GLIS3 MORPHANTS</i>	53
<i>V. GLIS3 KNOCKDOWN AND THYROID DEVELOPMENT</i>	54
<i>A. Induction of thyroid primordium</i>	54
<i>B. Differentiation and proliferation of thyroid follicles</i>	56
<i>C. Proliferation and apoptosis of thyroid primordium of glis3 morphants</i>	58

<i>D. T4 production and regulation of the HPT-axis in glis3 morphants</i>	60
<i>VI. RESCUE OF THYROID DEFECTS OF GLIS3 MORPHANTS</i>	62
<i>VII. EFFECTS OF GLIS3 OVEREXPRESSION ON THYROID DEVELOPMENT</i>	63
<i>VIII. GLIS3 ACTS AS AN EFFECTOR OF THE SONIC-HEDGEHOG PATHWAY</i>	66
<i>A. Shh and zebrafish thyroid development</i>	67
<i>B. Shh and glis3 overexpression</i>	69
<i>C. In vitro analysis of glis3 and sufu cellular localization</i>	71
<i>IX. ANALYSIS OF POSSIBLE GLIS3-NOTCH PATHWAY INTERACTION</i>	71
DISCUSSION	74
BIBLIOGRAPHY	81

ABSTRACT

Congenital Hypothyroidism (CH) is the most common congenital endocrine disease that can be broadly classified as failure of the gland to develop normally (dysgenesis) or inadequate thyroid hormone (TH) production from eutopic thyroid gland (dyshormonogenesis). Biochemically, CH patients are characterized by low circulating levels of T4 and T3 associated with an increased production of TSH due to the feedback mechanisms controlling the hypothalamic-pituitary-thyroid (HPT) axis.

CH is considered a disease with a strong genetic component, but with a largely missing explanation for its heritability. At present, genetic variants in candidate genes explain only the 10% of CH cases.

The extraordinary progresses in high-throughput screening technologies lead to the identification of several genes involved in the thyroid development and TH synthesis.

Recently, the transcription factor GLI-Similar protein 3 (*GLIS3*) has emerged as a new candidate gene for CH, but its role in thyroid development and function remains largely unexplored.

GLIS3 is a member of the Kruppel-like zinc-finger transcription factors that can acts as activator or repressor of gene expression. Homozygous and compound heterozygous *GLIS3* variants have been associated with NDH syndrome, characterized by neonatal diabetes (T1D and T2D), CH and polycystic kidney. Additionally, several missense heterozygous *GLIS3* variants have been also identified in cohorts of patients with isolated CH. Interestingly, heterozygous *GLIS3* variants are associated with other mutations in genes involved in thyroid functioning, supporting the hypothesis of the oligogenic CH origin.

In both NDH and isolated CH patients, the thyroid disease is extremely heterogeneous. In fact, most of the affected cases present variable thyroid dysgenesis (athyreosis, thyroid hypoplasia and ectopy), whereas dysmorphogenesis with eutopic *in situ* gland is also reported.

Evidences from *Glis3* knockout mice indicate a relevant role of *Glis3* in TH biosynthesis and postnatal follicle proliferation, with a mechanism of action downstream of the TSH/TSHR signalling and thyroid cell proliferation. However, no significant thyroid developmental defects were observed in this particular mice model.

Since *GLIS3* mutations are variably associated with thyroid dysgenesis, the aim of this study is to gain insight on *GLIS3* activity during the early steps of thyroid development, using zebrafish as a model system.

In zebrafish (zf), we observed the expression of *glis3* transcript from the early developmental stages onwards, with a particularly evident signal at 1 dpf (day post fertilization) in the pharyngeal endoderm, the embryonic tissue that will give rise to endocrine organs, like thyroid and pancreas, and in the pronephric ducts. In apparent contrast with mouse data, *glis3* is absent in the differentiated thyrocytes of zebrafish embryos at 2-3 dpf.

Transient knockdown zebrafish embryos (called *glis3*_MOs), obtained by the microinjection of specific *glis3* morpholinos, revealed a reduced expression of the early thyroid markers *nkx2.4*, and *pax2a*, at 1 dpf. The defective specification of the thyroid primordium at this early developmental stage was not associated with reduced proliferation or increased apoptosis of thyroid precursors, thus indicating that this phenotype was likely due to alterations in the commitment of endodermal cells toward the thyroid fate. Such defect resulted in a reduction in size of the differentiated thyroid precursors with a diminished expression of both *tg* and *slc5a5*, and later on in the number of functional thyroid follicles. At 5 dpf, the stage in which the thyroid gland is functional and responds to the HPT-axis, decreased levels of T4 associated with *tshba* elevation were also seen in *glis3*_MOs. The specificity of the thyroid defects was confirmed by the rescue phenotype after co-injection of the wild-type zf-*glis3* transcript (WT mRNA) and the *glis3* morpholino. In contrast with morpholino knock-down, the overexpression of the *glis3* mRNA leads to an increase of the number of the thyroid

precursors at 1dpf, thus leading to the differentiation of a larger thyroid tissue and an elevation of T4 levels at 5 dpf. Taken together, our results demonstrate that *glis3* acts at the endodermal level controlling the commitment of endocrine precursors, potentially representing a required factor for the early specification of thyroid primordium.

Given the current knowledge, GLIS3 is reported to interact with a pivotal element within the Sonic hedgehog (Shh) pathway. Previous experiments in the mouse model indicated a potential role for such pathway in thyroid development, but the underlying mechanisms and the stage of Shh action in this context are still elusive. Our experiments revealed that the expression of *shha* (the zf homologous of human Shh) was significantly reduced in the pharyngeal endoderm of *glis3*_MOs. Consistently, the injection of a morpholino against *shha* abolished the expression of *glis3* in the endodermal layer, as well as the treatment with Cyclopamine (a Shh-antagonist) caused a reduced or absent expression of *glis3*, thus confirming the co-involvement of *shha* and *glis3* during the thyroid cell specification. Interestingly enough, the overexpression of *glis3* mRNA failed to rescue the thyroid defects in the Cyclopamine-treated embryos, suggesting that *glis3* would act as downstream effector of the Shh pathway.

In conclusion, this is the first evidence of the possible interaction between Shh and Glis3 during the early specification of thyroid primordium. Since the mechanisms involved in such a delicate event are largely unknown, our data provide important insights as *glis3* appears as an endoderm factor required for the commitment of endoderm cells toward the thyroid fate. These data shed new light into the molecular mechanisms potentially involved in CH pathogenesis.

INTRODUCTION

I. THE THYROID GLAND: AN OVERVIEW

The thyroid gland, through the production of the thyroid hormones (TH), including thyroxine (T4) and the bioactive form triiodothyronine (T3), plays multiple roles during the embryonic development of several organs and regulates the homeostasis of several physiological mechanisms, including body growth and metabolism postnatally [1, 2].

In vertebrates, the thyroid is a gland composed by two lobes connected by an isthmus located adjacent to the trachea (Figure 1A).

The gland is composed by the fusion of primordial tissues that develop from the anterior foregut: the thyroid diverticulum that derived from the endoderm, and the ultimobranchial bodies, a bilateral structures that give rise form the neural crests. The diverticulum originates form the midline anlage located in the pharyngeal floor, which enclose a small group of endodermal cells, which will form the thyroid follicular cells [2]. The ultimobranchial bodies (UBB) are transient embryonic structures, located on the sides of the developing neck, containing the parafollicular calcitonin producing cells (C-cells).

During embryogenesis, the cells of the thyroid anlage and the UBB migrate and merge to form the definitive thyroid gland that is visible as a compact organ, in which the endoderm-derived cells organize the TH-producing thyroid follicles, whereas the C-cells are dispersed in the interfollicular space (Figure 1B). A rich network of capillaries surrounds the thyroid follicles providing the systemic delivery of released TH. Finally,

the stromal compartment, which encapsulates and separates the follicular thyroid tissue, consists mainly of *ectomesenchymal* fibroblast derived from the neural crest [2].

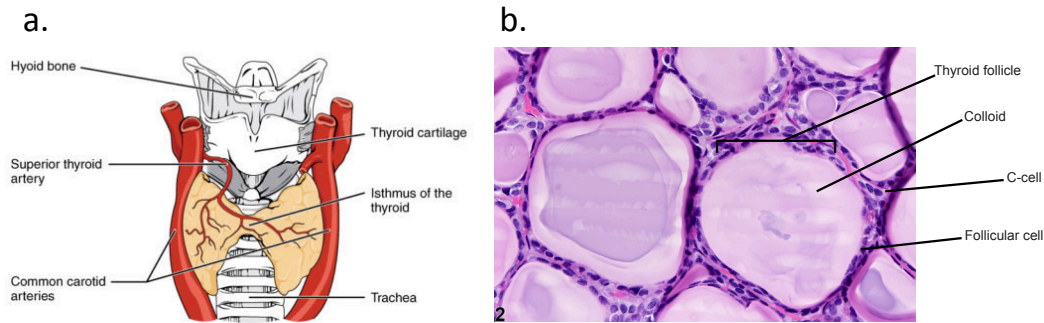


Figure 1. Thyroid gland anatomy. **a)** Gross anatomy, anterior view; **b)** Histology, showing the thyroid follicles formed by follicular cells and colloid, and nest of C-cells.

The thyroid follicular cell (or thyrocyte) is the functional unit of the gland, and is composed by a monolayer of cuboidal-epithelial cells that encloses a central lumen filled with colloid, a proteinaceous depot of TH precursors [2]. The thyroid epithelium is morphologically and functionally polarized, with the apical surface facing the colloid and a basolateral surface facing the interstitium (Figure 2a). Iodination and TH synthesis occur in the colloid at the apical plasma membrane. TH production starts with the synthesis of thyroglobulin (TG) that is secreted into the colloid of the thyroid follicles by exocytosis. Meanwhile, a sodium-iodide symporter (NIS or SLC5A5) pumps iodide actively into the cell and enters the follicular lumen from the cytoplasm by the transporter pendrin (SLC26A4) (Figure 2b). In the colloid, iodide is oxidized to iodine by thyroid peroxidase (TPO) and iodinate the TG at the level of the tyrosyl-residues to produce thyroxine (T4) and triiodothyronine (T3) (Figure 2c). TG re-enters the follicular cells by endocytosis and TH are liberated by proteolysis, whereas TG is degraded via lysosomes (Figure 2d). The efflux of TH into the bloodstream appears largely through the monocarboxylate transporters (MCT) 8 and 10 (Figure 2e) [2].

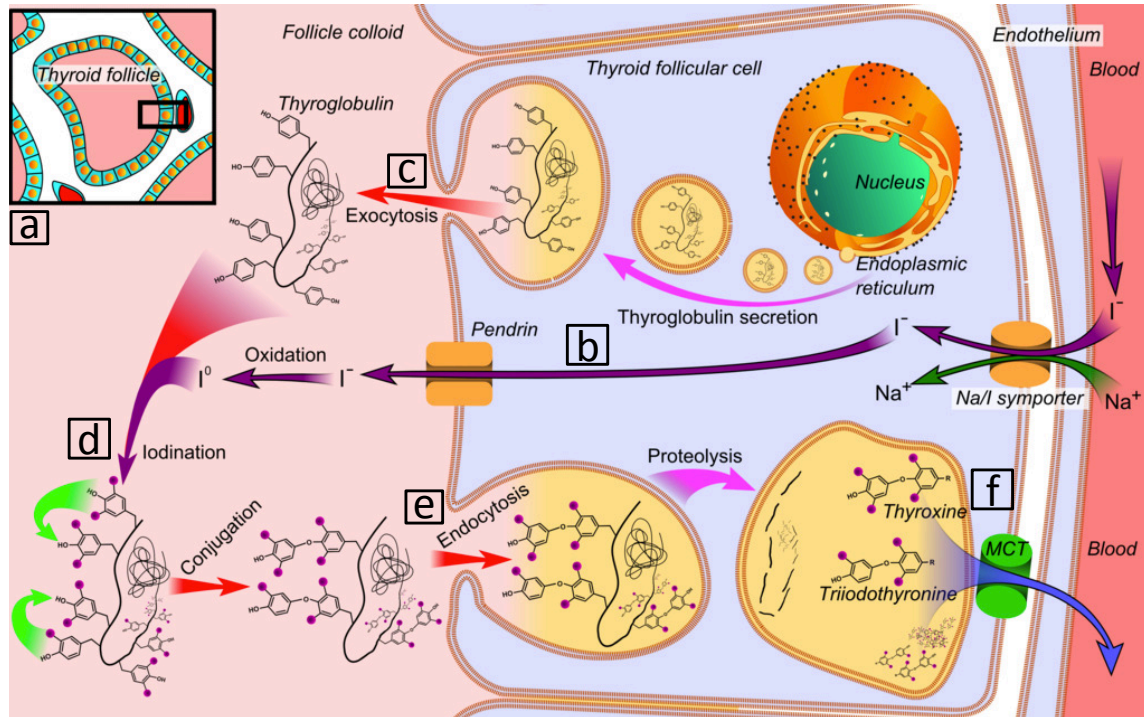


Figure 2. Synthesis of TH in the thyrocyte. (a) View of thyroid follicle structure; (b) Import of iodide into colloid; (c) Synthesis of TG and exocytosis into the lumen; (d) Iodination of the tyrosine residues of the TG; (e) Conjugation of the iodinated residues and endocytosis into the follicular cell; (f) Proteolysis of conjugated-TG and release of TH into the blood by specific transporters (MCT) [Modified from (Mikael 2014)].

The proper amount of TH is finely regulated by the removal of an atom of iodine from specific tyrosine residues. Most of the T3 is produced in the liver (in mammals) or the kidney (in fish), by outer ring deiodination (ORD) of T4 operated largely by the type-2 deiodinase (DIO2) enzyme, and to a lesser extent by the DIO1. Both T4 and T3 are inactivated by the inner ring deiodination (IRD) of DIO3 that produce reverse T3 (rT3) and T2, respectively. The T3 re-enters the bloodstream to reach the rest of the body (Figure 3).

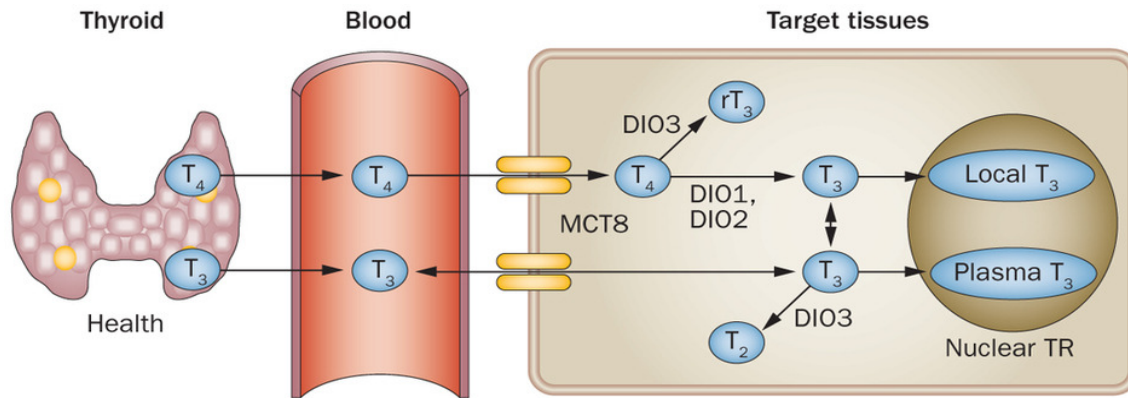


Figure 3. Metabolism of TH. T₄ is converted to T₃ by the DIO2 and DIO1. DIO3 produces the rT₃ and T₂, by the deiodination of T₄ and T₃, respectively. Modified from Williams and Bassett, 2011 [3].

Once reached the target cell, T₃ is actively transported into the nucleus where it binds specific thyroid hormone receptors (TRs) [4]. TRs, including the TR α 1, TR β 1 and TR β 2 isoforms, function as homodimers or heterodimers with the retinoic acid receptor (RXR) recognizing specific sequences (thyroid responsive elements, TREs) located in the promoter of target genes [5, 6]. In the absence of T₃, TRs repress basal transcription through association with a variety of corepressors that limits the access of the basal transcriptional machinery. The binding of T₃ induces structural changes that release the corepressors and recruit coactivators, that facilitate transcription [7]. Depending on the type of TRE, the TRs can positively or negatively regulate gene expression (Figure 4). Circulating TH levels are maintained within a narrow range by the control of the hypothalamic-pituitary-thyroid (HPT) axis. Low levels of T₃ trigger the release of the thyrotropin-releasing hormone (TRH) from the hypothalamus that in turn stimulates the anterior pituitary to secrete the thyroid-stimulating hormone (TSH). The TSH binds the TSH-receptor (TSHR) expressed on the basolateral membrane of the thyrocytes and thus activating the biosynthesis of TH. By negative feedback inhibition, elevated levels of T₃ repress the release of both TRH and TSH [8, 9]. (Figure 5).

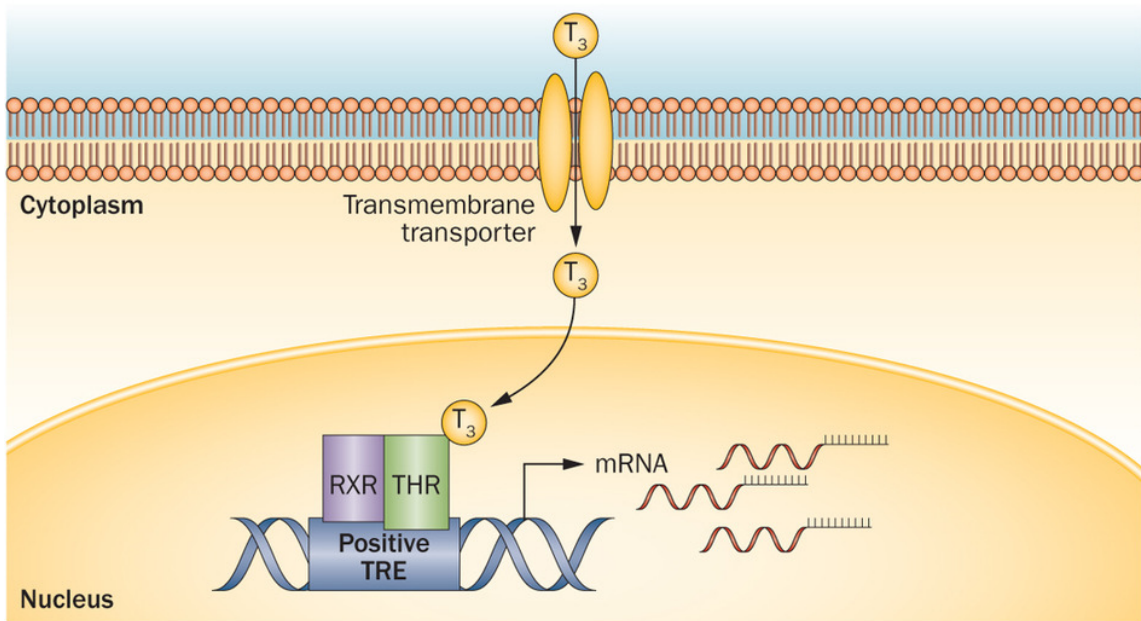


Figure 4. TH action. In this illustration, T₃ binds complex formed by TR, RXR and the positive TRE. The activation of the transcriptional machinery activates gene expression. Figure modified from [8, 9]

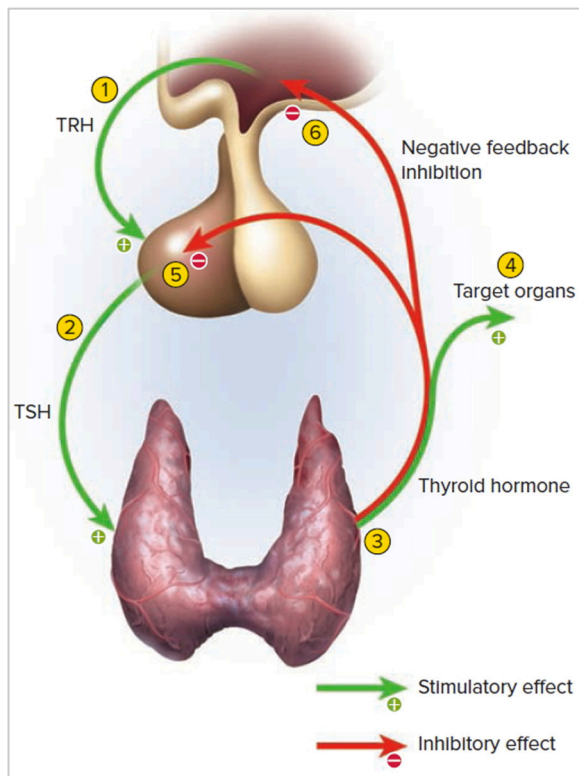


Figure 5. Control of TH secretion. Low T₃ levels trigger the synthesis of hypothalamic TRH and the pituitary TSH that stimulate the production of TH. Conversely, high T₃ levels produce opposite effects [8, 9].

II. THYROID MORPHOGENESIS: A MULTISTEP PROCESS

The formation of the three primary germ layers (ectoderm, mesoderm and endoderm) takes place during early gastrulation of the vertebrate embryo. The inner layer, endoderm, contributes to organize the digestive tract, the associated organs: liver, pancreas, lung and thyroid. The precise control of endoderm patterning is required for proper organogenesis [11-13].

During development, the thyroid gland undergoes a series of morphological changes, which are promoted by the expression of specific transcription factors [4, 15].

The multistep process of thyroid organogenesis, can be summarised as follow (Figure 6):

- 1) Formation of the thyroid placode through the assembling of the thyroid progenitors in the pharyngeal floor of the endoderm, upon the aortic sac. At the molecular level, these cells can be distinguished by the combined expression of *NKX2-1*, *PAX8*, *HHEX* and *FOXE1*. These transcription factors play a fundamental role not only in the formation of the thyroid bud, but also in the functional differentiation of the gland in late development and postnatally [4, 15].
- 2) The growing placode evaginates to form the thyroid bud.
- 3) Caudal migration of the thyroid placode along the anterior neck region, taking contact with the surrounded mesenchyme.
- 4) Bifurcation of the thyroid primordium that extends bilaterally along the pharyngeal arch arteries.
- 5) Bilobation, involving the fusion of the thyroid primordium with the ultimobranchial bodies (UBBs). An isthmus connects the two lobes.
- 6) Folliculogenesis, the last morphogenic step during which the follicles are functionally differentiated, and are surrounded by the C cells.

By this process, the final shape of the gland is established, and the thyrocytes start to express genes involved in iodine uptake and TH synthesis, such as the sodium-iodine symporter (NIS or SLC5A5), thyroglobulin (TG) and thyreoperoxidase (TPO).

In mice, the entire process takes place in one week, from E8.5 to E15.5, whereas in humans, the thyroid development occurs during the E20 to the E70 [2, 10].

Although the gland is completely formed, the embryo is still dependent by the maternal supply of TH. In fact, as evidenced by genetic deletion experiments, the thyroid-stimulating hormone (TSH), the fine regulator of thyroid function, does not participate in the early embryonic morphogenesis and growth of the gland. In mice this occur postnatally whereas in humans TSH regulates fetal thyroid growth in the third trimester [15].

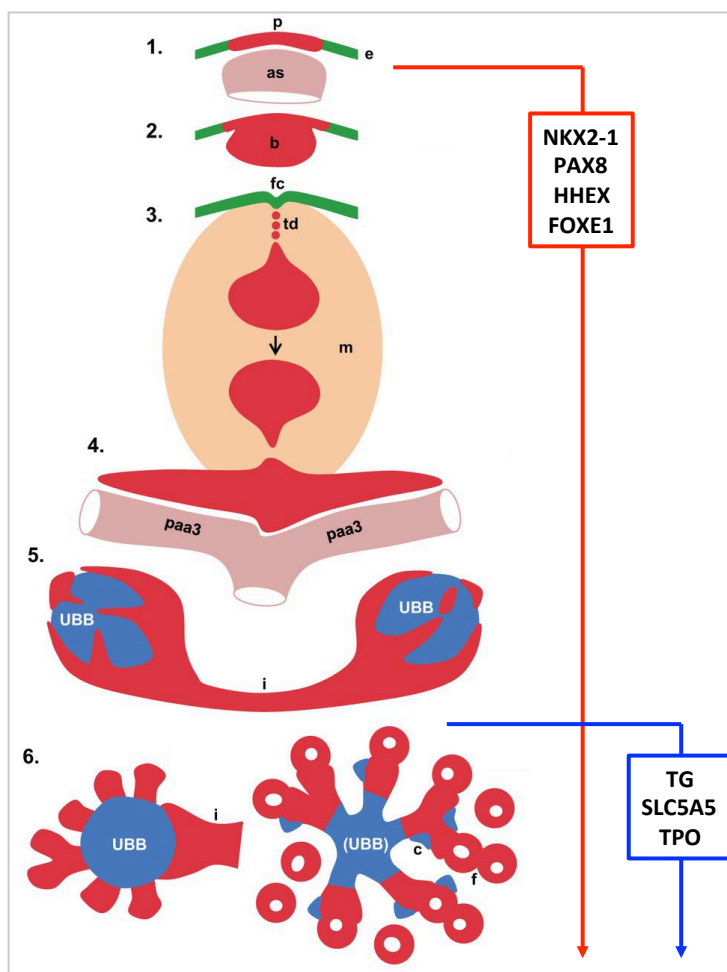


Figure 6. Morphogenesis of the thyroid gland. (1) Assembly of endoderm-derived thyroid progenitors to form the thyroid placode (p), above the aortic sac (as); (2) Emergence of the thyroid bud (b); (3) Migration of the thyroid primordium leaving the foramen caecum (fc), transiently connecting the thyroglossal duct (td) and reaching the final destination with the surrounding mesenchyme (m); (4) Bifurcation of the primordium that extends bilaterally along the pharyngeal arch arteries (aap); (5) Bilobation involving the fusion of the primordium with the UBBs. Right and left lobe are connected by an isthmus (i); (6) Lobe growth, migration of the C-cells (c) and differentiation of thyroid follicles (f). Figure modified from Nilsson and Fagman, 2017 [2].

A. Zebrafish thyroid gland: similarities and differences

With regard to zebrafish, the ontogeny of the thyroid follows the same pattern in all vertebrates and zebrafish, as previously described: the thyroid anlage always originates in the primitive pharynx and thyroid follicular cells migrate from the anlage to reach their definitive position and finally organize themselves into follicles in a specie-specific manner. Moreover, the expression of a conserved thyroid transcription factor network has been demonstrated in the developing thyroid of zebrafish (Figure 7).

However, differences exist in the anatomy of mature thyroid tissue and in the timing of specific morphogenetic events [11, 12]. The zebrafish thyroid completes its development without assuming a glandular organization, with rows of non-encapsulated thyroid follicles that are scattered between the first gill arch and the *bulbus arteriosus* within the sub-pharyngeal mesenchyme, along the ventral aorta (Figure 7). Moreover, the UBBs and the derived-C cells remain separated from the rest of the thyroid. In zebrafish, the onset of folliculogenesis takes place earlier than in mammals (T4 production assessed from 55 hours post-fertilization, hpf) [13, 14], and the final expansion of thyrocytes are TSH-dependent by 100hpf [15]. This is probably due to the fact that zebrafish embryos demand to become independent from maternal TH supply already in early development [13].

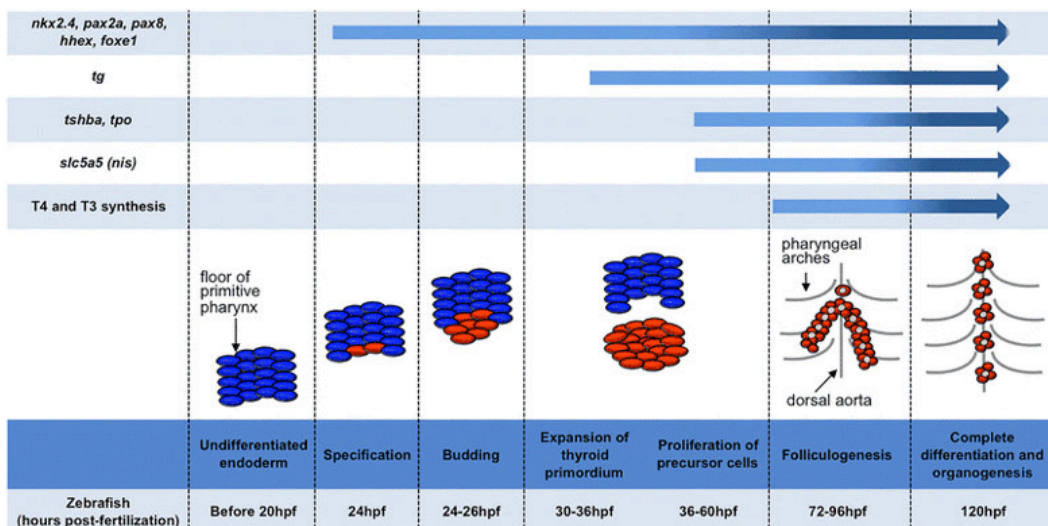


Figure 7. Events of the zebrafish thyroid development. The time to each step with the relative expression of early and late genes are reported as hpf (hours post-fertilization) [2, 16, 17].

III. GENETIC REGULATION OF THYROID DEVELOPMENT

In this section we report the current knowledge about the genetic factors involved in thyroid organogenesis.

As mentioned above, a set of genes, unique to the thyroid follicular cell type, has been identified as responsible for driving thyroid specific gene expression. It comprises the transcription factors *NKX2-1*, *PAX8*, *HHEX* and *FOXE1*, each of them is also expressed in different cell types. However, the combination of these factors to the thyroid primordium can be considered as a thyroid signature within the anterior foregut endoderm [18].

- **NKX2-1**

NKX2-1, primarily known as thyroid transcription factor-1 (TTF-1), is one of the main actors during the organogenesis from the pharyngeal endoderm [2]. *NKX2-1* is a member of the homeodomain transcription factor family, expressed in thyroid, lung and ventral forebrain of higher vertebrates [19]. It was identified as a nuclear protein able to recognise and bind specific DNA sequence on the thyroglobulin promoter [20].

As mentioned before, *NKX2-1* is expressed early during the specification of the thyroid placode where contributes to the specification and differentiation of the thyroid follicles [19]. *Nkx2-1* knockout (KO) mice present athyreosis and arrest the lung development at the early developmental stages [21]. Further investigations defined that in this mice the thyroid rudiment is initially formed but then it disappears through apoptosis [18, 21]. These results demonstrate that *Nkx2.1* is not required for the initial specification of thyroid, but is fundamental for the survival of the thyroid cells precursors, also controlling the expression of genes involved in thyrocyte differentiation, like thyroglobulin [2, 20].

In zebrafish, the transient KO of *nkx2.4* (homologous of the mammalian *NKX2-1*) by morpholino microinjection leads to defects in thyroid morphogenesis resulting in athyreosis, as confirmed by the absence of T4-producing follicle at 5dpf. Similarly, *nkx2.4* KO displays complete absence of the thyroid or severe thyroid hypoplasia at 55hpf [22]. Taken together, these data suggest that *NKX2-1* exhibits an evolutionary conserved role in regulating thyroid development.

- **PAX8**

PAX8 (paired box-8) gene is detectable only in the thyroid endoderm derived-organs [2] and, like *NKX2-1*, starts to be expressed in the thyroid primordium and it is maintained in the thyroid follicular cells during all stages of development and in adulthood [20].

In the *Pax8*^{-/-} mice the thyroid gland is severely affected, thyroid follicles are undetectable and C cells mostly compose the gland. KO mice died early after weaning due to the severity of the hypothyroidism that can be rescued by T4 administration [23, 24]. Further analysis confirmed that *Pax8* is required for the survival of the thyroid precursors rather than in thyroid differentiation. Moreover, it has been demonstrated that *Pax8* directly regulates the expression of the other early thyroid genes. In fact, in *Pax8* KO mice, the expression *Hhex* and *Foxe1* are strongly down-regulated [20].

In zebrafish, two *pax* genes (*pax2a* and *pax8*) are expressed in thyroid primordium at 24hpf. Zebrafish *noi* mutants (deficient in *pax2a* activity) develop the thyroid primordium and express *nkx2.4* and *hhex* until 30hpf, but no active follicles are detectable at 5dpf [11]. Phenocopying the thyroid phenotype of *noi* mutants, in the *pax2a* KO the thyroid anlage is formed, but the expression of thyroid markers becomes severely impaired or is absent [22]. The finding that the phenotypes of *noi* and *pax2a* mutants are similar to that of *Pax8* KO mice, suggests that zebrafish *pax2a*, acting upstream of *pax8*, plays a similar role in thyroid development [25].

In both mice and zebrafish, the anti-apoptotic factor Bcl2 strongly accumulates specifically in the thyroid bud, suggesting that anti-apoptotic signals are important in early thyroid development and that the mechanism is evolutionarily conserved [17, 26].

- **HHEX**

The haematopoietically homeobox transcription factor *HHEX* is a critical regulator of many aspects of vertebrate development, such as the formation of endoderm-derived organs: thyroid, pancreas, liver, lung and thymus [2, 27, 28]. *Hhex*-null mice display aplastic or hypoplastic at E10.5 and complete athyreosis at E13.5, suggesting a very early function of *Hhex* in thyroid development [18]. In zebrafish, the orthologous gene *hhex* is initially expressed in the anterior endoderm, co-localizing with *nkx2.1* in the thyroid primordium at 22hpf. Morpholino injected embryos result in a lack of T4-producing follicles at 5dpf whereas the evagination and localization of thyroid

primordium are not affected but the expression of *nkx2.1* and *pax2a* is lost at 60hpf. Furthermore, the overexpression of *hhex* increases the number of thyroid precursor cells in zebrafish. All together, these studies in zebrafish and mice emphasize the role that *HHEX* gene plays after induction and evagination of the thyroid primordium, when it appears to control thyroid differentiation and, perhaps, growth.

- **FOXE1**

FOXE1, previously known as thyroid transcription factor-2 (TTF-2) is identified as a nuclear protein able to bind at the thyroglobulin and thyroid peroxidase promoters under hormone stimulation [20, 29].

Like the other thyroid transcription factors, FOXE1 is expressed in the pharyngeal endoderm promoting the migration of thyroid precursors [20]. In *Foxe1* KO mice the thyroid bud is missing or remains a part of the pharyngeal endoderm, demonstrating that this factor has an important role during the thyroid primordium migration [30]. Further investigations described the importance of *Foxe1* in the maintenance of epithelial-phenotype of progenitor cells during migration and also as a promoter of cell survival, probably acting downstream of *Pax8*.

Although *foxe1* is expressed in thyroid primordium of zebrafish embryos at 24hpf, the knockdown of *foxe1* have no effects on thyroid morphogenesis. These authors argued that the zebrafish thyroid develops very early during development and *foxe1*'s role might be redundant in this context; it is thus possible that the role of FOXE1 in mammalian thyroid development may have been acquired during evolution [13, 31].

IV. INTERACTION BETWEEN ENDODERM AND MESODERM DURING THYROID DEVELOPMENT

The specification of the gut region and the derived organs also depends on the crosstalk between the endoderm and the mesoderm. Several studies highlight the importance of permissive signals sent from the mesoderm layer to promote endoderm organogenesis (i.e. during liver and pancreas development) [32-36]. A wide range of intrinsic or extrinsic pathways derived from the endoderm and/or the mesoderm has been described to contribute to thyroid development [37]. Each gene acts both individually and in concert to form a complex network that is required for the proper specification of endodermal cells into thyroid precursors, in the migration of thyroid primordium, as well as in the correct differentiation and expansion of the gland.

A. Nodal pathway

During embryogenesis, the Nodal pathway is involved in the definition of mesoderm and endoderm from a common territory, the so called *mesendodermal* layer, as well as in positioning of the anterior–posterior axis, neural patterning and left–right axis specification [38]. The Nodal gene encodes an activin-like member of the transforming growth factor β (TGF β), and it belonging a complex cascade of signals, it is involved in the activation of the transcription of the endoderm-specific genes, like *gata5*, *sox17* and *foxa2* [39-41]. Much of the role of Nodal signalling in thyroid has been elucidated in the zebrafish model. In the Nodal co-receptor *one-eyed pinhead* mutants (*oep*^{-/-}), the loss of endoderm is evident during gastrulation, with an overall failure in the mesodermal cells specification, leading to the absence of thyroid primordium [42]. Furthermore, zebrafish mutants in the downstream effectors of Nodal signalling like *bon*, *gata5* and *sox32* completely fail to develop the thyroid primordium, as a consequence of altered endoderm organization and of the loss of the direct inductive role that these factors play in specifying the thyroid primordium [42-44].

B. Notch pathway

Notch is a highly conserved, local cell-signalling mechanism that participates in a variety of cellular processes and it is involved in many aspects of development and disease. Notch signalling governs cell fate differentiation and critical cell fate decisions during development, the segmentation in lower organisms, somitogenesis, neurogenesis, vasculogenesis and cardiogenesis [45, 46]. In mammals there are four Notch receptors (NOTCH1-4). The receptors interact with different ligands, belonging to Delta-like (DLL1-3) and Jagged families (JAG1 and JAG2). Notch binding to ligand elicits several steps cleavage that culminates in the releasing of the Notch intracellular domain (NICD). NICD translocates into the nucleus, where it induces the expression of several genes [47]. Mice KO for the Notch effector *Hes1* show thyroid hypoplasia and diminished T4 production. *Jag1* KO mice present vascular defects that result in embryonic lethality before E11.5, precluding the study of thyroid development. However, the double heterozygous *Jag1/Notch2* mice strongly resemble those seen in patients with Alagille syndrome, which includes congenital hypothyroidism as a clinical feature [47, 48].

Studies conducted in zebrafish have shown that the Notch signalling is involved in the development of the thyroid gland. Perturbations of the Notch signalling are associated with increased (Notch silencing) or diminished (Notch over-activation) number of thyroid precursors committed to the thyroid fate. Furthermore, both *jag1a* and *jag1b* ligands (homologous of the human JAG1) co-localize with *tg* and play distinct roles during thyroid development. *Jag1a* appear to be important at 72hpf contributing to define the number of cells able to proliferate and move caudally to generate new follicles, whereas *jag1b* are involved earlier during the differentiation of the thyroid primordium (24-48hpf) [47].

Taken together these findings indicate a dual role of Notch signalling during zebrafish thyroid development: induction of thyroid primordium, restricting the number of endodermal cells that will differentiate to thyroid cells, and Jag1-dependent controls of differentiation and expansion of thyroid follicles [47]. However, since the Notch signalling is expressed in both endoderm and mesoderm, it is possible that permissive factors from the surrounding tissues (e.g. lateral plate mesoderm) contribute to the

observed phenotype. In fact, the cardiac plate mesoderm is known to be an important source of FGF signals that influence thyroid organogenesis, both in zebrafish and mouse model. This supports the existence of a common pathway regulating thyroid and heart development, and it can also explain the frequent association of cardiac defects in patients with thyroid dysgenesis carrying mutations in the *JAG1* gene [47, 49].

C. Sonic Hedgehog pathway

The Sonic Hedgehog (SHH) signalling is involved in several key events during embryogenesis of vertebrates, including left–right axis determination and organ development [50, 51] and it is also an important regulator of pharyngeal region development [52]. Upon secretion, SHH inactivates the transmembrane receptor Patched1 (PTCH1), which normally inhibits the activity of the transmembrane protein Smoothened (SMO), and resulting in the nuclear localization of glioma-associated (GLI) transcription factors, which are the terminal effectors of SHH signalling. It has also been described that, in absence of SHH, the Suppressor of Fused (SUFU) negatively regulates the pathway by directly binding to GLI and anchoring them in the cytoplasm, thus preventing the activation of GLI-target genes (Figure 8). SUFU has also been shown to form a repressor complex with GLI1, which translocate into the nucleus where it represses gene transcription [53].

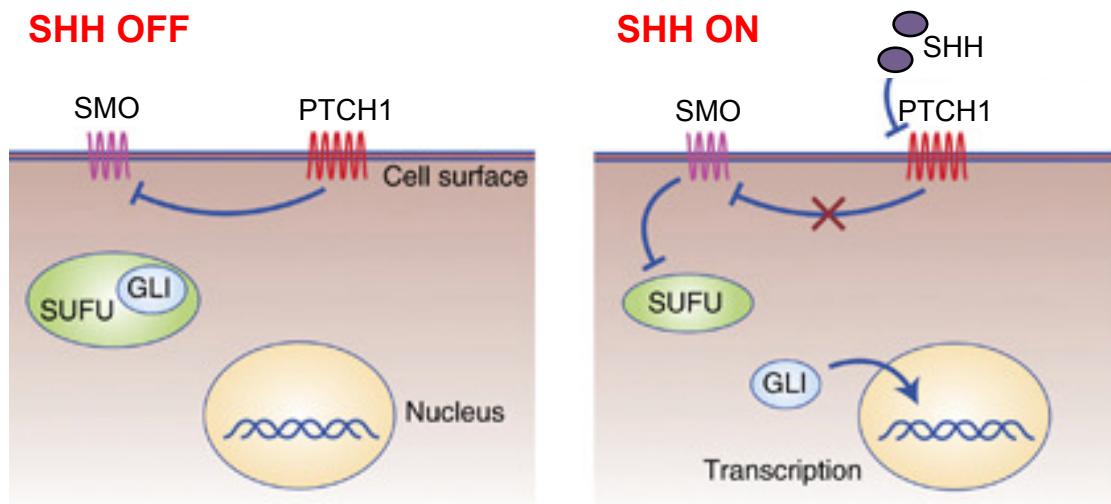


Figure 8. Sonic Hedgehog signalling. In absence of ligand, the transmembrane receptor SMO is maintained inactive by the binding with PTCH1. At the same time, the SUFU anchoring and inhibiting GLI activity, When SHH bind PTCH1, SMO is activated and release the inhibition mediated by SUFU, allowing the nuclear translocation of GLI and the activation of gene transcription [53].

In *Shh* KO mice, the thyroid primordium is correctly specified in the pharyngeal endoderm, but the thyroid fails to bifurcate developing a single unilateral gland, likely due to defective formation of pharyngeal arteries [54]. Defective activity of *Shh* and its receptor *Patched* both in thyroid and vessel wall strongly suggests that this phenotype primarily depends on defective *Shh*-signalling from the pharyngeal endoderm or loss of *Shh* response in other embryonic tissues that indirectly influence thyroid development [52]. However, in mice deficient for *Tbx1*, a mesodermal target of the *Shh* signalling, the number of cells in the thyroid placode is reduced, the thyroid budding is delayed and the thyroid primordium fails to migrate and takes contact with the aortic sac [55].

In zebrafish, the genes of *shh*-pathway are expressed in the pharyngeal endoderm at early developmental stages [56]. Three-dimensional reconstruction of zebrafish *shh* mutant embryos and rescue experiments shows that the thyroid primordium, after normal evagination, fails to bifurcate and is mislocated due to the asymmetrical development of pharyngeal arteries [42, 56].

These results suggest that SHH contributes through the definition of the foregut territory for thyroid specification, regulating thyroid migration and bifurcation during the later phases of thyroid development [54].

V. CONGENITAL HYPOTHYROIDISM (CH)

Primary Congenital Hypothyroidism (CH) is the most common endocrine disease that can be broadly classified as failure of the gland to develop normally (dysgenesis) or inadequate hormone production from eutopic thyroid gland (dysmorphogenesis). Biochemically, CH patients are characterized by low circulating levels of T4 and T3 associated with an increased production of TSH due to the positive activation of the HPT axis. Clinically, the reduced action of TH in the peripheral tissues results in a wide spectrum of manifestations, including delayed bone development, mental retardation and altered metabolism. The implementation of universal newborns TSH-screening in the '70s and the timely treatment with L-thyroxine, virtually eradicated significant intellectual disabilities due to severe CH [57]. More recently, the increased of stringent screening strategies allows the detection of milder cases, and resulting in a dramatic increase of the incidence of CH from 1:4000 to 1:2000 over the last years [58]. Several concomitant factors (eg, improved outcome of CH more frequently allowing transmission of heritable defects, endocrine disrupting chemicals) can contribute this phenomenon, but the lower threshold of neonatal TSH screening represents the main cause of the increased CH detection [57]. CH has been considered a disease with a strong genetic component, but with a largely missing explanation for its heritability.

Thyroid dysgenesis (TD), which includes thyroid agenesis, hypoplasia, and ectopy, occurs in about 80% of CH cases, and its incidence (1:4000) has not significantly changes over the past decades. The underlying causes of TD, however, remains obscure in the vast majority of cases, with only 2-5% of cases being attributable to genetic mutations [20, 59]. Nevertheless, the known genetic causes of TD provide an important window into basic thyroid ontogeny (Figure 9).

Inactivating mutations that contribute to thyroid dysgenesis have been identified in genes expressed in thyroid tissues during embryogenesis and in the normal functioning thyroid gland (e.g. *NKX2-1*, *NKX2-5*, *TSHR*, *PAX8*, *FOXE1*), resulting in a misspecification or dislocation of thyroid follicular cells [60]. Since the expression of the transcription factors is not restricted to the thyroid, CH is frequently associated to additional syndromic features, such as interstitial lung disease and chorea (*NKX2-1*),

and renal abnormalities (*PAX8*), cleft palate, bifid epiglottis, choanal atresia, and spiky hair (*FOXE1*).

Unlike TD, the incidence of dyshormonogenesis has been increased of 15-20% in the last years. Known genetic causes of dyshormonogenesis are reported in Figure 9 [58, 61].

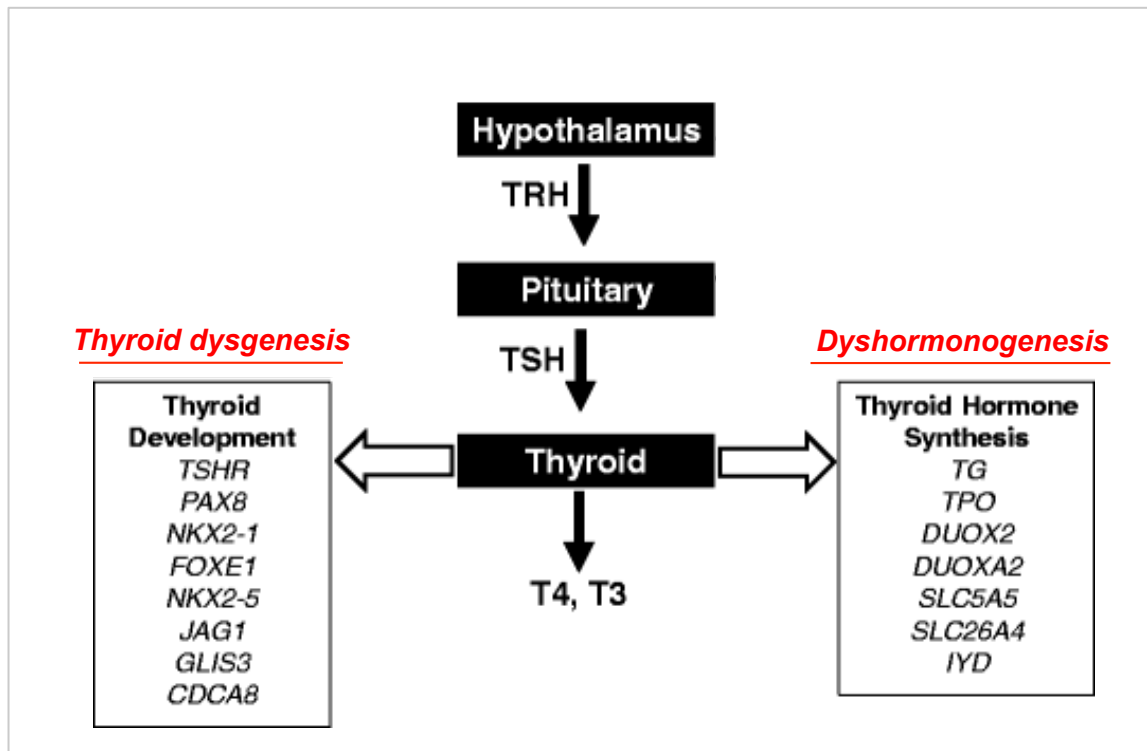


Figure 9. Genetic causes of CH. Modified from [62].

Despite the growing number of genes associated with CH, the precise portion that can be attributed to mono- or polygenic causes, can explain only the 10% of affected cases. The influence of non-genetic factors, such as epigenetics variations and the exposure of endocrine disruptors, may contribute to the aetiology of CH. However, further work is needed to identify the entire causative factors underlie the multifactorial and polygenic origin of CH [57, 63]. Nonetheless, recent studies examining larger sets of candidate genes, using next-generation techniques, identified causative variants in a higher portion of patients than older studies. For instance, a recent analysis, conducted by our group, of 11 genes in 177 Italian CH patients demonstrates a prevalence of mutation in 58% of cases that is even higher (75%) in patients with eutopic gland. The 23% of cases harboured variants in more than one gene, similar to other reports [62, 63]. These results

suggest that the apparent low heritability of CH may be explained by the confluence of rare variants in several genes. Furthermore, in this study, variants in genes typically associated with TD (eg. *NKX-2-1*, *FOXE1*) has been identified in patients with dysmorphogenesis, and vice versa. This finding suggests a crossover in the etiopathogenesis between TD and dysmorphogenesis.

An example of this potential phenotypic overlap is *JAG1*, the ligand of the Notch pathway that is critical for thyroid development in zebrafish [47]. Heterozygous *JAG1* variants have been described in cohorts of patients with Alagille syndrome (multisystemic disorder) and non-syndromic CH. Interestingly, the thyroid phenotype of patients with *JAG1* variants included not only TD, as to be expected from the zebrafish model, but also dysmorphogenesis. Taken together, the current knowledge highlighted the complexity of thyroid development and function and that the genetic component underlying the different manifestations of CH may overlap.

VI. THE TRANSCRIPTION FACTOR GLI-SIMILAR 3 (*GLIS3*)

The transcription factor Gli-similar 3 (*GLIS3*) belongs to the family of the Krüppel-like zinc finger transcription factor [61] and it is involved in several cellular processes, including proliferation, apoptosis, differentiation and development [64].

The human *GLIS3* gene is located on chromosome 9p24.2 and encodes a full-length protein of 90 kD in size. *GLIS3* is expressed in a tissue-specific manner, with highest levels in kidney, thyroid gland, endocrine pancreas, thymus, testis and uterus. Lower levels of expression have also been reported in brain, lung, ovary and liver [61, 65].

The *GLIS3* protein consists of a centrally located zinc finger domain (ZFD) (five tandem Cys₂-His₂ zinc finger motifs), a C-terminal transactivation domain (TAD) and a relatively large N-terminus that is important in the regulation of *GLIS3* stability and its transcriptional activity [61, 66] (Figure 10). The five Cys₂/His₂ zinc finger domain (ZFD) dictates *GLIS3* cytosolic or nuclear localization and it is responsible for the recognition of specific DNA responsive elements, the GlisBS (Glis3-binding site, 5-(G/C)TGGGGGGT(A/C)) localized within the regulatory regions of target genes [64].

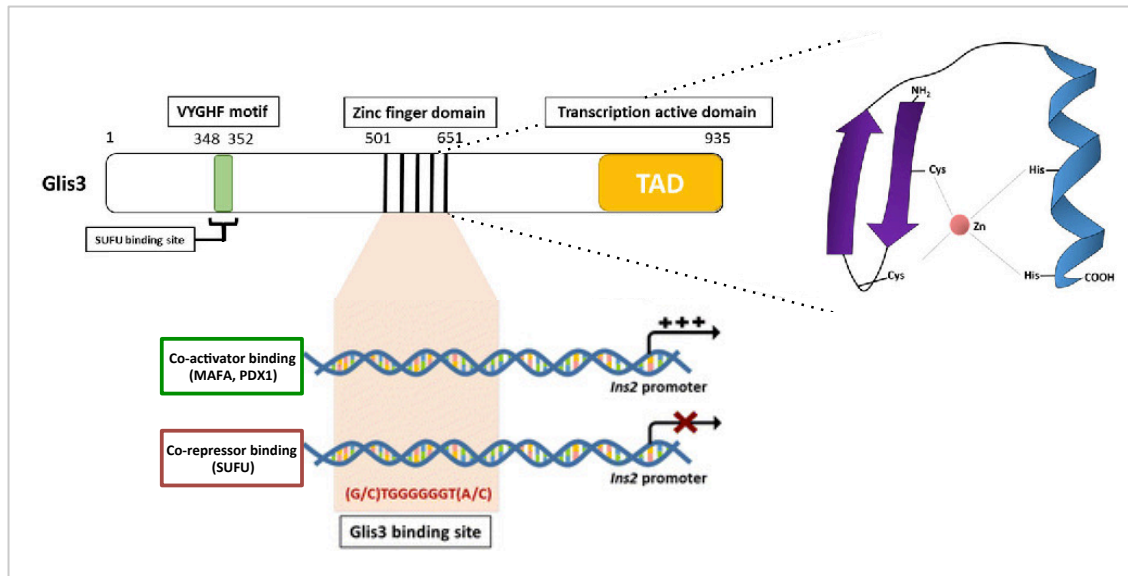


Figure 10. Schematic structure of GLIS3. The SUFU-interaction motif VYGHF within the N-terminus, the zinc finger domain (ZFD) and the C-terminal transactivating domain (TAD) are along the Glis3 protein structure. The illustration of the Cys2/His2 zinc finger is indicated by the dotted lines. Below is reported the positive or negative regulation of *Ins2* expression, dictated by the interaction with co-activators (green box) or co-repressor (red box). Modified from [67].

Several alternate transcripts of *GLIS3* have been reported so far in humans. Senee *et al.* established the gene structure of *GLIS3* and characterized the alternative transcripts and the predicted protein products. Twenty-five putative transcription start sites located in 12 exons and four transcription termination sites located in four exons have been identified. The predicted translation products of these transcripts encode nine variants of the *GLIS3* protein, most containing the five intact zinc finger domains, with variations in the N- and C- terminal regions that might affect the function of the encoded proteins. Some transcripts have limited or no coding capacity and may have regulatory function [65]. The larger transcript (7.5kb) is predominantly expressed in pancreas, thyroid, and kidney, whereas the smaller isoforms (0.8-2kb) are mainly localized in heart, kidney, liver and skeletal muscle [68]. Despite the distinct pattern of expression, the pathophysiological functions of the variable-length isoforms remain unknown.

The role of N- and C-terminus of *GLIS3* has been determined by the comparison of the activity between the full-length and truncated constructs. The deletion of the first 254 residues in the N-terminus results in a significant increment of transcriptional activity, whereas the truncation of 306 residues abolishes such activity [64,63]. Moreover, truncations in the C-terminal domain always diminished the activity of *GLIS3* [64].

These data suggests that different regions within the N- and C-terminuses contribute to its transcriptional activity.

Once bound to the DNA, GLIS3 can interact with co-activators or co-repressors, thus enhancing or silencing the expression of several target genes [69]. For instance, it has been reported that Glis3 has a dual role in controlling the transcription of the *Ins2* gene (Figure 10). *Glis3* directly binds the Glis3-BS localized in the promoter of *Ins2* and interact with the co-activators MafA and Pdx1 to activate *Ins2* expression [70]. On the other hand, *Glis3* can also bind the co-repressor suppressor of fused (SUFU) through the conserved motif VYGHF [71] (Figure 10). This complex is able to translocate into the nucleus where it suppresses the expression of *Ins2* [67]. SUFU is a negative regulator of the Sonic Hedgehog (SHH)/GLI signalling, implicated in several developmental processes and tumorigenesis (see Section IV-C for details) [69, 72]. However, the precise function of SUFU in GLIS3-mediated transcriptional regulation is not fully clarified [69, 71].

SUFU plays also an essential role in protecting the degradation of GLIS3. In fact, it has been reported that N-terminus of GLIS3 interacts with cullin-RING ubiquitin ligase 3 (CUL3) and with the ubiquitin ligase ITCH, promoting the poly-ubiquitination and the degradation *via* proteasome of GLIS3. Indeed, SUFU anchoring GLIS3 at the N-terminus, hiding the residues recognized by the ubiquitin ligases, thus protecting and stabilizing GLIS3 activity [66, 69, 71]. Taken together these findings suggest that SUFU, belonging the SHH pathway, modulates GLIS3 functions by both cytoplasmatic stabilization and nuclear transcriptional regulation [61, 73].

Furthermore, GLIS3 has been also described to interact with TAZ (*WWTR1*), a PDZ binding motif-containing transcriptional co-activator, in the primary cilium [74]. TAZ is part of the Hippo signalling pathway that regulates its nuclear localization and activity [69, 75]. The Hippo pathway plays a role in the regulation of many biological functions, including cell migration, differentiation, proliferation, and cell polarity. The WW-domain of TAZ recognizes a P/LPXY motif in the C terminus of GLIS3 [74] [61].

In vitro experiments demonstrate that the co-expression of these two transcription factors promotes the translocation of TAZ from the cytoplasm to the nucleus where it co-localizes with GLIS3. Into the nucleus, TAZ appears to function as a co-activator of GLIS3 enhancing its transcriptional activation. The localization at the primary cilium

and also the interaction with TAZ are reported to be the key elements of the GLIS3 signalling pathway underlying the renal polycystic disease, described in patients with mutations in *GLIS3* and *WWTR1* [74, 76, 77].

VII. *GLIS3* AND CONGENITAL HYPOTHYROIDISM

Based on the current knowledge, *GLIS3* represents a new candidate gene for congenital hypothyroidism (CH) but its role in thyroid development and function remains largely unexplored.

Homozygous and compound heterozygous mutations in the *GLIS3* gene have been associated with a rare syndrome, called NDH, characterized by neonatal diabetes (ND) and CH. NDH patients are characterized by intrauterine growth retardation and onset of non-immune diabetes mellitus (both Type-1 and -2). Other manifestations include renal parenchymal disease, primarily renal cystic dysplasia, and hepatic disease, with hepatitis in some patients and hepatic fibrosis and cirrhosis in others. Facial dimorphism and congenital glaucoma are also been reported in some affected cases [61, 65, 74, 78]. Regarding the thyroid gland, high TSH and low T4 characterize all of NDH patients reported so far, but in presence of a wide spectrum of structural thyroid abnormalities including athyreosis, hypoplasia, perifollicular and interstitial fibrosis, and normal thyroid anatomy. Similar phenotypic variability has been also observed in patients with mutations in *NKX2.1* and *PAX8* genes, involved in the specification of thyroid primordium, and the subsequent expression of genes (*TG*, *TPO*, *TSHR*, and *NIS*) responsible for the differentiation and proliferation of thyroid follicles and the synthesis of thyroid hormones (TH) [79, 80].

NDH patients are also characterized by variable sensitivity of TSH suppression after L-thyroxine treatment, resulting in a difficult normalization of thyroid parameters [69]. Several patients with elevated TSH and TG levels appear to be resistant to increasing doses of thyroxine therapy despite normalisation of free T4, thus excluding alterations in the L-T4 absorption [68, 80].

One possible explanation for the variable clinical manifestations described in patients could be attributed to the tissue-specific expression of variable-length transcripts of *GLIS3*, and the type of the mutation. The overall variants of the *GLIS3* gene identified

in NDH patients include large or small frameshift deletions that mainly localised in the N-terminus, and point mutations within the ZF domain. It has been reported that large deletions or frame shift mutations, causing profound disruptions of *GLIS3* structure, are associated with the most severe manifestations of NDH. Instead, milder phenotypes seem to be correlated to missense substitutions that preserve a residual function of one or more *GLIS3* transcripts [69, 80].

However, the lack of a distinctive clinical picture makes difficult the recognition and the treatment of these patients. Therefore, additional work is required to understand the genotype/phenotype correlations and, in particular, to determine whether *GLIS3* acts upstream of genes involved in pathways regulating thyroid development, hormonogenesis, and the peripheral response to T4.

In our laboratory, we have recently identified rare heterozygous *GLIS3* missense variants in a large cohort (18/177) of patients with isolated CH [63]. Clinically, half of the affected cases presented variable thyroid dysgenesis (athyreosis, thyroid hypoplasia and ectopy), whereas the remaining part have *in situ* thyroid gland [63]. Interestingly, these *GLIS3* variants are associated in all 18 cases with other rare variations in genes involved in thyroid pathology, supporting a frequent oligogenic origin of CH. Supporting our data, the NGS screening conducted in a cohort of 592 Chinese patients with CH reported a prevalence of the *GLIS3* mutations of the 0.3% [81].

In addition, a number of genome wide association studies (GWAS) have associated several *GLIS3* single nucleotide polymorphism (SNPs) with elevated circulating TSH levels and low T4 [61].

Taken together all of these data support a relevant role of *GLIS3* in thyroid function and in the onset of CH, possibly contributing to the explanation of the missing heritability of CH and the prevalent sporadic presentation of the disease [63].

Although hypothyroidism is associated with *GLIS3* variants, the absence of consistent pathological features in patients makes unclear the identification of a causative mechanism [69].

VIII. ANIMAL MODELS OF NDH

Up to now, the pathological mechanism underlying the multisystem clinical presentation of NDH syndrome has been studied in mice, and most of the researches have been focusing on pancreas development and the onset of diabetes.

The *Glis3*-null mice die within one week after birth due to the severity of neonatal diabetes [74]. The mutant mice *Glis3^{zf/zf}* and *Glis3^{-/-}* mutant mice develop neonatal diabetes, characterized by increasing blood sugar levels and decrease insulin secretion due to the early apoptosis of the β -cell mass [74, 82].

Regarding the control of insulin secretion, it has been reported that Glis3 knockdown drastically reduces the expression of both *Ins1* and *Ins2* genes by the binding to specific GLIS-responsive elements located in their promoter regions. Both *in vivo* and *in vitro* data prove that Glis3 is able to physically interact with *Pdx1*, *MafA* and *NeuroD1*, forming a transcriptional complex that activate the expression of the *Insulin* genes [74, 83]. Furthermore, the mRNA expression of the glucose transporter *Glut2* and the ATP-transporter SUR1 (*Abcc8*) are also reduced in the pancreas of *Glis3^{-/-}* mice. SUR is a sensor of intracellular levels of ATP and ADP and enhance insulin secretion in response to anti-diabetic drugs. These data highlight the post-developmental role of Glis3 in controlling insulin transcription and secretion, thus explaining the pathological mechanism underlying the onset of T1D in NDH patients [84]. However, as T2D is concerned, the *Glis3^{+/-}* mice develop overt diabetes and hypoinsulinemia when exposed to high-fat diet (HFD). Specifically, Glis3 deficiency is associated to downregulation of *Ccnd2*, a regulatory factor that is essential for postnatal β -cell growth and mass expansion in response to HFD and insulin resistance. An additional role of *Glis3* in T2D is its association with apoptosis. Glis3 KD in INS-1 cells increases the expression of several inflammatory cytokines and modulating the alternative splicing of the pro-apoptotic BimS leading to β -cells death [84].

All of these studies indicate that GLIS3 has multiple critical regulatory functions during pancreas development and also in the adult pancreas: regulating the development of endocrine progenitors, the generations and maturation of pancreatic β -cells, regulation of insulin expression, as well as in maintaining normal duct morphology [69].

As for NDH patients, the *Glis3* mutant mice also develop polycystic kidney disease [77], pointing up the role of *Glis3* in the maintenance of the normal renal function. Kang and co-workers demonstrate that *Glis3* and its co-activator Wwtr1/TAZ are part of transcriptional regulatory networks that are critical in the function of the primary cilium [77].

As far as thyroid gland is concerned, the Refetoff's group has recently described that *Glis3* is essential for TH biosynthesis and postnatal thyroid gland proliferation in mouse, acting down-stream of TSH/TSHR system [79]. In the mouse thyroid tissue, *Glis3* is highly expressed into the follicular cells, co-localizing with *Pax8* in the nuclei. *Glis3* KO mice present decreased levels of both free and TG-bound T4 and T3 accompanied with an elevation of TSH, suggesting its role in TH biosynthesis. RNA-seq and CHIP-seq analyses of mice thyroid confirm that *Glis3* directly regulates the expression of *Nis*, *Pds*, *Tpo*, *Duoxa2* and *Mct8*, the key components of the TH biosynthesis machinery [79]. Furthermore, *Glis3* deficiency results in structural changes of the thyroid gland that appears smaller size with a diminished number of follicular cells per follicle. Its role in follicles proliferation is further confirmed by the treatment of KO mice with low-iodide diet (LID). Both WT and *Glis3* KO mice present a dramatic increase of TSH in presence to LID, but in contrast, the thyroid gland of *Glis3* KO mice fail to adequately respond to the activation of the HPT-axis with follicular hypertrophy [79]. Data obtained by gene-expression analyses also indicate that *Glis3* deficiency is associated with a strong down-regulation of several cell proliferation-related gene, such as *Ccnd2* and *Cdca2* [79]. Interestingly, this scenario is similar to what was described in the pancreas during postnatal period, where the lack of *Glis3* leads to low insulin secretion and inability of the β -cells to growth and expand their mass in presence of HFD. These results indicate that GLIS3 is primarily involved in the postnatal control of TH synthesis and follicle proliferation downstream the TSH/TSHR system [79]. The expression levels of *Pax8*, *Nkx2.1*, and *Foxe1* are not significantly changed in thyroid glands from *Glis3* KO mice. Although in the first week after birth, the size of the thyroid follicles is smaller in *Glis3*-deficient mice, the thyroid gland and the TH levels are well conserved, suggesting that the subsequent hypothyroidism in this particular KO model is related to a hormonogenesis disorder rather than to thyroid gland dysgenesis.

In mice, *Glis3* appears to be important for the expression of *Slc5a5* (Na/I Symporter) and *Slc26a4* (Pendrin), channels responsible for iodine uptake and TH synthesis. The authors also report that the repression of proliferation of *Glis3*-deficient thyroid follicular cells is caused by the inhibition TSH-mediated mTOR pathway as well as the reduced expression of several genes involved in cell-division, which are directly regulated by Glis3. However, despite the relevant role of Glis3 described during pancreas organogenesis, no significant thyroid developmental defects were observed in *Glis3*^{-/-} mice. These data are partially in contrast to those observed in the NDH patients, in which thyroid dysgenesis is a common feature. However several factors, including the type and site of the mutation, can contribute the variable expression of the thyroid phenotype [79].

Although the available *Glis3* models greatly increase the comprehension of the molecular mechanisms underlying pancreas development and function, they not fully recapitulate the clinical manifestations of the NDH patients, in particular regarding the thyroid gland. Therefore, we address the possibility of zebrafish as a viable vertebrate model to study in more details the role of GLIS3 in thyroid dysfunction.

IX. ZEBRAFISH AS A MODEL TO STUDY THE ROLE OF *GLIS3* DURING THYROID DEVELOPMENT

Zebrafish (*Danio rerio*) has emerged as an important and useful model system to study different human diseases. Zebrafish possesses a unique combination of features that makes it particularly well suited for experimental and genetic analysis of vertebrate development. It has a short reproductive cycle with external fertilization and lays a large numbers of embryos per mating that can be analysed under microscope because of their optical transparency. Somitogenesis begins at about 9hpf and at 24hpf the zebrafish embryo has already formed all the major tissues and many organ precursors, such as a beating heart, circulating blood, nervous system, eyes and ears, all of which can be readily observed under a simple dissecting microscope. Larvae hatch by about 2.5dpf and they are swimming and feeding by 5–6dpf.

A variety of tools and methodologies have been developed to exploit the advantages of the zebrafish system. Zebrafish embryos and early larvae are optically clear, allowing for direct, non-invasive observation or experimental manipulation at all stages of their development, such as whole mount *in situ* hybridization analysis of gene expression patterns with extraordinarily high resolution. The microinjection of morpholinos (MOs), specific antisense oligonucleotides, is a useful method to investigate gene function *in vivo* by gene-specific inhibition of mRNA translation or by modifying pre-mRNA splicing events. It is possible to knockdown two or more different genes simultaneously by the injection of different MOs. Moreover, the genome editing techniques such as TALENs and CRISPR/CAS9 allow to generate stable mutant lines, permitting to overcome some limitations dictated by the morpholino microinjection [85].

Importantly, this model has been more and more frequently used in studies on thyroid pathophysiology because of its versatility, limited costs, and the relatively shortened time to obtain significant results when compared with other animal models as well as the broad conservation of the molecular mechanisms involved in thyroid development and function and TH action [2, 13, 17, 86].

X. AIM OF THE PROJECT

The aim of my PhD thesis is to deeply investigate the *glis3* function during the early steps of thyroid gland development, taking advantages of the zebrafish model system. In particular, we focus the attention on the possible *glis3* interaction with the SHH pathway during the commitment of the endocrine precursors towards the thyroid fate. The comprehension of the molecular mechanism of *glis3* activity will provide new insights into the etiopathogenesis of CH.

MATERIALS & METHODS

I. ZEBRAFISH MAINTENANCE

- Ethical statement

Current Italian national rules: no approval needs to be given for research on zebrafish embryos. Fish were maintained and raised according to EU regulations on laboratory animals (Directive 2010/63/EU).

- Zebrafish line and maintenance

Breeding fish were maintained at 28°C on a 14 hours light/10 hours dark cycle. They are bred in 3-5 litre tanks in three different systems.

Embryos were collected by natural spawning and staged according to Kimmel et colleagues (1995) [87]. They were raised in an incubator at 28°C in fish water with 0,1% Methylene Blue in petri dishes. The following Wild Type (WT) zebrafish line was used: AB strain, obtained from Wilson lab, University College London.

Stock solution for fish water: 34 g of Instant Ocean Sea Salt dissolved in 1 l of deionised H₂O.

Fish water: 50 ml of stock solution in 10 l of deionised H₂O.

II. REAL-TIME qRT-PCR

Real-Time qRT-PCR (Real-Time Quantitative Reverse Transcription PCR) was used for the detection and quantification of cDNA targets. This technique used fluorescent

reporter molecules (SYBR™ Green) to monitor the production of amplification products during each cycle of the PCR. Before the Real-Time PCR, this technique required the extraction of RNA from tissues and then its retrotranscription in cDNA.

A. Total RNA extraction and cDNA synthesis

Total RNA was extracted from embryos of different developmental stages and from several adult tissues using the TRIzol™ (Thermo Fisher Scientific). Tissues and organs were dissected under a stereomicroscope, frozen in TRIzol™ and stored at -80°C until further processing. Total RNA was extracted from pools of 20 embryos for each developmental stage and stored at -80°C. Frozen specimens were homogenized in TRIzol™. The RNA was then purified according to standard protocols and resuspended in 20–50µl of RNase- free water, 0.1mM EDTA, or 0.5% SDS solution.

The reaction was carried out following the protocol of GoScript™ Reverse Transcription System (Promega).

B. Real-Time PCR

Real-time analysis was performed by ABI PRISMTM 7900HT Fast Real-Time PCR System) using SYBRGreen MasterMix (Invitrogen).

The PCR reaction comprised an initial denaturation step at 95 °C for 30 s, followed by 40 cycles at 95 °C for 5 s, 60 °C for 15 s, and 72 °C for 45 s. A melting temperature-determining dissociation step was performed at 95 °C for 30 s, 60 °C for 30 s, and 72 °C for 60 s at the end of the amplification phase. The dissociation curve was used to check the specificity of PCR products.

For each developmental stage and for each tissue 50ng of cDNA were used. Elongation factor 1-alpha 1 (eEF1a1) gene was used as endogenous control. Quantification of the targets was normalized using the comparative CT method (also known as the $\Delta\Delta CT$ method), after ensuring that the targets and endogenous control had similar or relatively equivalent PCR efficiencies. Each experiment was conducted as a triplicate and repeated three times.

The following specific primers for the real-time PCR are used:

eef1a FW	5' CTGGTGTCCCTCAAGCCTGGTA 3'
eef1a REV	5' ACTTGACCTCAGTGGTTACATTGG 3'
glis3_qRT_FW	5' GACGCCAGCAGGTGTTTGCT 3'
glis3_qRT_REV	5' CAGAGACTCTCTGGAGAGCA 3'

III. SYNTHESIS OF PROBES FOR *IN SITU* HYBRIDISATION

To perform the whole mount *in situ* hybridisation assay we synthesised, *in vitro*, the *glis3* antisense digoxigenin (DIG) riboprobe, that consequently binds to the endogenous *glis3* mRNA during the hybridisation. In order to synthesize the probe we designed two primers to amplify a 1024bp long sequence for *glis3* (ENSDART00000142833.2). Then we performed a RT-PCR reaction on total RNA extracted from WT 26-48hpf (hours post fertilisation) embryos.

The primers used for probe amplification are the following:

glis3_WISH_FW	5' TGGGAAAGGCTGTAACCTGA 3'
glis3_WISH_REV	5' GGACACCTCAAACCTGAAGCG 3'

To evaluate the development and function of the thyroid we also used the following probes: *nkx2.4*, *pax2a*, *tg*, *slc5a5* [56], *tshba* [88], *shha* [89], and *wwtr1* [90].

A. Cloning and transformation reaction

The RT-PCR product was cloned in the pCRTM II-TOPO[®] vector (Figure 11) following manufacturer's instructions of TOPO TA Cloning[®] kit (Invitrogen), that provide for the cloning of PCR product in the plasmidic vector and then its bacterial transformation using One Shot[®] TOP10 (Invitrogen) competent cells.

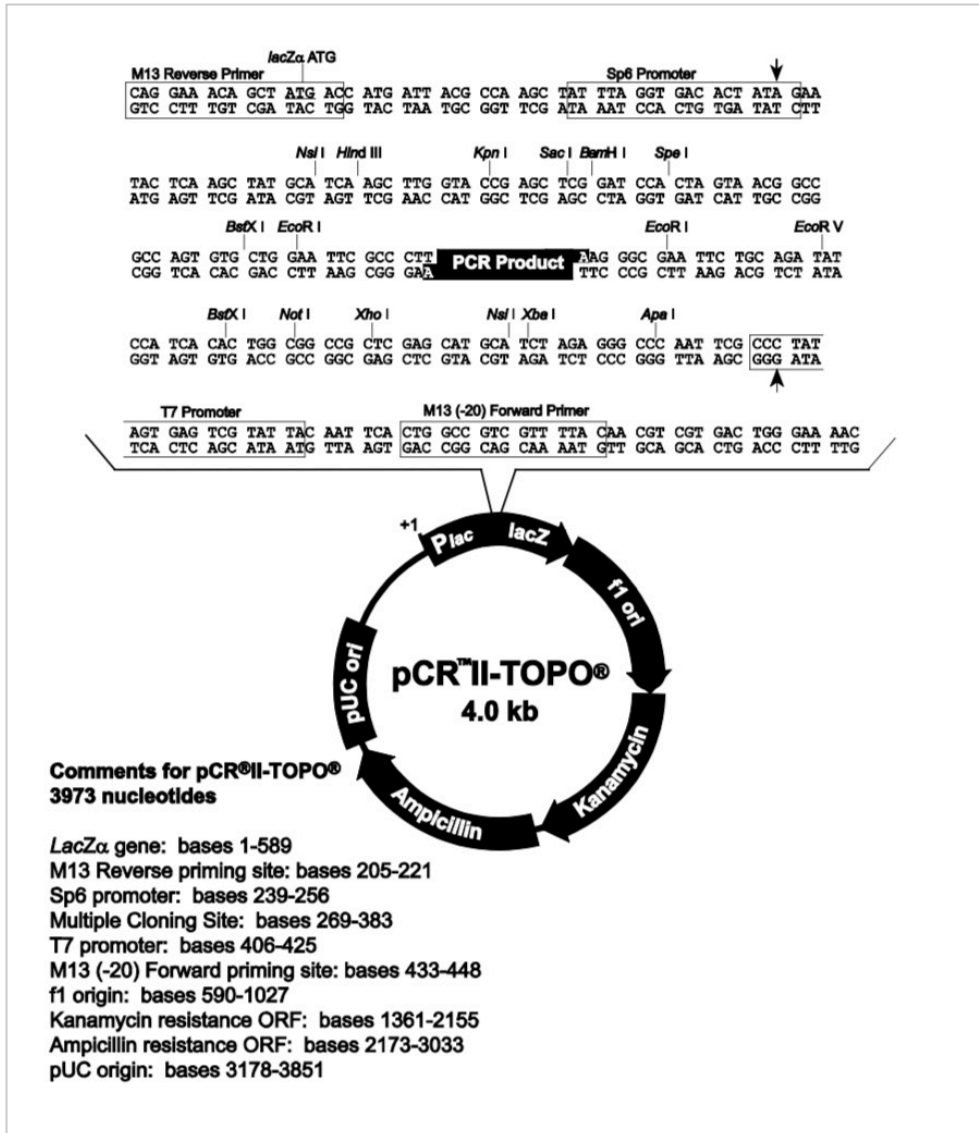


Figure 11. Schematic representation of the pCR™II-TOPO® vector. (from TOPO® TA Cloning® Kit user manual Invitrogen).

B. Isolation of plasmid DNA

Recombinant colonies were screened and preparation of plasmid was performed using PureLink™ HiPure Plasmid Filter Maxiprep system (Invitrogen) according to the manufacturer's instructions.

C. Probes labelling and synthesis

The linearized plasmids were then used as templates for antisense digoxigenin-UTP labelling and for *in vitro* riboprobe synthesis following the DIG RNA Labelling Kit (SP6/T7; Roche) manufacturer's instructions.

IV. WHOLE MOUNT *IN SITU* HYBRIDISATION (WISH)

Embryos at the appropriate stage were fixed in 4% paraformaldehyde (PFA)/ phosphate buffered saline (PBS) over night at 4°C; then they were dechorionated and they were dehydrated in 100% methanol and stored at -20°C until used for whole mount *in situ* hybridisation (WISH). WISH experiments were performed according to Thisse *et al.*, [91].

The synthesized DIG-probes were detected using anti-DIG-alkaline phosphatase (AP) and NBT/BCIP staining.

After WISH experiments, the embryos were post-fixed in 4% PFA and analysed in glycerol 85% under a stereomicroscope.

To evaluate the thyroid volume (*tg*) and the proper synthesis of *tshba* the respective DIG-probes were stained with Fast Blue that is able to produce fluorescent signals. These signals were detected by confocal microscopy.

For confocal microscopy, fixed embryos were embedded with 0.8% low-melting agarose and placed on a Petri capsule. Stacks were recorded using a 40x immersion objective (Nikon C2+ confocal system; Nikon). The fluorescence signals were quantified using ImageJ software (<http://rsb.info.nih.gov/ij/>).

V. LOSS-OF FUNCTION ANALYSIS

The embryos were injected with a specific Morpholino (MO), a specific antisense oligonucleotide to transiently knock down the gene function.

The specific *glis3* morpholino was designed by Gene Tools (LLC, Philomath, OR), in order to recognize the splice donor site of the exon2-intron2 boundary of the pre-mRNA.

- *GLIS3MO_SPL*: 5' - TTCTTGTTTTTACCTTTCATACCGC - 3'

As a negative control we injected standard control morpholino (std ctrl-MO) that targets human β -globin gene. This oligo has not been reported to have other targets or generate any phenotypes in any known test system except human β -thalassemic hematopoietic cells.

- std ctrl-MO : 5' CCTCTTACCTCAGTTACAATTTATA 3'

Morpholinos were dissolved in Danieau's buffer (58mM NaCl; 0,7mM KCl; 0,4mM MgSO₄.H₂O; 0,6mM Ca(NO₃)₂; 5mM Hepes pH 7.2) at 2mM concentration and stored at -80°C.

Embryos were microinjected at the 1–4 cells stage and Rodamine dextran (Molecular Probes) was usually co-injected as a tracer.

Microinjection was performed through a micromanipulator (Micromanipulator 5171; Eppendorf), and a microinjector (Femtojet; Eppendorf.)

Escalating doses of MO were tested for phenotypic effects and to establish the correct dose to perform the experiments.

The embryos were treated with PTU 1X (1-Phenil-2-thiourea, SIGMA; stock PTU 10X 0.015 g of PTU powder in 50 ml of fish water) to inhibit pigment formation [92].

For a better observation the injected embryos (called morphants) were anaesthetized using tricaine 1X (Ethyl 3-aminobenzoate methanesulfonate salt, SIGMA; stock tricaine 25X 0.08 g in 20 ml of distilled H₂O) in fish water and PTU 1X.

The morphants were observed up to the stage of interest and they were fixed in PFA 4%/PBS at 4°C over night, dehydrated and stored in 100% MeOH at -20°C.

RT-PCR and qRT-PCR on total RNA, extracted from 30–40 embryos at 2 days post-fertilization (dpf), were used to found out the molecular mechanism of action and to check the efficiency of splicing MO.

The primers used for RT-PCR are the following:

<i>glis3</i> _MO_FW	5' AAACCGGGCCCTGATGAATA 3'
<i>glis3</i> _MO_REV	5' AAGCAGGACTGAGACTCTGG 3'

The primers used for qRT-PCR are the following:

WT_FW	5' ATGAAAGGTTACAGAAGGGT 3'
WT_REV	5' AGCAAACACCTGCTGGCGT 3'
Intr2_FW	5' ATGAAAGGTAAAAACAAGAAT 3'
Intr2_REV	5' ATTAGTTGACTTTACCTTCAAA 3'

To confirm the results obtained by the *GLIS3*MO_SPL, we used a second *glis3* splicing morpholino (*GLIS3*_MO2) that has been already validated [93].

- *GLIS3*_MO2: 5' - ACCTGCTGCAAGAGATCAGTTAAAA - 3'

To investigate the relationship between *glis3* and Shh or Notch pathway the MOs used are the following, which have been already validated:

- *shha*_MO: 5' - CAGCACTCTCGTCAAAAGCCGCATT - 3' [94]
- *jag1a*_SPL_MO: 5' - AAACAGCCTCTGAAACTCACCGGCC - 3' [47]
- *jag1b*_SPL_MO: 5' - AATCCTGCTACTCACTTTCCTGCTGGC - 3' [47]

VI. RESCUE EXPERIMENTS

Full-length zebrafish wild type *glis3* cDNA was cloned into pcs2+ vector (Invitrogen; Figure 12) between BamHI and EcoRI restriction sites, upstream the Sp6 promoter sequence and downstream the polyadenylation signal.

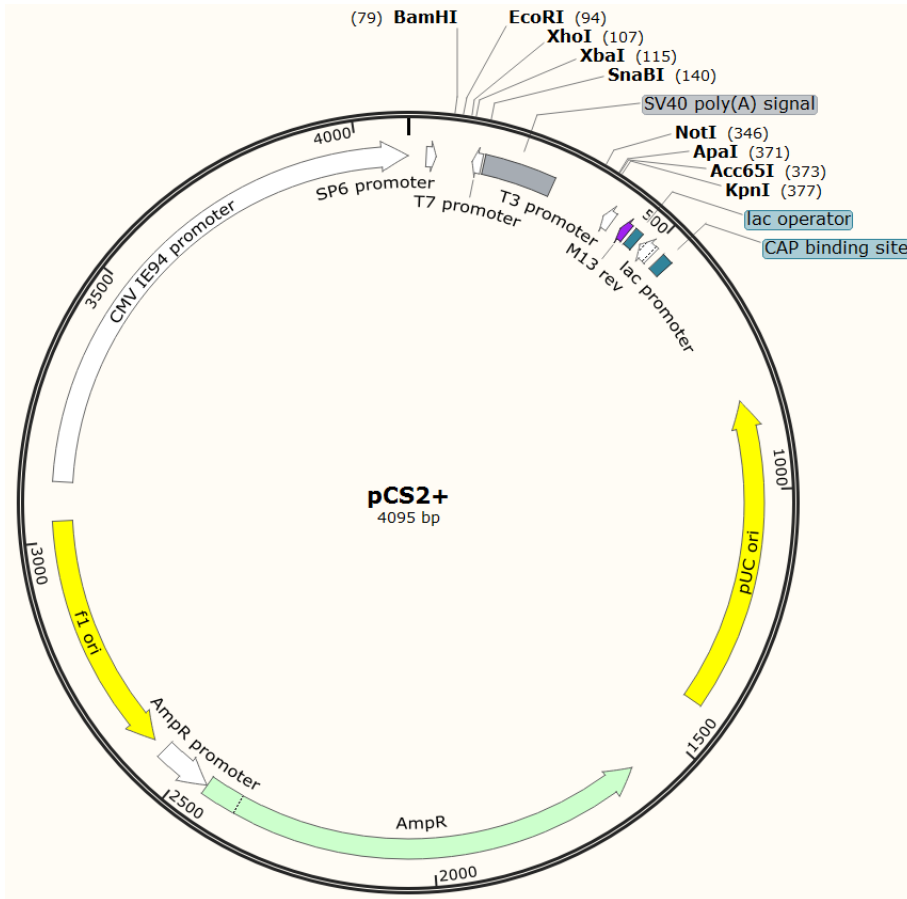


Figure 12. Schematic representation of the pcs2+ vector (Invitrogen).

Primers used to obtain the full-length zebrafish *glis3* coding sequence (CDS) are the following:

<i>glis3</i> CDS_FW	5' ATGGACATGAATGGGAAAG 3'
<i>glis3</i> CDS_REV	5' TCAGCCTTCAGTGAACACACA 3'

After transformation in TOP10 cells, the wild type positive clone was selected and confirmed by complete automated sequencing. The mutated *glis3* mRNA was generated introducing a point mutation GGA>TGA in the position 1223bp, causing the formation of a premature stop codon upstream the Zinc-Finger functional domain.

The primers used for mutagenesis are the following:

<i>glis3</i> MUT_FW	5' TGCACTGCTGAGCCATCTACAGCC 3'
---------------------	--------------------------------

<i>glis3</i> MUT_REV	5' GGCTGTAGATGGCTCAGCAGTGCA 3'
----------------------	--------------------------------

Both constructs (wild-type and mutated) were linearized with Not1 and the efficiency of was checked on agarose gel electrophoresis. The mRNAs were *in vitro* transcribed using the mMessage mMachine Sp6 kit (Thermo Fisher Scientific), following the manufacturer's instructions.

The obtained mRNAs were purified using the phenol/chloroform extraction and quantified by Nanodrop.

As control of *glis3* mRNAs microinjection, we used the mRNA of GFP, which has no targets in zebrafish.

VII. IMMUNOFLUORESCENCE

The qualitative analysis of TH production was performed by immunofluorescence according to standard procedures using the rabbit anti-T4 BSA serum (1:1000; ICN Biochemicals, Aurora, OH) and the AlexaFluor 555 anti-rabbit IgG as secondary antibody (Invitrogen) [11, 47].

To test proliferation and apoptosis, after WISH with *nkx2.4*-DIG riboprobes and Fast Blue staining, embryos were stripped and rinsed in PBS. Anti-phospho-histone H3 (PH3) and antiactive caspase-3 (AC-3) antibodies (1:250; Cell Signaling, Beverly, MA), followed by antirabbit IgG secondary antibody/AlexaFluor 488 (1:500; Invitrogen) were used [47].

VIII. IMMUNOCYTOCHEMISTRY

COS7 cells were plated (2×10^5) on sterile coverslips placed in 35 mm Petri dishes and transfected with 1 μ g of plasmids (for co-transfection was used 0.5ug of pEGFP_sufu cDNA and 0.5ug of pcDNA4/His-Myc_A_glis3 cDNA). Twenty-four hours after transfection, cells were washed with PBS, fixed with PBS containing 3%

paraformaldehyde (Sigma-Aldrich St. Louis, MO, USA) for 10 min at room temperature and rinsed twice with PBS. Cells were permeabilized with 0.1% Triton X-100 (Sigma-Aldrich, St. Louis, MO, USA), blocked for 30 min with PBS-goat serum 2% (Invitrogen, Auckland, NZ), incubated with α -c-Myc primary antibody 1:100 (Life Technologies, Carlsbad, CA, USA) in PBS-goat serum 2% (1:100) overnight at 4°C and incubated with the appropriate secondary antibodies (Alexa Fluor 555 goat anti-mouse IgG, Life Technologies, Carlsbad, CA, USA) 1:500 for 1 h at room temperature. Finally cells were mounted with Slow-Fade Gold antifade reagent with Dapi (Life Technologies, Carlsbad, CA, USA). Images were acquired by using a laser scanning confocal system installed on a Nikon Eclipse Ti microscope with a 60x oil immersion objective. Alexa Fluor 555 was excited with a 555-nm argon laser and detected with a 568-nm band pass filter.

IX. CYCLOPAMINE TREATMENT

For the inhibition of the Shh pathways, embryos were rinsed in fish water with 10 μ M Cyclopamine (Sigma-Aldrich) from 50% epiboly stage up to fixation in PFA at 26 and 48 hpf. Controls consisted of corresponding incubations in 1% DMSO (dimethylsulfoxide) [95, 96].

X. DAPT TREATMENT

For the inhibition of the Notch pathways, the γ -secretase inhibitor DAPT (N-[N(3,5-difluorophenacetyl)-l-alanyl]-S-phennylglycine t-butyl ester) (Sigma-Aldrich) was diluted in fish water at 100 μ M. The embryos were dechorionated and treated with DAPT from 50% epiboly stage up to 24 hpf at 30°C. As controls, the embryos were treated with fish water containing 1% DMSO [47].

XI. STATISTICAL ANALYSIS

All data were shown as means \pm standard error (SEM) or percentages. The *t*-student test was used to comparison of differences between groups. The $p < 0.05$ was considered statistically significant (* $p < 0.05$; ** $p < 0.01$; *** $p < 0.001$). All analyses were conducted with the software package GraphPad Prism 4.0 (GraphPad, San Diego, CA).

RESULTS

I. STRUCTURE AND CONSERVATION OF ZEBRAFISH *GLIS3*

The *glis3* gene is evolutionary conserved across species dating back to fishes. In zebrafish *glis3* (NM_001080607) is localized on the chromosome 10 and encodes for a full-length protein of 804 aminoacids and 88.45kDa in size (UniProt F1QB13). Recently, a shorter isoforms (787aa) with unknown functions has been deposited (UniProt A0A0R4IU85).

As reported in Figure 13, the full-length protein is composed of several domains. The Serine-Rich (SR) and Proline-Rich (PR) domains localized in the N-terminus seem to be important for the interaction with Hnf6, a critical regulator in early endoderm development (Kim, 2012). The five zinc-finger (ZF) motifs positioned in the middle of the protein are crucial for the recognition and binding of the GLIS3-binding sites (Glis3BS). Finally, the nuclear localization signal (NLS) partially overlapping with the 5th ZF allows the translocation of the transcription factor into the nucleus.

The alignment conducted with ClustalW2 software (www.clustal.org) revealed the rather low conservation between zebrafish and human (47.23%) or murine (46,52%), which is mainly restricted in the ZF domain (Figure 13B and C) [97].

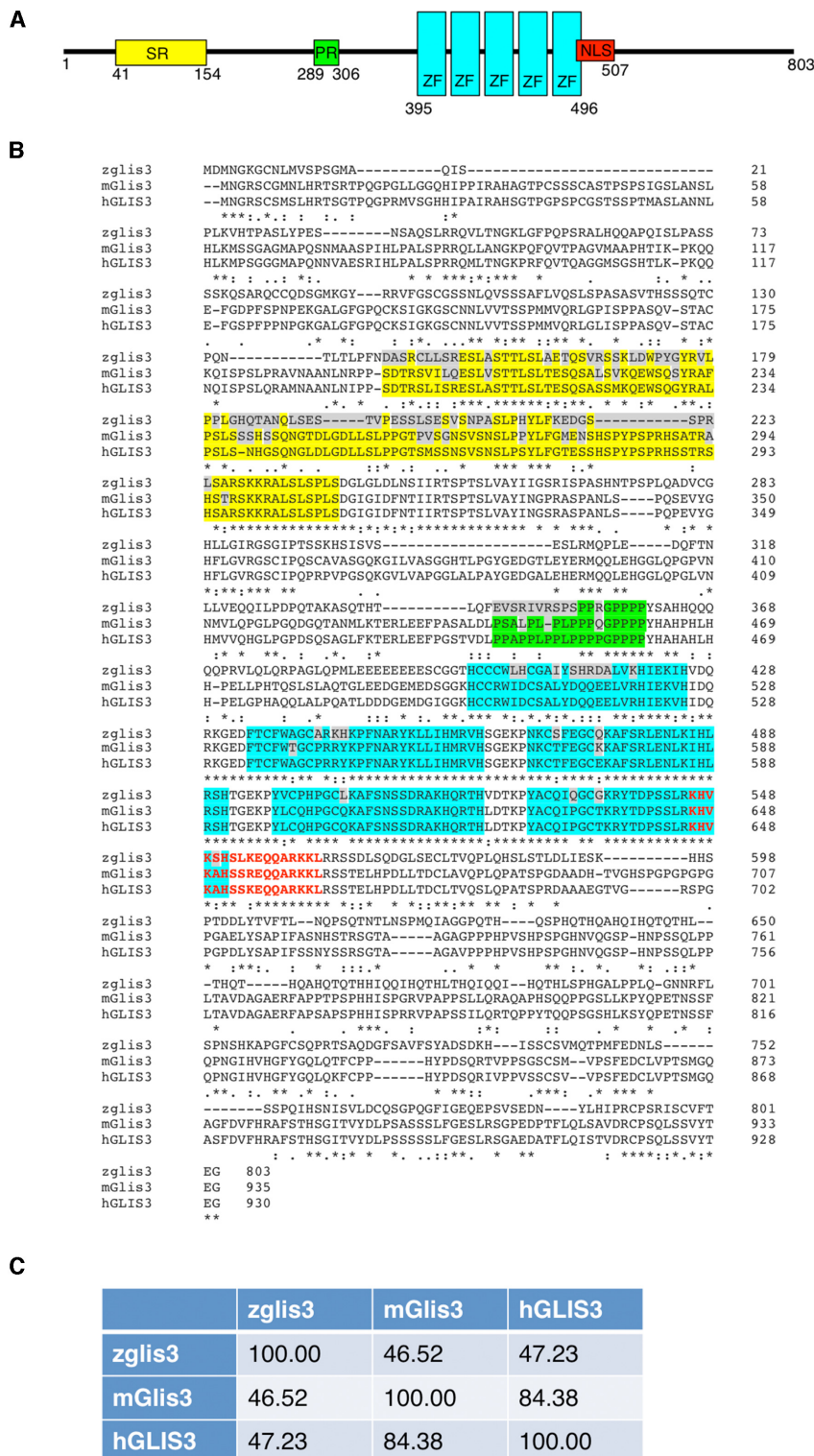


Figure 13. (A) Schematic representation of the zebrafish *glis3* protein (UniProt F1QB13). Yellow = Serine-Rich (SR) domain; Green = Proline-Rich (PR) domain; Light Blue = Zinc-Finger (ZF) domain; Red = Nuclear Localization Signal (NLS). (B) Alignment of the GLIS3 protein sequencing of the zebrafish (UniProt F1QB13), mouse (UniProt Q0GE24) and human (UniProt Q8NEA6). The colour code of the different domains is reported above. The residues that differ between species are highlighted in grey. (C) Aminoacid identity between zebrafish, murine and human GLIS3 proteins, performed using ClustalW2 software [97].

II. EXPRESSION OF *GLIS3* DURING ZEBRAFISH DEVELOPMENT

To explore the function of *glis3* activity *in vivo*, we examined its expression in zebrafish embryos by qRT-PCR and WISH. *Glis3* expression is dynamically regulated in a spatio-temporally specific manner during embryonic development (Figure 14).

As reported in the histogram 14A, *glis3* mRNA has not maternal origin, since it was undetectable before the maternal to zygotic transition (MZT) stage, occurring at 2.5-3hpf. The expression of the zygotic *glis3* mRNA started from the late somitogenesis (20 somite-stage, 19hpf) onwards. During the later phases of embryonic development and larval transition, the levels of *glis3* increased exponentially by 3-5 fold at 1-3dpf, and 8-fold at 5dpf [97].

By WISH we also characterized the tissue-specific expression of *glis3* during embryonic development. At 20hpf, *glis3* is widely expressed in head and trunk regions (Figure 14C and C'), whereas at 24hpf, it appears restricted in brain, pronephric ducts and pharyngeal endoderm, the tissue that will give rise to the endocrine organs, such as thyroid and pancreas (Figure 14D). In particular, *glis3* is expressed in a "salt and pepper" manner, in the portion of the endodermal pouches and the medial endoderm (Figure 14D'), and well localized with cells that constitute the pancreatic bud (Figure 14D''). At 36hpf, the mRNA was also detectable in the hypothalamus, medial endoderm, otic vesicle, and pronephric ducts (Figure 14E-E'). At 2dpf, the signal is restricted to heart, hypothalamus and pronephric ducts (Figure 14F). Of note, *glis3* is not detectable in the developed thyroid gland (2dpf).

In adult zebrafish, the expression of *glis3* is maintained at high levels in kidney, pituitary and pancreas. Lower levels of mRNA are also present in testis, ovary, brain and pectoral fins (Figure 14B). Given the lack of a compact thyroid gland in zebrafish, it was not possible to dissect the single follicles for the analysis of the *glis3* expression [97].

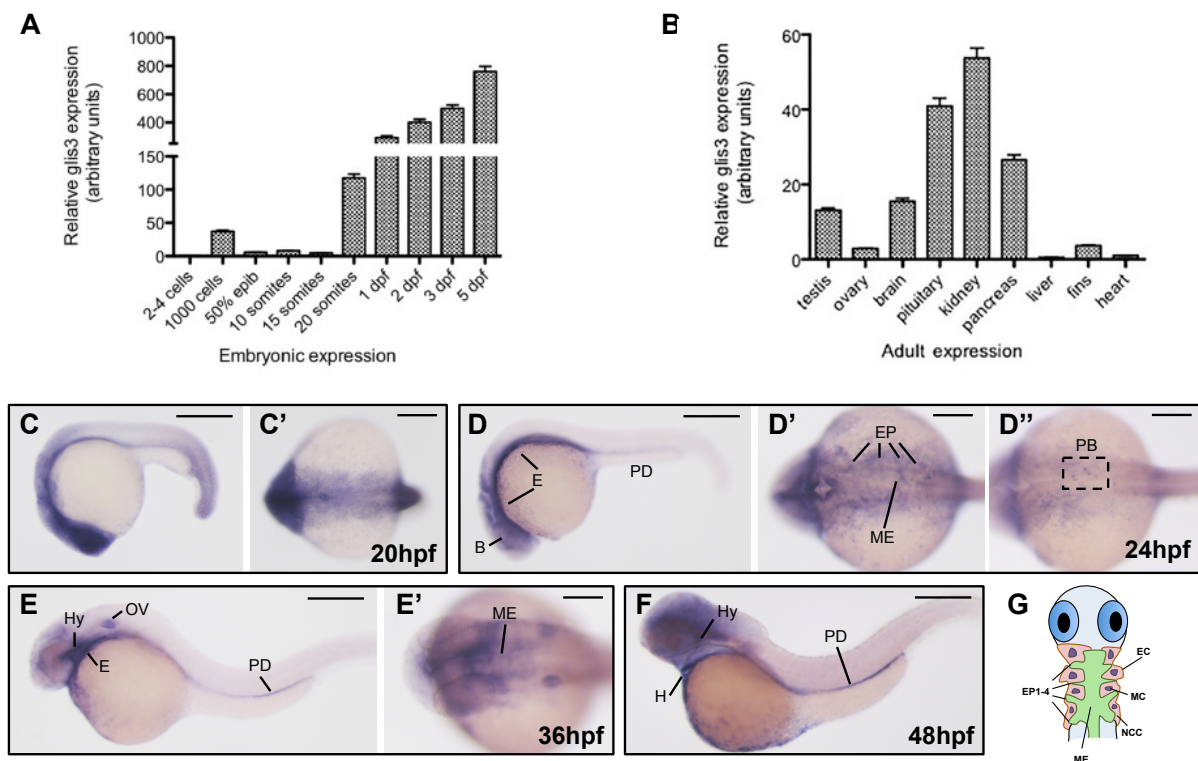


Figure 14. Ontogenetic pattern of *glis3* expression in zebrafish. (A-B) qRT-PCR of *glis3* relative mRNA expression during embryonic development and adult tissues. Total RNA is extracted from pools of 50 embryos/stage and from 3 adults, respectively. cDNA synthesis and qRT-PCR following standard procedures. Experiments are performed in triplicate and results are expressed by Mean \pm SD. (C-F) Tissue specific expression of *glis3*, at different developmental stages, analysed by WISH using *glis3* antisense riboprobe followed by NBT/BCIP staining. Images are representative of three experiments (30 embryos each). Embryos were acquired in lateral and dorsal view. Scale bars: 100µm and 250µm. B: brain; E: endoderm; PD: pronephric ducts; EP: endodermal pouches; ME: medial endoderm; PB: pancreatic bud; Hy: hypothalamus; OV: otic vesicles; H: heart. (G) Schematic representation of zebrafish pharyngeal region composed by the endodermal pouches (EP1-4), medial endoderm (ME), mesodermal core (MC), neural crest cells (NCC) and ectoderm (EC). Adapted from Rurale *et al.*, 2018 [97].

III. KNOCKDOWN EXPERIMENT WITH *GLIS3* MORPHOLINO ANTISENSE OLIGO

To further characterize the role of *glis3* in zebrafish embryonic development and during thyroid organogenesis and function in particular, we performed knockdown experiments by the microinjection of specific *glis3* morpholino into zebrafish embryos (called morphants) and comparing them with controls.

The control embryos were generated by the injection of a standard control morpholino (Std_CtrlMO) that has no target in zebrafish to discriminate possible off target effects or alterations due to the injection manipulation.

The spliced-blocking morpholino against *glis3* was designed to recognize the splice donor site of the exon2-intron2-3 boundary of the pre-mRNA (*glis3MO_SPL*) (Figure15A). The *glis3MO_SPL* was validated injecting different doses (0.3, 0.5, 0.7 and 1 pmol/embryo) in the zebrafish embryos at one-cell stage. The total RNA was extracted from pools of injected-embryos at 1 and 2dpf, and retrotranscribed into cDNA. The RT-PCR performed using a specific set of primers confirmed that the *glis3MO_SPL* alters in a dose-dependent manner the normal splicing, causing a strong reduction of the wild-type transcript and the production of a longer mRNA that retained part of the intron2-3 (340 bases) (Figure 15B). Additionally, by qRT-PCR we observed that the expression aberrant *glis3* mRNA is correlated with the amount of the *glis3MO_SPL* injected (Figure 15C).

The bioinformatic analysis of this aberrant transcript revealed the formation of a frameshift mutation and thus leading to the translation of a non-functional protein.

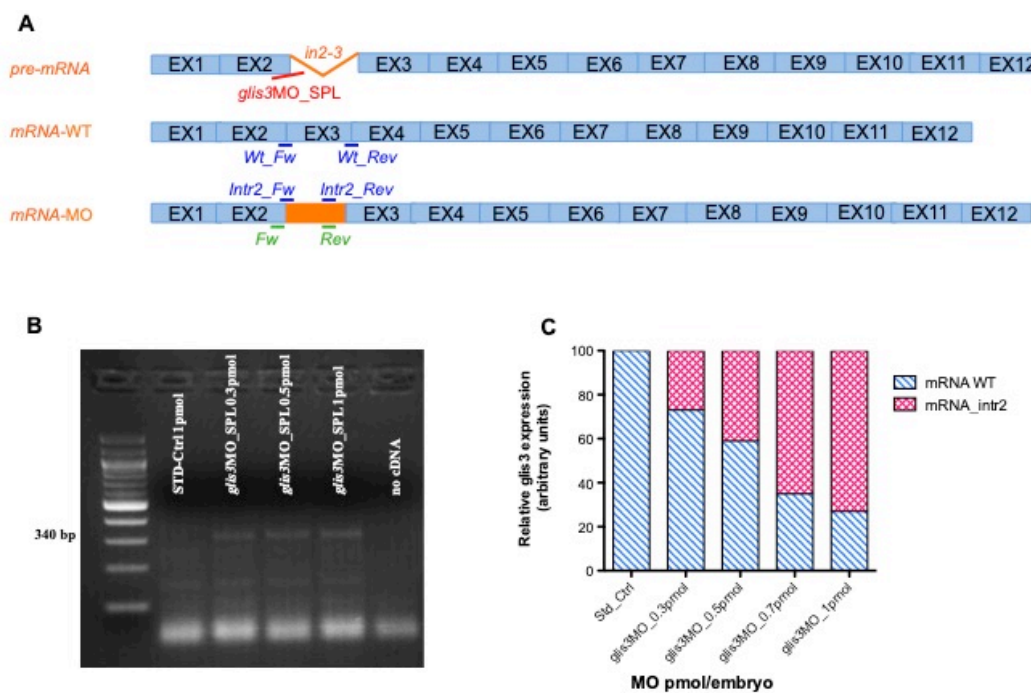


Figure 15. Morpholino-mediated knockdown of the *glis3* genes in zebrafish. (A) *glis3* gene structure: the squared boxes correspond to the exons, the orange lines correspond to the introns. *glis3SPL_MO* is targeted to the splice donor site between exon 2 and intron 2-3 (E2i2-3). The position of primer sets used in RT-PCR and qRT-PCR to analyse the altered splicing are indicated in green and in blue, respectively. (B) RT-PCR analysis of *glis3* expression in STD_Ctrl and *glis3SPL_MO* injected embryos at different doses. The *glis3SPL_MO* causes the retention of a part of intron2-3 producing a PCR product of 340bp. (C) qRT-PCR of WT (mRNA WT) and aberrant (mRNA_intr2) *glis3* transcripts expressed after injection of growing doses of *glis3SPL_MO*.

IV. EVALUATION OF THE PHENOTYPE OF *GLIS3* MORPHANTS

During embryonic development, the *glis3* morphants presented a series of morphological defects, which can be divided into three phenotypic classes: normal, moderate and severe (Figure 16). The normal ones are indistinguishable from the controls (Figure 16A, E and I) and developed without any visible alteration (Figure 16B, F and L). The moderate class included morphants with curved tail, cardiac edema and impaired circulation (Figure 16C, G and M). The third class displayed severely affected phenotypes: shortened body, small head, cardiac edema, notochord abnormalities and twisted or truncated tail (Figure 16D, H and N). The frequencies of the morphants belonging these 3 phenotypic classes were strongly dependent on the dose of *glis3*MO_SPL injected (Figure 16O). Since the highest dose (1pmol/e) was associated with the most severe phenotype and with the higher mortality, we decided to use the 0.3 and 0.5pmol/e for the subsequent analysis.

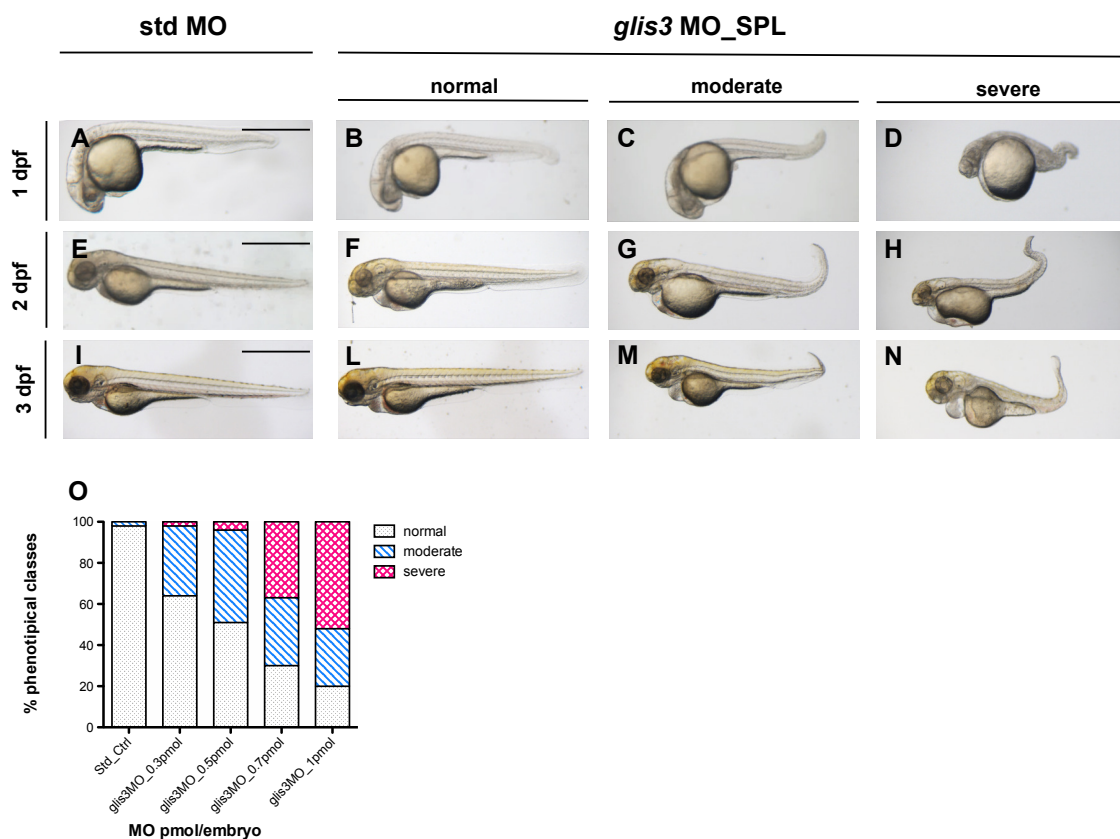


Figure 16. Phenotypic classes of embryos injected with *glis3*MO_SPL. (A_N) Three phenotypic classes normal, moderate and severe analysed at three different developmental stages (1, 2, and 3 dpf). The normal embryos (B, F and L) are indistinguishable from the controls (A, E and I). The moderate

class (**C, G and M**) presents embryos with curved tail, cardiac edema and impaired circulation. The severe embryos (**D, H and N**) are strongly affected by necrosis, cardiac edema, reduced circulation and stasis. (**Graphic O**): frequencies of the morphants belonging these phenotypic classes according to the injected doses. Scale bar: 250µm.

V. *GLIS3* KNOCKDOWN AND THYROID DEVELOPMENT

Following the set up of *glis3* gene knockdown and embryonic phenotype analysis, we performed whole mount *in situ* hybridization to test whether *glis3* plays a role in zebrafish thyroid organogenesis. To this purpose, we analysed the expression of the early transcription factors *nkx2.4* and *pax2a*, and the differentiated markers *tg* and *slc5a5* at different time points.

All of the results were confirmed by using a second *glis3* splicing morpholino that had been previously validated [93] (data not shown).

A. Induction of thyroid primordium

The thyroid primordium originates from the pharyngeal endoderm by 1dpf and starts to differentiate in thyroid precursors thanks to the combined expression of *nkx2.4*, *pax2a*, *hex* and *pax8* [56].

At 1dpf, the *glis3* morphants exhibited a deficient formation of thyroid primordium with a reduction or absence of *nkx2.4* and *pax2a* expression (Figure 17A-C and E-G).

After WISH, we acquired the embryos in dorsal view and we quantified the volume of *nkx2.4* and *pax2a* in the thyroid primordium (Figure 17A'-D' and E'-H').

Regarding *nkx2.4*, the 34.4% of embryos injected with 0.3pmol/e of *glis3*MO_SPL was comparable to controls; the 42.8% presented a marked reduction of the *nkx2.4* signal that was instead undetectable in the remaining 22.8%. Consistently with the lower levels of the wild-type transcripts, the 74.3% of the embryos injected with 0.5pmol/e, the *nkx2.4* signal was absent, while it appeared reduced in the remaining 25.7% of the morphants (Figure 17D).

The evaluation of *pax2a* gave similar results (Figure 17E-G). At 0.3pmol/e we observed: normal expression in the 48.5% of morphants, reduced or absent expression

in 17.6% or 33.9%, respectively. At 0.5pmol/e, the expression of *pax2a* was reduced or absent in the 31.2% and 68.8% of morphants, respectively (Figure 17F).

Regarding the volume of thyroid primordium quantified in embryos classified as reduced or absent expression of *nkx2.4* and *pax2a* we observed a >50% and >95% reduction than normal embryos, respectively (Graphs D' and H').

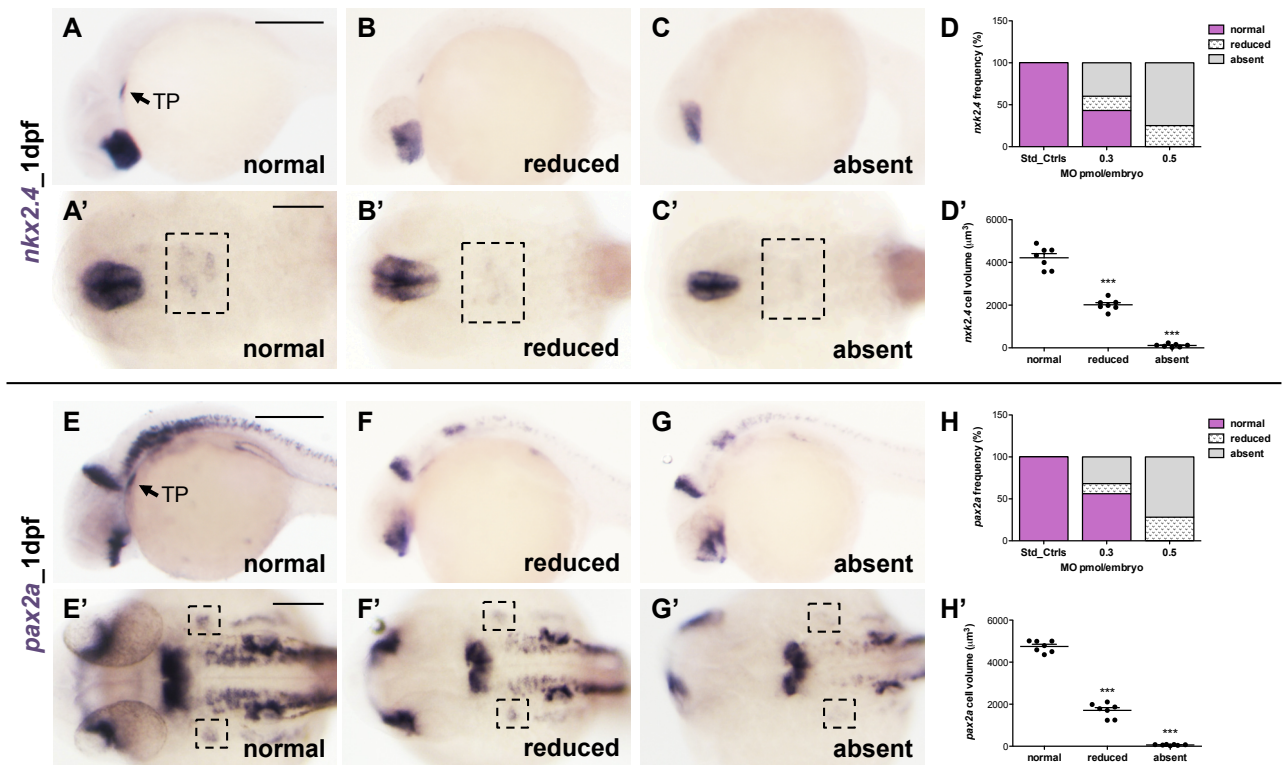


Figure 17. Expression of *nkx2.4* and *pax2a* in the developing thyroid primordium (TP).

(A-C and A'-C') WISH of *nkx2.4* expression in embryos injected with Std-CtrlMO and glis3MO_SPL at 0.3 and 0.5pmol/e. Images are representative of injected embryos that expressed normal, reduced or absent *nkx2.4* signal acquired in lateral and dorsal view. (E-G and E'-G') *pax2a* expression in the injected embryos at 1dpf. The embryos were subdivided belonging the three phenotypic classes described above. Each experiment was performed in triplicate, using 40 embryos per MO injected. Scale bar: 250µm. TP: thyroid primordium. (Graphs D, H) Bars indicated the percentages of the injected embryos belonging the different phenotypic classes. (Graphs D', H') Quantification of *nkx2.4* and *pax2a* at 1dpf in the control and morphant embryos belonging the thyroid phenotypic classes (Normal; Reduced and Absent). Data were obtained from 10 embryos for each class. Statistical significance was calculated using Student's t-test (***)P<0.001).

B. Differentiation and proliferation of thyroid follicles

At 2dpf the precursors of thyroid primordium differentiate into thyroid follicles, which express the functional markers *tg* and *slc5a5*, and proliferate along the ventral aorta by 3dpf [98].

In agreement with what previously described, at 2dpf the embryos injected with 0.3pmol/e and 0.5pmol/e exhibited a dramatic reduction of *tg* in the 51.7% and 74.4%, respectively (Figure 18A-C). Similarly, comparing with the normal *slc5a5* expression (Figure 18D), we observed a marked reduction in the 42.6% of morphants injected with 0.3pmol/e and the 32.3% of 0.5pmol/e (Figure 18E and G). Furthermore, in the half of latter ones, the *slc5a5* signal was undetectable (Figure 18F and G).

At 3 dpf, the thyroid gland elongates in the midline forming the classical V-shape (Figure 18H). In morphants, the staining of *tg* continued to be reduced in the 32% and 50% of embryos injected with 0.3pmol/e and 0.5pmol/e, respectively (Figure 18I and K). Notably, a considerable number of morphants exhibited a normal expression of *tg* but the thyroid follicles were disorganized and ventrally displaced along the ventral aorta (Figure 18J).

After WISH, we flat mounted the embryos and counted the number of cells expressing *tg* and *slc5a5*. The number of positive cells in normal, reduced or disorganized thyroid tissues was calculated by dividing the area of positive staining by the average area of a single cell (Figure 18L and M). The difference between embryos with normal and reduced *tg* expression was significantly different at both 2 dpf (N: 48.5 ± 2.9 ; R: 15.2 ± 1.8 ; $P < 0.001$) and 3 dpf (N: 79.45 ± 4.3 ; R: 10.8 ± 2 ; $P < 0.001$). No significant differences between normal and disorganized signal have been observed in the embryos stained with *tg* (N: 79.45 ± 4.3 ; D: 74.7 ± 3.9 ; $P = ns$). Similarly, at 2 dpf, the number of *slc5a5* expressing cells in normal embryos (N: 51.2 ± 2.3) was significantly higher compared to reduced (R: 18.7 ± 2.5 ; $P < 0.001$) and absent (A: 0.45 ± 0.05 ; $P < 0.001$) signals.

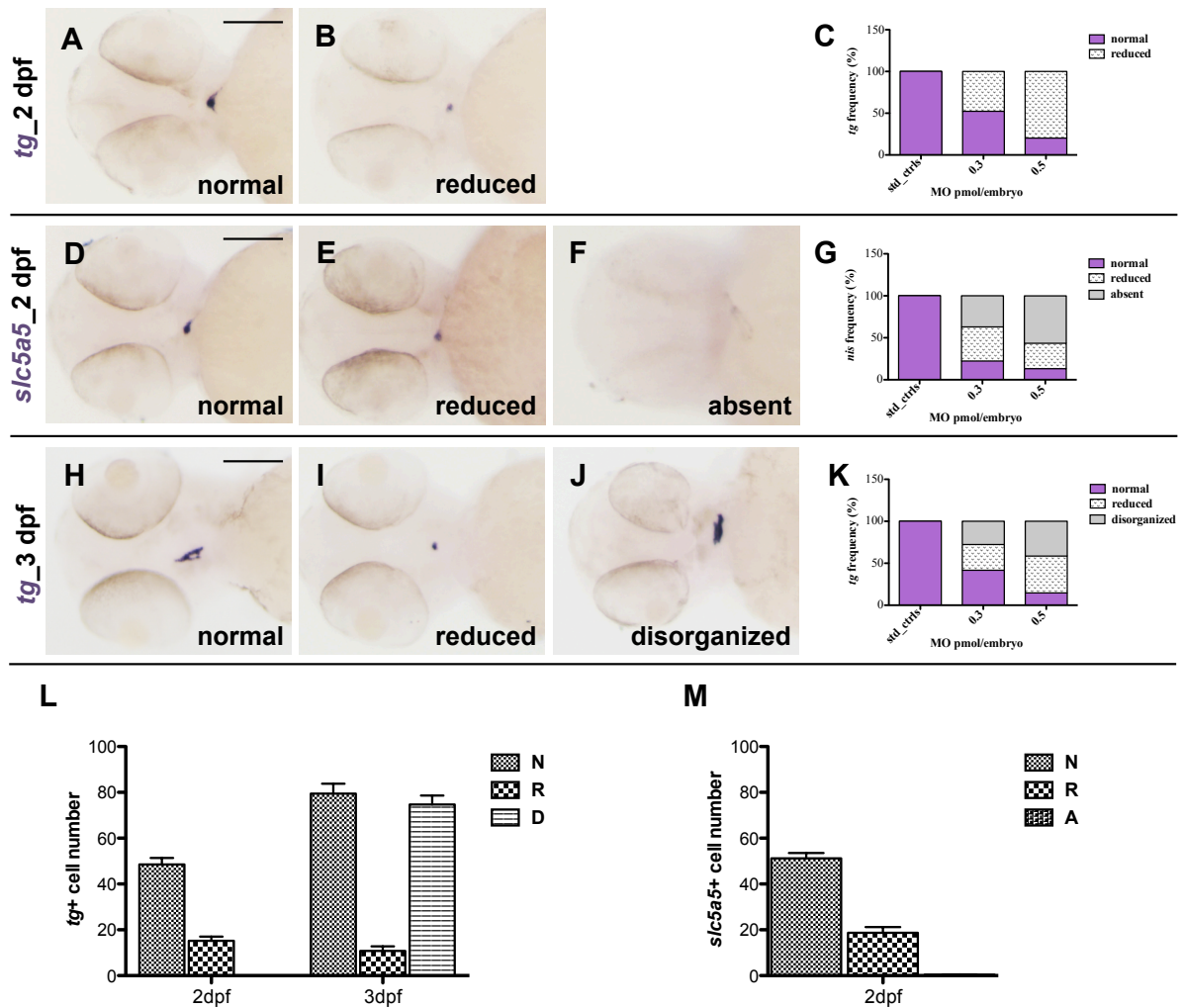


Figure 18. Expression of *tg* and *slc5a5* in the developing thyroid gland. (A-B) WISH of *tg* expression in embryos injected with Std-ctrlMO and *glis3*MO_SPL at 0.3 and 0.5 pmol/e. Images are representative of injected embryos that expressed normal or reduced *tg* signal. (D-F) *slc5a5* expression in the injected embryos at 2 dpf as described above. The embryos were subdivided belonging these three phenotypic classes: normal, reduced or absent. (D-F) analysis of thyroid elongation using WISH of *tg*, in the injected embryos at 3 dpf. Morphants presented, at various degrees, a normal formation of the V-shape thyroid, a reduction or a disorganization of follicles. (Graphs C, G and K) Bars indicated the percentages of the injected embryos belonging the different phenotypic classes. Each experiment was performed in triplicate, using 40 embryos per MO injected. Embryos were acquired in ventral view, anterior to the left. Scale bar: 250 μ m. (Graphs L and M) Quantification of *tg* and *slc5a5* expressing cells at 2 and 3 dpf in the control and morphant embryos belonging the thyroid phenotypic classes (Normal = N; Reduced = R; Disorganized = D and Absent = A). Data were obtained from 10 embryos for each class. Statistical significance was calculated using Student's t-test (***) $P < 0.001$.

C. Proliferation and apoptosis of thyroid primordium of *glis3* morphants

The mechanisms underlying the altered thyroid phenotype after *glis3* knockdown were investigated by WISH of thyroid primordium using *nkx2.4* followed by activated caspase-3 (AC-3) and phospho-histone H3 (PH3) immunostaining as markers of apoptosis or proliferation, respectively (Figure 19). At 24hpf, no significant differences in AC-3 (Figure 19C-D) or PH3 (Figure 19E-F) immunostaining were seen by confocal microscopy in the area of *nkx2.4* expression in all morphants analysed. These findings confirmed that the reduced expression of the early thyroid markers was not associated to a decreased proliferation nor to an increased apoptosis of the endocrine precursors committed to thyroid fate.

At this point we wondered if the reduced expression of the thyroid primordium in the *glis3* morphants is the result of a global impairment of the pharyngeal endoderm. To explore this possibility we analysed the expression of *foxa2*, an early endoderm-specific transcription factor (Figure 20). When the thyroid start to develop (22hpf) the endoderm appeared unaffected in *glis3* morphants (Figure 20B), compared to controls (Figure 20A).

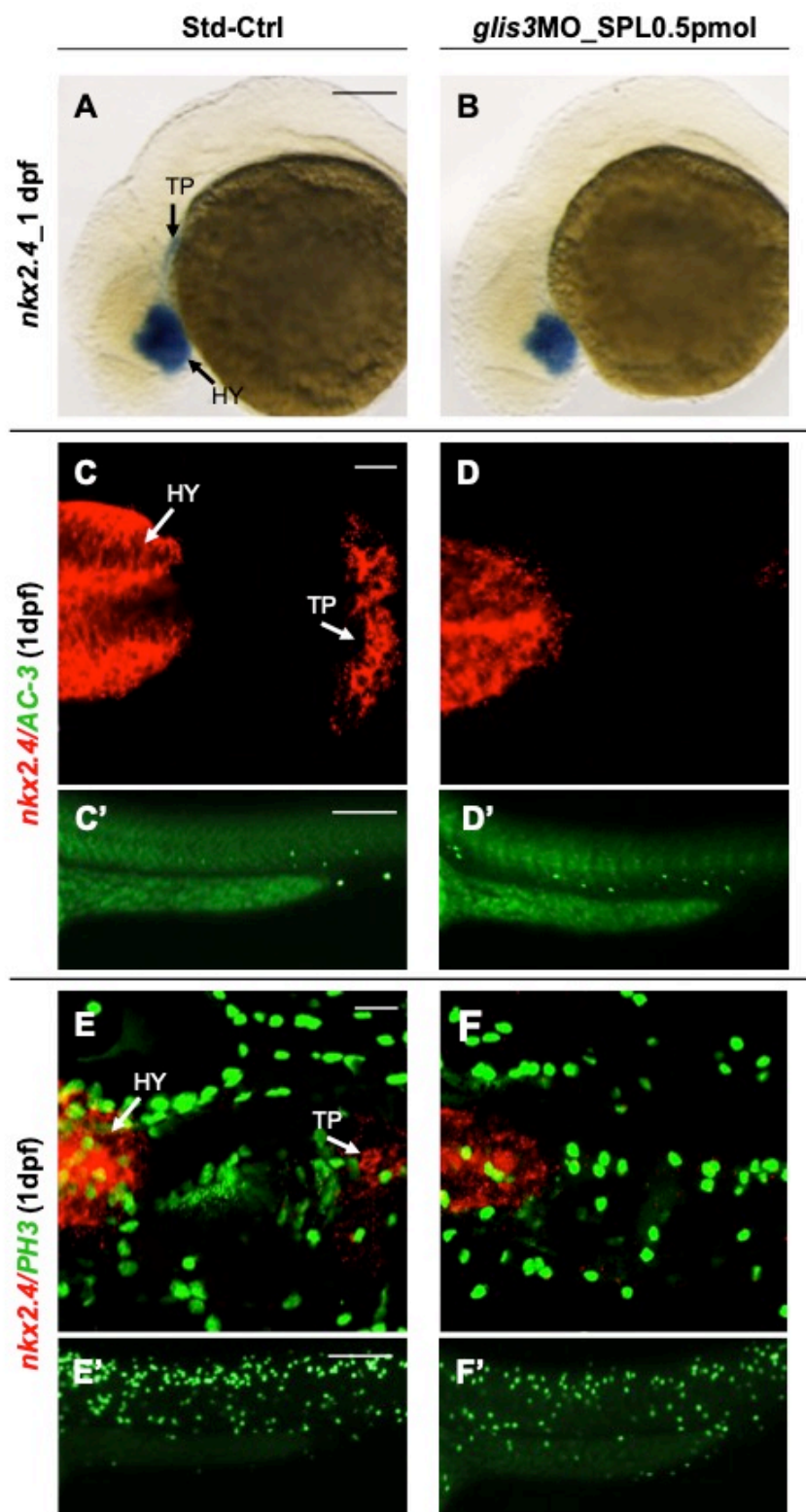


Figure 19. Analysis of apoptosis and proliferation in *glis3*-morphants. (A-F) WISH of *nkx2.4*, at 1dpf, using FastBlue staining for the acquisition of the fluorescence signal, followed by activated caspase-3 (AC-3) (C-D) and phospho-histone H3 (PH3) (E-F) immunostaining. Std-ctrl embryos reveal the correct development of the thyroid primordium. In *glis3*-morphants the thyroid primordium is absent.

No differences in AC-3 or in PH3 immunostaining were observed in morphants, compared to controls. (C'-D' and E'-F') AC-3 and PH3 staining of the trunk-tail regions were used as control of experimental conditions. Each experiment was performed in triplicate, using 40 embryos per MO injected. (A-B) Embryos were acquired in lateral view; scale bar: 250 μ m. (C-F) Embryos are all flat mounted, in ventral view, with anterior to the left. Scale bar: 100 μ m. HY: hypothalamus, TP: thyroid primordium.

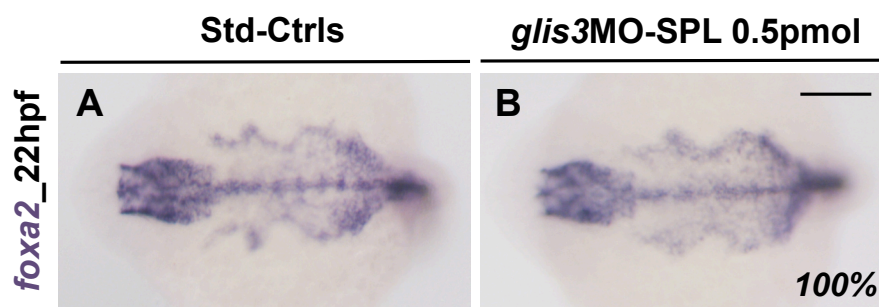


Figure 20. Analysis pharyngeal endoderm in *glis3* morphants. WISH showing *foxa2* expression in Std_Ctrls (A) and *glis3* morphants (B) at 22hpf. Each experiment was performed in triplicate, using 40 embryos per MO injected. The embryos were acquired in dorsal view, anterior to the left. Scale bar: 100 μ m.

D. T4 production and regulation of the HPT-axis in *glis3* morphants

We performed T4 whole mount antibody staining to assess the status of thyroid function in *glis3*-injected larvae and controls at 5dpf. In control larvae, a growing number of T4-producing follicles was detectable in the pharyngeal area, spread in the pharyngeal jaw (Figure 21A). By counting the single T4-positive follicles, we observed that the *glis3* morphants (0.5pmol/e) exhibited the reduced number of follicles (n: 3 \pm 1) compared to the control fish (n: 5 \pm 1) (Figure 21B and C).

Given the primary regulatory role of TSH on thyroid function, we also investigated the expression of the pituitary *tshba* (homologous of the human TSH β), by WISH using the FastBlue dye followed by confocal acquisition (Figure 21D-E). At 5dpf, the 85% of the *glis3* morphants (0.5pmol/e) presented a significant increased in the number of the *tshba* positive cells (n: 13 \pm 2) when compared with controls (n: 4 \pm 1) (Figure 21D-F).

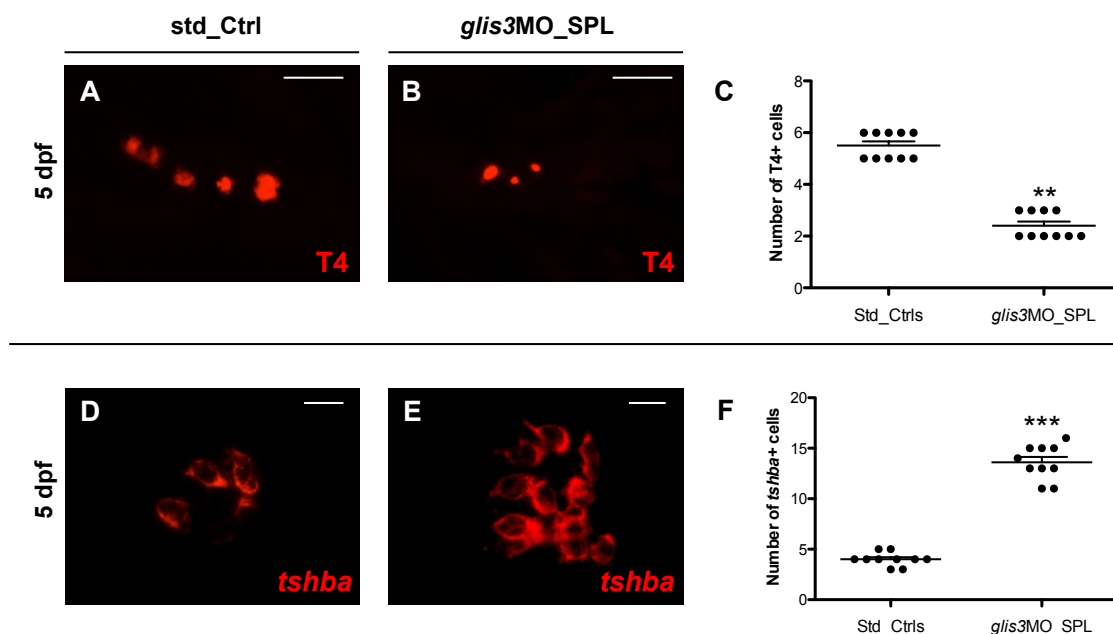


Figure 21. Analysis of T4 and *tshba* levels in *glis3*-morphants. (A-B) T4 whole mount antibody staining, at 5dpf, in control and in *glis3MO_SPL* larvae at 0.5pmol/e. Distinct follicles were visible in a row along the anterior-posterior axis, at the pharyngeal midline. (C) Count of the number of T4-producing follicles in Std_CtrlMO and in *glis3MO_SPL* injected larvae. (D-E) WISH of *tshba* using FastBlue staining for the acquisition of the fluorescence signal, at 5 dpf, in control and in *glis3MO_SPL* larvae at 0.5pmol/e. (F) Count of the number of *tshba*-producing follicles in Std_CtrlMO and in *glis3MO_SPL* injected larvae. Embryos were all flat mounted, in ventral view, with anterior to the left. Each experiment was performed in triplicate, using 40 embryos per MO injected. Scale bar: 100 μ m. Statistical significance was calculated using Student's t-test (**P<0.01; ***P<0.001).

Taken together, our results indicated that *glis3* is involved zebrafish thyroid development. The knockdown of *glis3* was associated with an early impairment of thyroid primordium induction thus leading to the differentiation of a reduced number of thyroid follicles.

This defect was not associated to changes in proliferation/apoptosis of thyroid precursors, suggesting a role of *glis3* for the quantitative regulation of endodermal precursor specification, thus restricting the number of cells committed to a thyroid fate. In later stages the low T4 production and the high *tshba* expression observed in *glis3* larvae well recapitulate the clinical findings described in patients with congenital hypothyroidism.

VI. RESCUE OF THYROID DEFECTS OF *GLIS3* MORPHANTS

To have a confirmation of the specific thyroid phenotype resulting from *glis3* morpholino activity, we performed mRNA rescue experiments co-injecting the *glis3MO_SPL* with the wild type and mutated forms of the zebrafish *glis3* transcript.

The mutated *glis3* mRNA was generated introducing a point mutation GGA>TGA in the position 1223bp, causing the formation of a premature stop codon upstream the ZF domain.

Considering that *glis3MO_SPL*-injected embryos showed curved trunk, pericardial edema, and impaired circulation, independently of the class they belong to, we decided to check the recovery of these specific features, in association with a moderate mortality and reduced number of morphants with severe phenotype. Since high doses of mRNA injection resulted in increased mortality, the zebrafish embryos co-injected with 0.5 pmol/e of *glis3MO_SPL* and 100pg/e of the WT or MUT *glis3* mRNAs gave the best results, with a recovery of a normal phenotype in 50-60% of embryos with the affected phenotype of the *glis3* morphants.

In this experiment, the control embryos were generated by the injection of 100pg/e mRNA of GFP that has no target in zebrafish and does not cause any modification in the injected embryos.

At this point, we focused our attention on the thyroid phenotype, analysing the expression of *nkx2.4* and *tg* at 1 and 2dpf, respectively (Figure 22). No changes in the expression of both markers have been observed in the uninjected (Figure 22A and F) or in embryos injected with the GFP mRNA (Figure 22B and G). The co-injection with the *glis3MO_SPL* and the WT mRNA was able to normalize the expression of *nkx2.4* and *tg* in the vast majority of the embryos (Figure 22D and I), in comparison with the *glis3MO_SPL* injected alone (Figure 22C and H). Interestingly, the co-injection of the *glis3MO_SPL* and the MUT mRNA (Figure 22K) failed to rescue the thyroid defects of *glis3* morphants and even worsened the phenotype. Finally, no significant differences were observed after the injection of 100pg/e of both WT and MUT mRNA alone (Figure 22E, J and L).

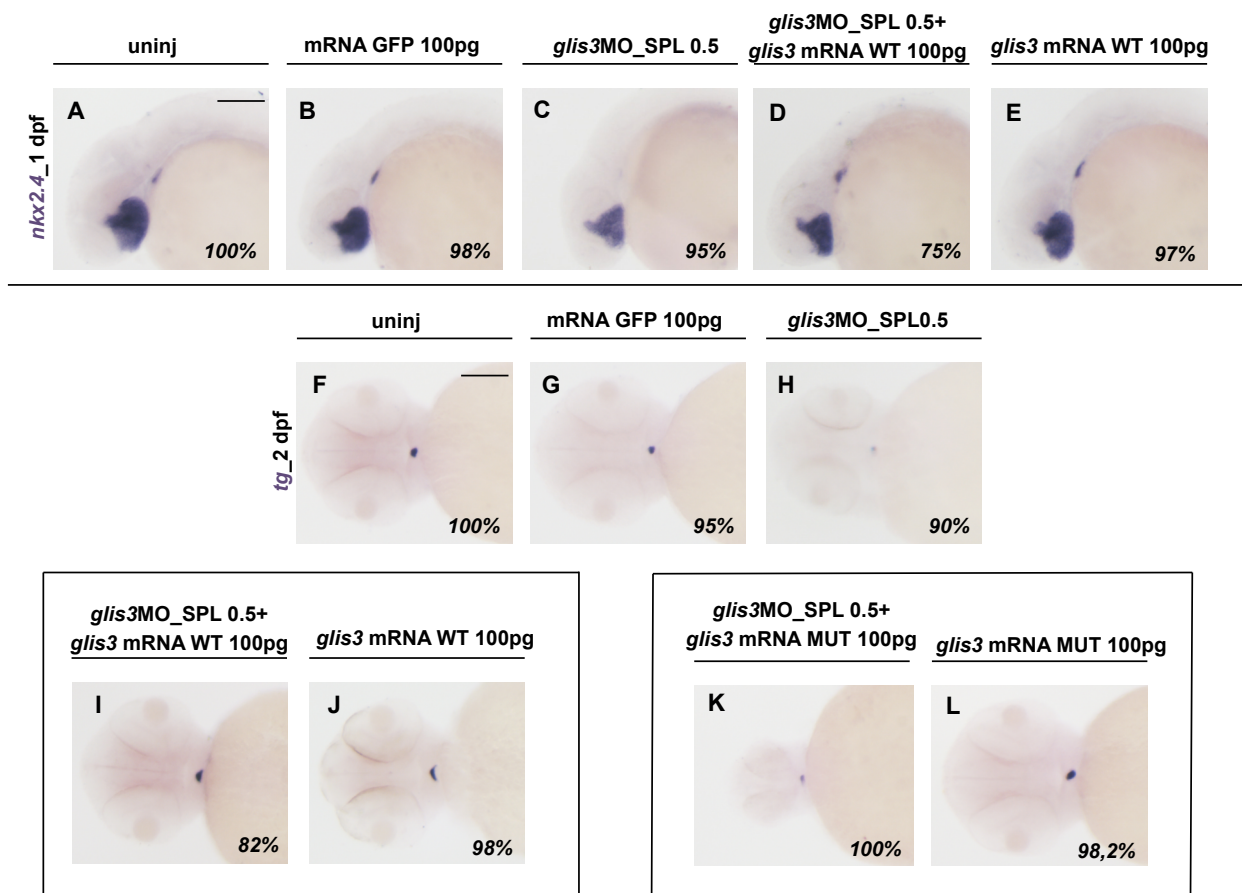


Figure 22. Molecular analysis of the rescue of thyroid defects of *glis3* morphants. (A-E) WISH of *nkx2.4* expression, at 1 dpf, in the uninjected embryos, embryos injected with mRNA GFP 100pg/e, *glis3MO_SPL* at 0.5pmol/e, with both *glis3MO_SPL* at 0.5pmol/e and *glis3* mRNA WT100pg/e and only *glis3* mRNA WT100pg/e. (F, L) WISH of *tg* expression, at 2 dpf, in the uninjected embryos, embryos injected with mRNA GFP 100pg/e, *glis3MO_SPL* at 0.5pmol/e, with both *glis3MO_SPL* at 0.5pmol/e and *glis3* mRNA WT100pg/e (I) with only *glis3* mRNA WT100pg/e (J), with both *glis3MO_SPL* at 0.5pmol/e and *glis3* mRNA MUT100pg/e (K) and with only *glis3* mRNA MUT100pg/e (L). Each experiment was performed in triplicate, using 40 embryos per each injection. Embryos were acquired in lateral (A-E) and ventral (F-L) views, anterior to the left. Scale bar: 250 μ m.

VII. EFFECTS OF *GLIS3* OVEREXPRESSION ON THYROID DEVELOPMENT

To further define whether *glis3* gene dosage contribute to the onset of thyroid defects, we performed an over-expression experiment, microinjecting growing doses of WT *glis3* mRNA. When compared with controls at 1dpf (Figure 23A), the injection of 200 or 250pg/e was associated with an increase of the *nkx2.4* signal at the level of the thyroid primordium in 56.5% or 68% (Figure 23B,C) of the embryos, respectively.

Similarly, we observed an upregulation of *tg* expression at 2dpf in the 68% (200pg/e) and 75% (250pg/e) of embryos (Figure 23D-F).

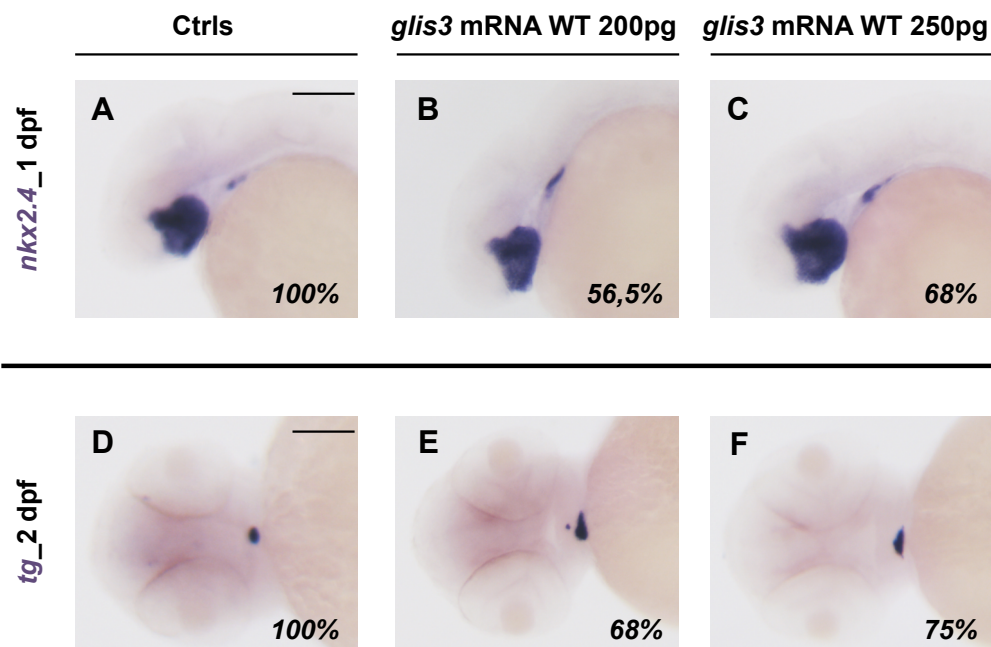


Figure 23. Expression of *nkx2.4* and *tg* in the *glis3*-overexpressed embryos. (A-C) WISH of *nkx2.4* expression in embryos injected with GFP RNA 250pg/e (Ctrl) and *glis3* mRNA WT at 200pg and 250pg/e. (D-F) WISH of *tg* expression in embryos injected with GFP RNA 250pg/e (Ctrl) and *glis3* mRNA WT at 200pg and 250pg/e. Embryos were acquired in lateral view (A-C) and in ventral view (D-F). Each experiment was performed in triplicate, using 40 embryos per each doses injected. Scale bar: 250 μ m.

To quantify the impairment of thyroid specification after *glis3* knockdown as well as the induction of thyroid growth following *glis3* overexpression, we measured the *tg* and T4 levels in embryos injected with *glis3*MO_SPL (0.5pmol/e) and the WT mRNA (200pg/e). At 2dpf, the injected embryos were analysed by WISH (FastBlue) of *tg* followed by confocal acquisition and quantification. ImageJ software was used to quantify both the number and the intensity of fluorescent pixels of the same area and number of stacks for each sample, thus defining the volume of *tg*-positive cells. In parallel, the number of T4-producing follicles in embryos at 5dpf was determined by IHC and fluorescence acquisition.

Confirming the previous results, the thyroid gland was smaller in 87% of *glis3* morphants compared to controls (Figure 24A, B and D) and the number of T4-

producing follicles was reduced by 50% (Figure 24E, F and H). On the contrary, the overexpression of *glis3* led to an enlargement of the thyroid gland (+130% than controls) at 2dpf (Figure 24C and D), as well as in a significant increase of the T4 production (Figure 24G and H).

Taken together these data support the idea that *glis3* is a key regulator of thyroid development, and that the proper amount of *glis3* is critical for the adequate specification of thyroid precursors.

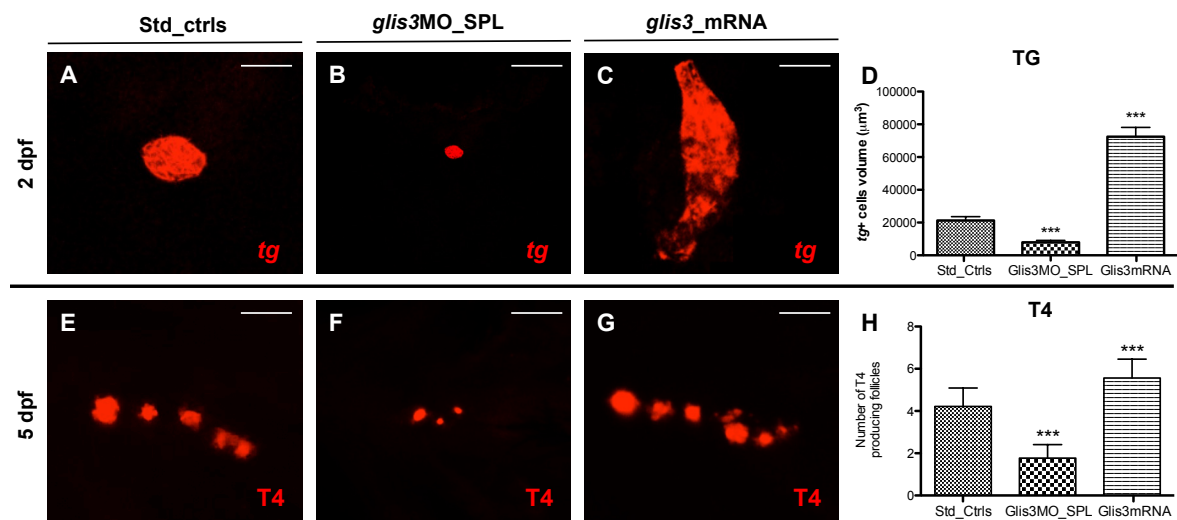


Figure 24. Analysis of *tg* and T4 levels in *glis3* overexpressing embryos. (A-C) WISH of *tg* using FastBlue staining for the acquisition of the fluorescence signal. Std_Ctrl embryos revealed the normal distribution of *tg*-expressing cells at 2dpf. (D) Quantification of the thyroid volume (μm^3) in Std_Ctrl, *glis3*MO_SPL and *glis3*_mRNA 200pg/e injected embryos. The bars indicate the average of the total thyroid volume of 10 embryos per group. (E-G) T4 whole-mount antibody staining in larvae at 5dpf. Distinct follicles were visible in a row along the anterior-posterior axis, at the pharyngeal midline. (H) Count of the number of T4-producing follicles in Std_Ctrl, *glis3*MO_SPL and *glis3*_mRNA injected larvae. Embryos were all flat mounted, in ventral view, with anterior to the left. Scale bar: 100 μm . Asterisks indicate statistically significant differences (Mann-Whitney test; ***, $P < 0.001$).

VIII. GLIS3 ACTS AS AN EFFECTOR OF THE SONIC-HEDGEHOG PATHWAY

Several findings support the idea that *glis3* is one of the transcription factors belonging to the Sonic-Hedgehog (SHH) signalling: **i)** the members of GLI-family are reported to be the main effectors of the SHH pathway [50]; **ii)** the stability of the GLIS3 is regulated by the binding with the Suppressor of Fused (SUFU), a negative regulator of SHH [71]; **iii)** SHH is known to be an important regulator of endoderm specification and thyroid development [52].

To study the relationship between *glis3* and *Shh*, we first analysed the expression of *shha* in *glis3* morphants by WISH. When compared with controls at 2dpf (Figure 25A-A'), the 100% of *glis3* morphants injected 0.3pmol/e and 0.5pmol/e, presented a significant reduction of *shha* expression in the pharyngeal endoderm (Figure 25B-B'). Interestingly, the *shha* signal appeared upregulated in the hypothalamus and nervous system of morphants (Figure 25B-B').

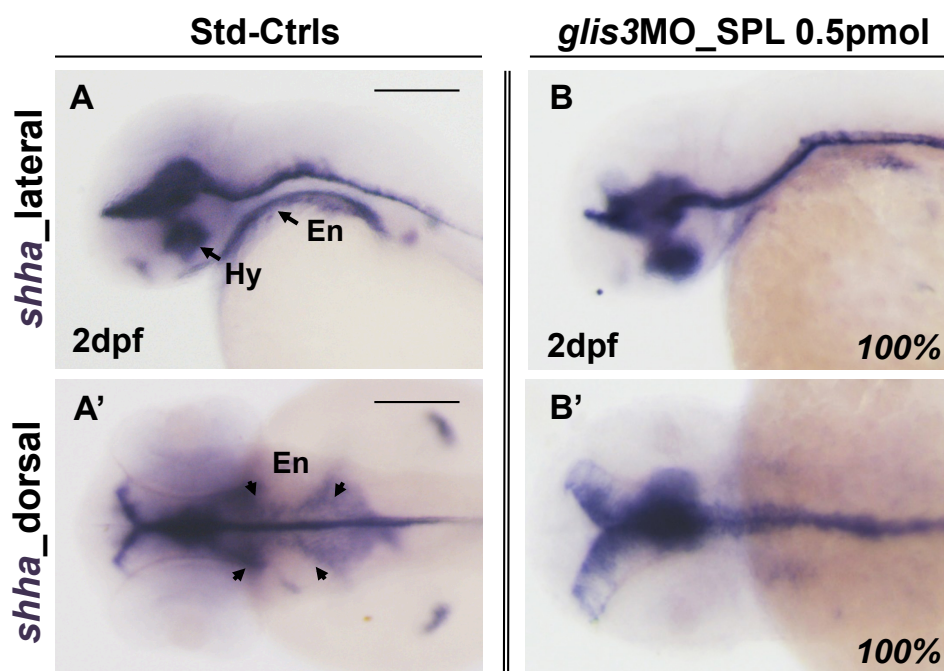


Figure 25. Expression of *shha* in the *glis3* morphants. (A-B) WISH of *shha* expression in embryos injected with Std-ctrl (A-A') and *glis3*MO_SPL at 0.5pmol/e (B-B'). Each experiment was performed in triplicate, using 40 embryos per MO injected. Embryos were acquired in lateral (A, B) and dorsal (A'-B') views, anterior to the left. Scale bar: 250 μ m. En: endoderm; Hy: hypothalamus.

To further confirm this association, we blocked the Shh signalling by the microinjection of a morpholino against *shha* [94] and by the treatment with the Shh antagonist cyclopamine and we analysed the expression of *glis3*. Cyclopamine is a pharmacological inhibitor of the Shh receptor smoothed (SMO), that through its binding to the receptor SMO is able to block the downstream Shh signal [95, 96].

When compared with controls at 1 and 2dpf (Figure 26A and C), the injection of *shha*_MO (1.25pmol/e) abolished the expression of the *glis3* in brain and in the pharyngeal endoderm (Figure 26B and D). Similar results were obtained by the treatment with 10µM of cyclopamine (Figure 26E-H).

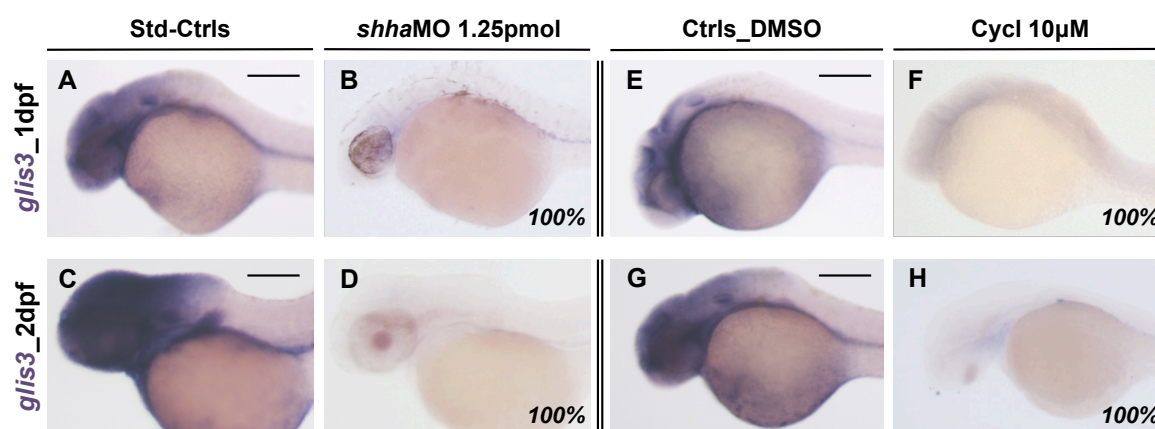


Figure 26. Analysis of *glis3* expression in *shha*-deficient embryos. (A-H) WISH of *glis3* expression at 1 and 2dpf. (B-D) The *glis3* expression is absent, at the endoderm level, in the embryos injected with *shha*_MO at 1.25 pmol/e. (F-H) The treatment with Cyclopamine 10µM abolish the *glis3* expression, compared with DMSO controls (E-G). Each experiment was performed in triplicate, using 40 embryos per each experiment. Embryos were acquired in lateral view, anterior to the left. Scale bar: 250µm.

A. *Shh* and zebrafish thyroid development

To test whether SHH signalling plays a role in thyroid development, we blocked the SHH pathway by Cyclopamine and analysed the expression of thyroid markers by WISH (Figure 27).

At 1dpf, both *nkx2.4* and *pax2a* signals were absent at the level of thyroid primordium in the 100% of the cyclopamine-treated embryos (Figure 27A-D). At 2 and 3dpf, the *tg* expression was reduced in 68% or absent in 32% of treated-embryos (Figure 27E-K).

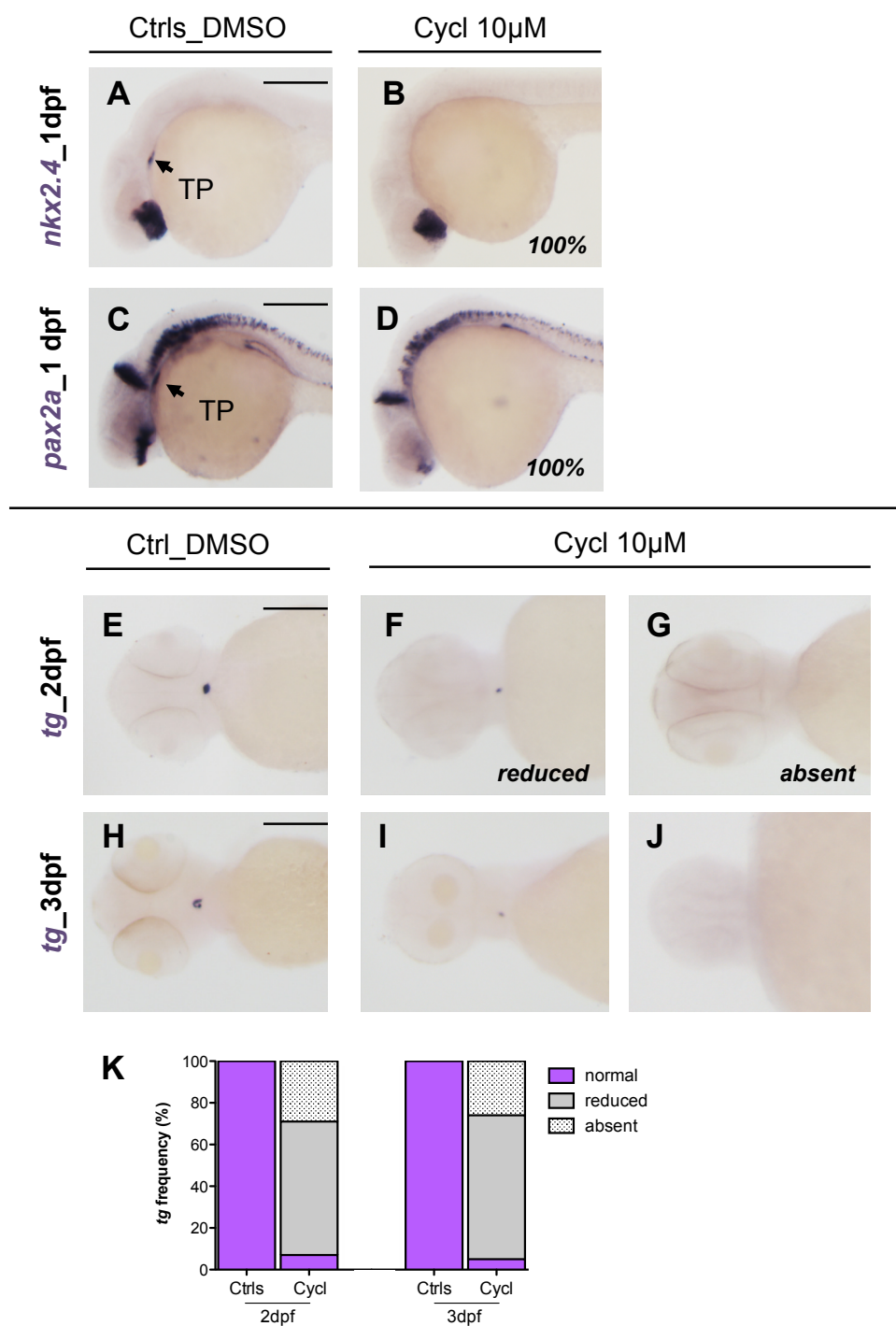


Figure 27. Analysis of thyroid gland development in Cyclopamine treated embryos. (A-D) WISH of *nkx2.4* and *pax2a* expression at 1dpf in control embryos (DMSO1%) and treated with Cyclopamine 10μM. **(E-J)** WISH of *tg* expression at 2 and 3dpf in control embryos (DMSO1%) and treated with Cyclopamine 10μM. The embryos were subdivided as normal, reduced or absent *tg* signal. The frequency of the embryos belonging each phenotypic class is reported in the histogram **K**. Each experiment was performed in triplicate, using 40 embryos per treatment. Embryos were acquired in lateral **(A-D)** and ventral **(E-J)** views, anterior to the left. Scale bar: 250μm. TP: thyroid primordium.

B. *Shh* and *glis3* overexpression

To further investigate the role of Shh-*glis3* pathway in thyroid development, we first analysed the expression of *shha* in *glis3*-overexpressing embryos. At 2dpf, no alterations of the *shha* signal at the level of the pharyngeal endoderm and nervous system have been observed in these conditions (Figure 28A-D). However, the overexpression of *glis3* resulted in an excess of *tg*-expressing cells (see Section 7). When compared with controls (Figure 28E), the treatment with cyclopamine was able to abolish the expression of *tg* even in the *glis3*-overexpressing embryos (Figure 28H), similarly to what happened in fish with normal *glis3* expression (Figure 28F).

These results suggest that *glis3* acts downstream the SHH pathway, likely controlling the specification of the endoderm precursors committed to the thyroid fate, and that Shh is necessary for *glis3* activity.

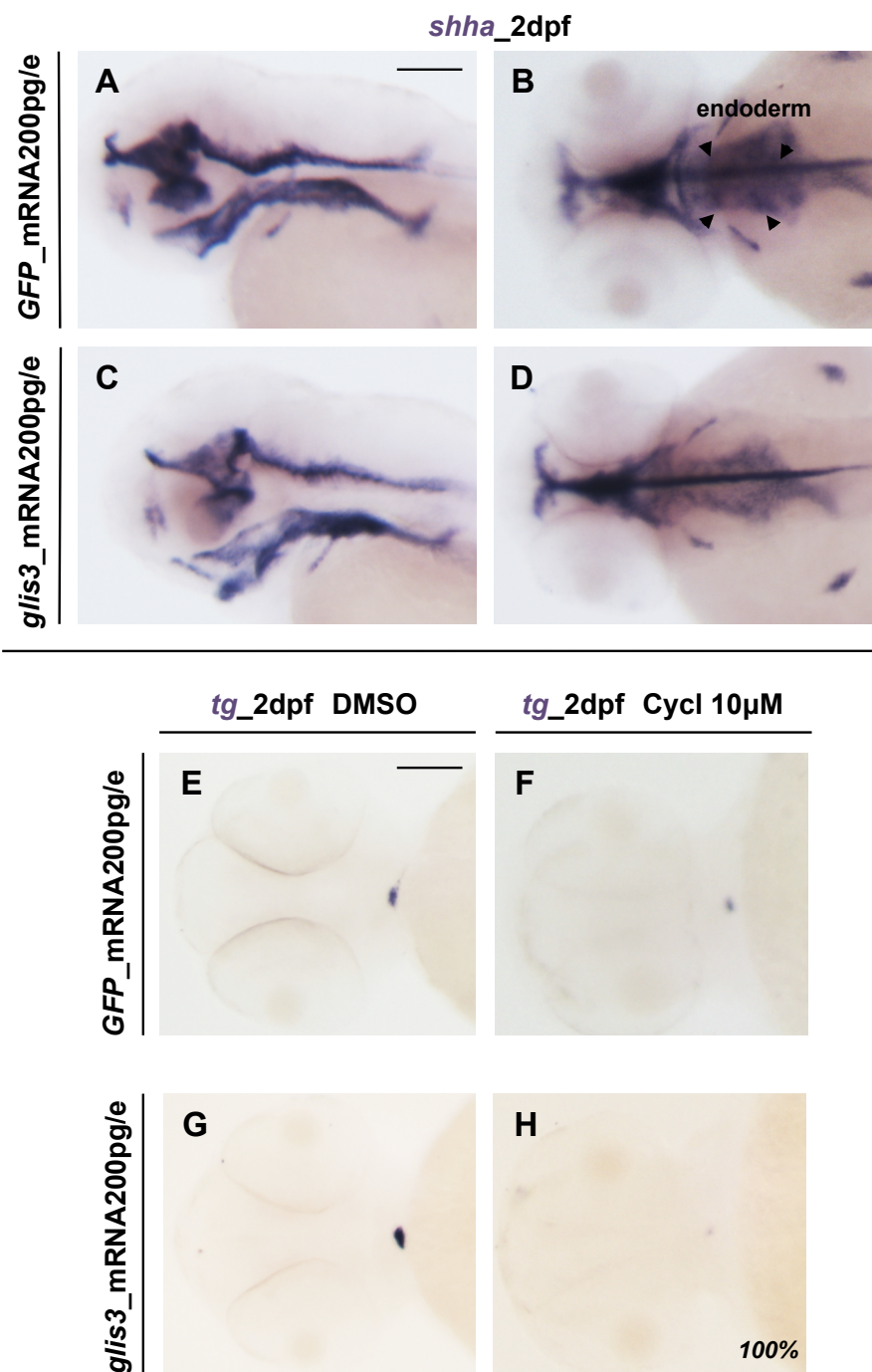


Figure 28. Analysis of *shha* in *glis3* overexpressing embryos. (A-D) WISH of *shha* expression in embryos injected with GFP mRNA 200pg (Ctrl) and *glis3* mRNA WT 200pg/e at 2dpf. No differences are detectable between Ctrl and *glis3* overexpressing embryos. (E-H) WISH of *tg* expression, at 2dpf, in embryos injected with 200pg of GFP and *glis3* WT mRNAs, followed with treatment with DMSO1% and Cyclopamine 10μM. The cyclopamine treatment abolishes the expression of *tg* in the *glis3*-overexpressing embryos (H). Each experiment was performed in triplicate, using 40 embryos for each experiment. Embryos were acquired in lateral (A, C), dorsal (B, D) and ventral (E-H) views, anterior to the left. Scale bar: 250μm.

C. In vitro analysis of *glis3* and *sufu* cellular localization

Given the findings that demonstrated the importance of the interaction between Sufu and Glis3 for its cellular localization and transcriptional activity [71], we also wondered if this mechanism is conserved also in zebrafish.

COS7 cells were co-transfected with plasmids that contained the entire coding sequences of zebrafish *sufu* and *glis3*. As reported in Figure 29, *glis3* co-localized with *sufu* into the nucleus of transfected cells, whereas a fraction of *sufu* is detectable into the cytoplasm.

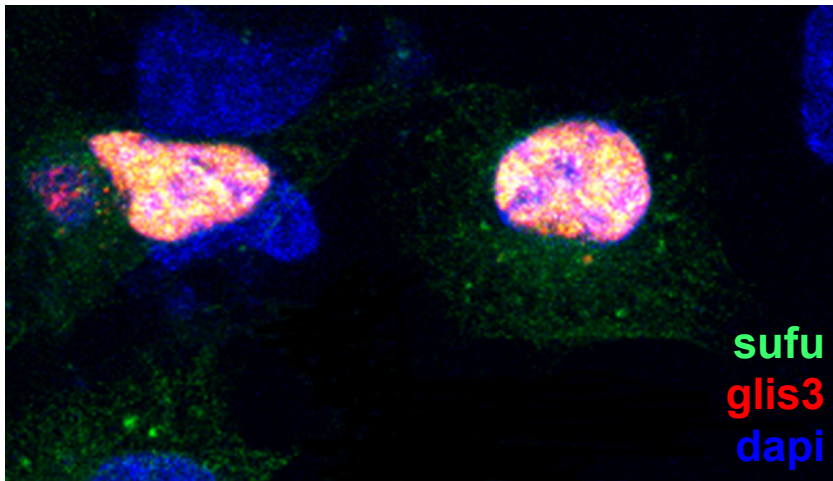


Figure 29. Immunolocalization of zebrafish *sufu* and *glis3* in COS7 cells. pEGFP_ *sufu* is visible in green whereas the pcDNA4/His-Myc_A_ *glis3* was incubated with secondary antibody Alexa Fluor 555 and is visible in red. Dapi (in blue) marks the nucleus of cells. The experiment was performed in triplicate.

IX. ANALYSIS OF POSSIBLE *GLIS3*-NOTCH PATHWAY INTERACTION

Several findings, previously obtained in our Lab, demonstrated that Notch signaling is important for the correct thyroid development and function [47]. Differently, TAZ (transcriptional co-activator with PDZ-binding motif), also referred as *Wwtr1*, acts as a potent regulator of Pax8 and Nkx2, suggesting that TAZ within the hippo pathway may play a role in the control of the thyroid gland development [99]. It was also shown that both *Glis3* and *Wwtr1* contribute to renal function [77]. Since *wwtr1* is known to

interact with the Notch signaling for the determination of cell fate in the zebrafish pronephric duct [100], we hypothesized a possible interaction between *glis3* and *wwtr1* during thyroid development. For these reasons we decided to investigate the possible *glis3* interactions with both Notch pathways and *wwtr1* in the zebrafish thyroid development.

Firstly, we decided to analyse by WISH the *glis3* expression after down-regulation of the Notch signaling through the treatment with DAPT, an inhibitor of the Notch signaling, and through the injection of both MO against *jag1a* and *jag1b* [47]. *Jag1a* and *jag1b* are the ligands of the Notch receptors; it has been demonstrated that, in zebrafish, the knockdown of both genes results in thyroid hypoplasia and TSH elevated levels [47].

At 24hpf, the *glis3* expression in the embryos treated with DAPT 100 μ M [47] (Figure 30A-B) was unaffected.

The same result was obtained by in the *jag1a* + *jag1b* morphants, in which *glis3* signal remained unchanged, compared to control embryos (Figure 30C-D).

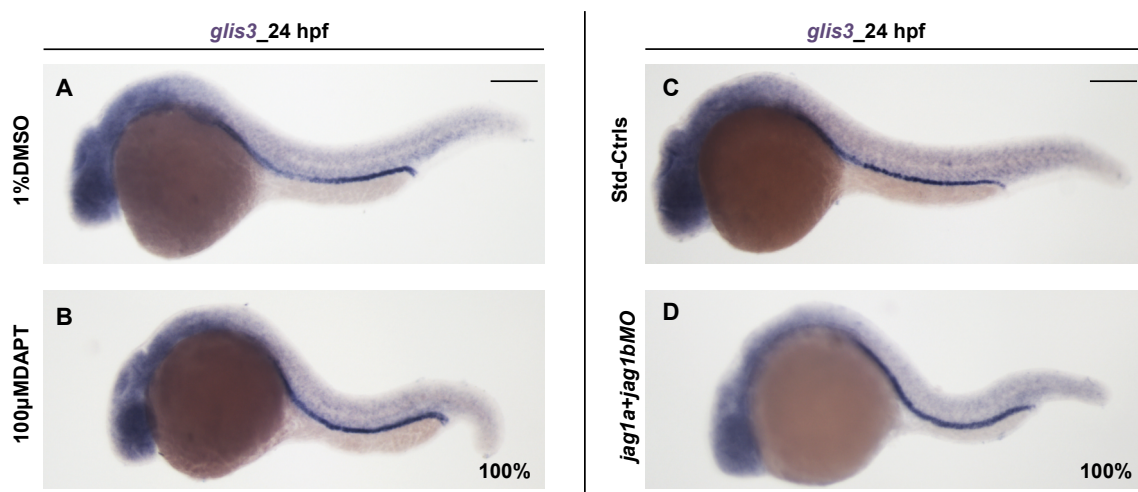


Figure 30. Analysis of the possible *glis3*-Notch pathway interaction. (A-B) WISH of *glis3* expression in embryos treated with 1%DMSO and 100 μ M DAPT, at 24hpf. No alterations in *glis3* signal are observed compared to controls. **(C-D)** WISH of *glis3* expression in embryos injected with Std_CtrlMO and *jag1a*MO+*jag1b*MO at 24hpf. The *glis3* expression in the *jag1*-morphants is maintained. Each experiment was performed in triplicate, using 40 embryos per each experiment. Embryos were acquired in lateral view, anterior to the left. Scale bar: 250 μ m.

Then, we analysed the *wwtr1* expression in the *glis3*MO_SPL injected embryos at 0.5 pmol/e and no differences were observed in the *wwtr1* signal in the *glis3*-morphants at both 26 and 48hpf (Figure 31).

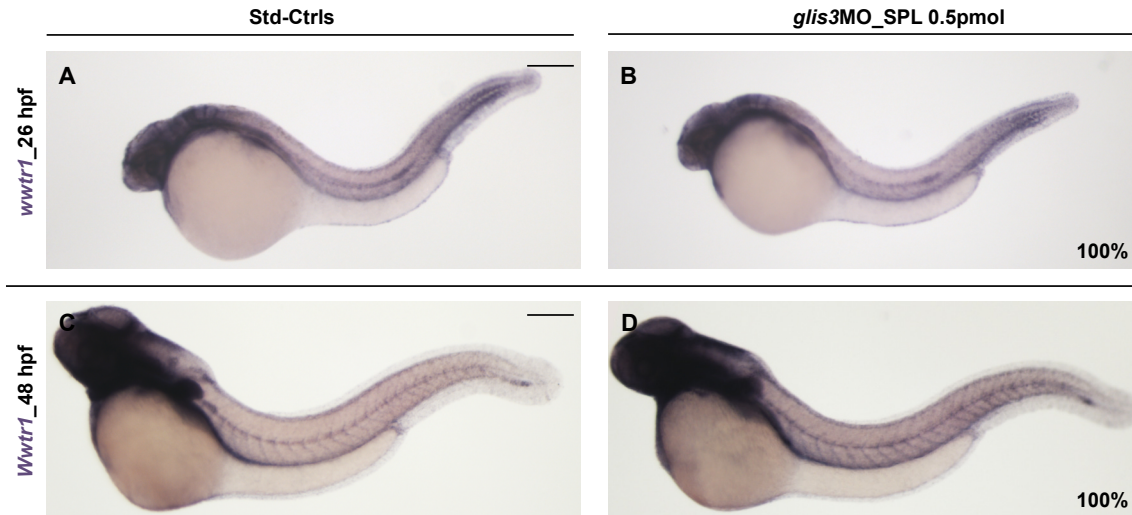


Figure 31. Analysis of *wwtr1* in *glis3*-morphants. (A-D) WISH of *wwtr1* expression in embryos injected with Std_CtrlMO and *glis3*MO_SPL at 0.5pmol/e at 26 (A-B) and 48hpf (C-D). The *wwtr1* expression in the *glis3*-morphants was unaffected. Each experiment was performed in triplicate, using 40 embryos per each experiment. Embryos were acquired in lateral view, anterior to the left. Scale bar: 250 μ m.

Taken together, these results indicated that *glis3*-Shh and jagged-Notch and *wwtr1*-Hippo pathways act in an independent manner during the early phases of the zebrafish thyroid formation.

DISCUSSION

Although a clear phenotype/genotype correlation has not been observed in CH, several factors, including type and site of mutation, should be taken in consideration [79]. Hence, there is an urgent need to improve our understanding in the pathophysiology underlying GLIS3 action, specially to determine whether *GLIS3* acts upstream of genes involved in pathways regulating thyroid development, hormonogenesis, and the peripheral response to T4.

To better characterize the role of *GLIS3* in the CH pathogenesis and to overcome the limits of the KO mouse model, we decided to take advantage of the zebrafish model to deeply investigate the *glis3* role in particularly during the thyroid gland development and function. Zebrafish is widely used in thyroid research thanks to the easy genetic manipulation, the rapid development and the high conservation of the pathways involved in thyroid morphogenesis [13, 17, 20].

Although the knockdown of *glis3* has been previously associated with pancreatic and renal dysfunction in zebrafish [61, 90, 93], few data are available in literature regarding its expression and activity. Therefore, we first analysed *in silico* the protein structure of the zebrafish *glis3* in comparison with the mammalian orthologues. Despite the low conservation between the zebrafish and human or mouse *GLIS3* proteins, we observe high identity in the zinc-finger functional domain, suggesting that the molecular mechanism of the transcription factor can be evolutionary conserved.

The analyses of the temporal and tissue-specific expression indicate that *glis3* is detectable at higher levels from 1dpf onwards in brain, pronephric ducts, and in pouches and medial region of pharyngeal endoderm, emphasizing its possible involvement during the specification of the endoderm-derived organs, like thyroid and pancreas. Of note, no *glis3* expression is observed in the differentiated thyroid at 2dpf [97].

In adults, *glis3* is still present in pancreas, kidney, and pituitary, and at low levels in brain and gonads, suggesting a post-natal activity in the regulation of some organ functions. Given the lack of a compact thyroid gland in adult zebrafish, it was not possible to dissect the single follicles for the analysis. However, further experiments are needed to get through this limitation.

To gain insights into *glis3* function, we analysed the progression of embryonic thyroid development after the knockdown of *glis3* mRNA expression using specific antisense morpholino oligonucleotide.

At 1dpf, when the thyroid precursors arise from the pharyngeal floor of the endoderm, the *glis3* morphants displayed a significant reduction or absent expression of the transcription factors *nkx2.4* and *pax2a* in the thyroid primordium. At this point, we wondered if the thyroid phenotype associated with *glis3* KD results from an increased apoptosis or decreased proliferations of thyroid precursors, as well as from a global alteration of the endoderm. Since no changes in proliferation/apoptosis rates and in *foxa2* expression were detected in *glis3* morphants when compared with controls, we can conclude that *glis3* is early involved in endoderm specification, likely regulating the number of endodermal cells committed to thyroid fate. These data are in contrast with what seen during the early phases of thyroid development that appeared almost uneventful in *Glis3*-KO mice, but are consistent with the previously demonstrated bimodal action of GLIS3 during pancreatic development and function and with the thyroid morphogenetic defect seen in patients with homozygous mutations and complete *GLIS3* loss-of-function.

We also detected a defective amount of thyroid precursors at later stages, in which the expression of *tg* and *slc5a5* is reduced or absent in most of the analysed embryos. The role of Glis3 in controlling *Slc5a5* expression was previously reported in mice. RNA-seq and CHIP-seq analyses of mice thyroid tissue confirm that Glis3 interacts and enhance the expression of *Nis*, directly regulating the synthesis of TH. In fact, *Nis* is suppressed in the thyroid gland of the *Glis3*-KO mice [79]. The specificity of the defects in thyroid development observed in morphants is also confirmed by the rescue experiment. The co-injection of the wild type form of the zebrafish *glis3* mRNA and the *glis3*MO_SPL is able to restore the proper thyroid specification and normalizes the expression of both early and late thyroid markers. More interestingly, the

overexpression of the *glis3* mRNA is sufficient to increase the number of the thyroid precursors at 1dpf, thus leading to the differentiation of a larger thyroid tissue and an elevation of T4 levels at later stages.

Taken together, we propose *glis3* as a key regulator of thyroid development and, in particular, in the specification of thyroid precursor cells, acting upstream the transcription factors *nkx2.4* and *pax2a*. The defective thyroid tissue associated with low T4 synthesis and the high *tshba* levels observed in *glis3* knockdown embryos resemble the biochemical features and thyroid dysgenesis reported in patients carrying biallelic mutations leading to a complete *GLIS3* loss-of-function. Interestingly and consistently with our proposal of an early action of GLIS3 during thyroid specification, another group previously reported the existence of GLIS3-binding-sites in *PAX8* promoter (10). The molecular mechanisms involved in Glis3 action have been extensively investigated during pancreas development, to gain insight into its role in diabetes. Three groups independently generated *Glis3*-deficient mice models and identified *Ngn3*, *Insulin* and *Ccnd2* as direct downstream targets of Glis3 in the pancreatic progenitors and β -cells [74, 82, 84, 101]. The *Glis3*^{-/-} mice display decreased expression of *Ngn3* in the embryonic pancreas resulting in reduced differentiation of β -cells and severe hyperglycaemia and ketoacidosis in littermates [74, 83]. *In vitro* experiments demonstrate that Glis3 binds the endocrine lineage-defining transcription factors *Hnf6* and *Foxa2* and the promoter/enhancer of *Ngn3*, synergistically transactivating its transcription [83].

Given the *Glis3* dual role in pancreas organogenesis and in regulation of insulin secretion and sensitivity, we propose the conservation of these two distinct physiological mechanisms also in thyroid. In fact, our zebrafish model supports the early involvement of *glis3* during the specification of thyroid precursor, whereas the murine KO model [79] recapitulate the involvement of Glis3 controlling the TH synthesis and follicle proliferation in response to HPT-axis activation.

In the last decade most of the thyroid research is engaged in the identification of those signals that induced the endodermal cells to a thyroid fate. Recently, Antonica *et al.*, for the first time, generate a functional thyroid from embryonic stem cells [102]. In this work it has been demonstrated that, in presence of doxycycline (Dox) and rhTSH in the medium, the overexpression of the transcription factors *NKX2.1* and *PAX8* is sufficient

to differentiate mouse embryonic stem cells (mESC) into thyroid follicular cells which organized in a functioning follicle structure. Importantly, when these follicles are grafted into athyreoid mice they are able to recovery thyroid hormone plasma levels [102]. Conversely, the mice transplanted with cells differentiated without Dox and rhTSH treatment remained hypothyroid, highlighting the need for more information regarding the signals that are required for the correct differentiation of thyroid precursors [102].

As far as we know, the Notch, Shh, and Bmp/Fgf pathways are reported to be involved in the commitment of the endocrine precursors [34, 45, 47, 49, 52, 54]. The SHH pathway is known to be a regulator of the endoderm specification and thyroid development [54]. In our work, we investigate, for the first time, the role of the *glis3*-*shh* pathway during the development of thyroid primordium. Our data strongly suggest that *glis3* acts within the Shh pathway during this early developmental window.

We observed that the expression of the *shha* in *glis3* morphants is significantly reduced in the pharyngeal endoderm. When we blocked the Shh signalling, by injection of a specific *shha* morpholino or by treatment with the Shh-antagonist Cyclopamine, we detected an absent *glis3* expression in the pharyngeal endoderm, pointing to a potential cross-talk mechanism between *glis3* and Shh pathway in the endoderm. In addition, in Cyclopamine-treated embryos, we observed a lack of thyroid primordium as shown by the absent expression of both *nkx2.4* and *pax2a* at 1dpf. At 2 and 3dpf, the tg-expressing follicles are also strongly reduced or absent in the treated embryos, confirming that *glis3* acts downstream the Shh pathway during thyroid development.

Interestingly, the overexpression of *glis3* mRNA in Cyclopamine-treated embryos (in which Shh pathway is off) fails to rescue these thyroid defects, suggesting that *glis3* may require an active Shh signals for its transactivation activity.

Although the specific molecular mechanisms are far from being understood, by similarity with the GLI-proteins, GLIS3 may act downstream the SHH signals, controlling the expression of several targets, like the *Ins2* gene. It has been demonstrated that the binding of GLIS3 with the Suppressor of Fused (SUFU), a negative regulator of SHH signalling, is important for GLIS3 stability and activity [71]. In the absence of SHH, SUFU anchors GLIS3 in the cytoplasm and prevents its interaction with the ubiquitin ligase CUL3 and ITCH, thus protecting GLIS3 from

proteasome degradation [69]. The GLIS3-SUFU complex is also able to translocate into the nucleus, where it suppresses the transcription of some target genes, such as *Ins2*. Conversely, when SHH is on, GLIS3 is released and forms a nuclear complex with coactivators, inducing the expression of *Ins2* [67].

Our preliminary data obtained *in vitro* by immunocytochemistry revealed that, like mice, the zebrafish *sufu* and *glis3* proteins co-localized into the nucleus of the transfected cells. Hence, we can speculate that similarly to those observed with the insulin gene, *glis3* through the interaction (direct or indirect) with *sufu*, is involved in the activation of specific early thyroid genes. In our proposed model, in the absence of the Shh signal, *glis3* is maintained inactive by the binding with co-repressors, such as *sufu*. This complex represses the transcription of the early thyroid genes, maintaining the endodermal cell in the undifferentiated state (Figure 32A). In the presence of Shh, the *sufu* localization is restricted to the cytoplasm, and *glis3* is able to translocate into the nucleus and forms a multi-protein complex that activates the transcription of target genes, like *nkx2.4* and *pax2a*. As a result through the activation of Shh-*glis3* signal the undifferentiated endodermal cell is committed to the thyroid fate (Figure 32B).

In the last part of this work, we wondered if Shh-*glis3* signalling interacts with other pathways, such as Notch/Jag1 and Hippo/Wwtr1 during zebrafish thyroid development. Notch is a highly conserved, local cell-signalling mechanism that participates in a variety of cellular processes and is involved in many aspects of development and disease. Several findings demonstrate that also the Notch signalling is important for the correct thyroid specification [47]. In fact, perturbations of the Notch signalling are associated with increased (Notch silencing) or diminished (Notch over-activation) number of thyroid precursors committed to the thyroid fate [49]. Furthermore, the knockdown of both ligands of the notch receptor, *jag1a* and *jag1b*, leads to thyroid hypoplasia and TSH elevated levels in zebrafish embryos [47].

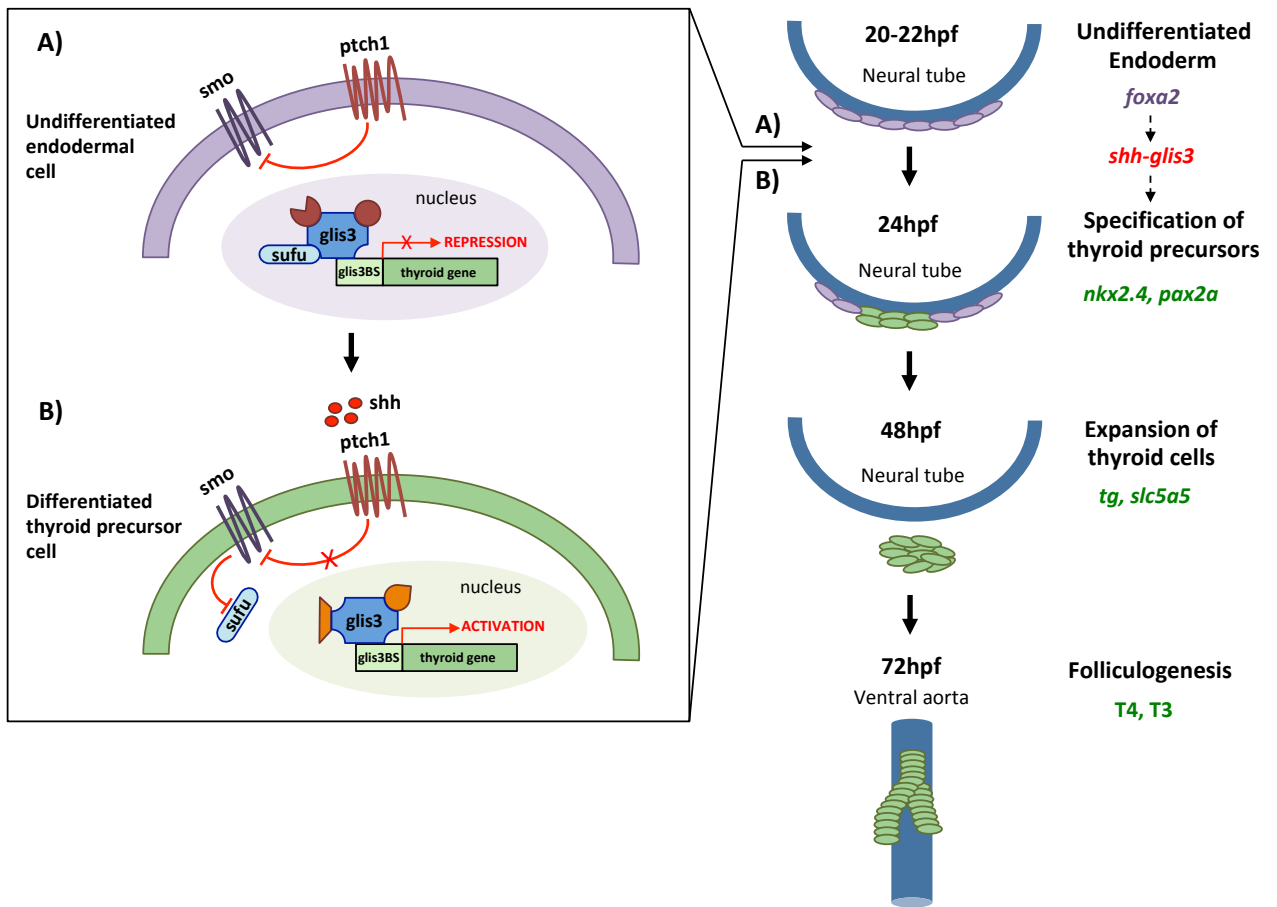


Figure 32. Proposed mechanism of *glis3*-SHH signaling during zebrafish thyroid development. In the right part of the figure we described the different phases of the thyroid development. The genetic markers involved in each step are reported. In the left box we illustrate the activity of *glis3* in the presence or absence of Shh signal. **(A)** Undifferentiated endodermal cell in which Shh is off and *glis3* is maintained inactive by *sufu*. **(B)** Differentiated thyroid precursor cell in which Shh is on, *sufu* is blocked by *smo* and *glis3* form a transcriptional complex that induce the expression of the early thyroid genes.

Regarding the Hippo pathway, it has been described that the transcriptional co-activator TAZ, also referred as Wwtr1, acts during the thyroid development [69, 75]. The Hippo pathway plays a role in the regulation of many biological functions, including cell migration, differentiation, proliferation, and cell polarity. *In vitro* experiments demonstrate that Wwtr1 is able to bind the C-terminus of Glis3 and function as co-activator of Glis3 activity [61, 74]. In zebrafish *wwtr1* gene is expressed in thyroid primordium; the analysis of the *wwtr1* morphants reveal significant reduction of the number of thyroid follicle cells and also the lumen of follicles appear smaller compared

to control embryos [90]. It is also known that *Wwtr1* is a potent regulator of *Pax8* and *Nkx2.1* controlling the thyroid gland development and differentiation [99]. Furthermore, it has been described that *wwtr1* interacts with the Notch signalling for the regulation of cell-fate decision during zebrafish kidney development [100].

Our results exclude a direct interaction and the mutual regulation between Shh-gl_{is}3 and Notch and Hippo pathways.

In conclusion, we demonstrate the key role of gl_{is}3 during the zebrafish thyroid development. The whole of these data suggests Glis3 as an element, acting within the Shh pathway, that is required for the thyroid commitment of the endoderm precursors through a direct or indirect regulation of the expression of specific transcription factors, such as *nkx2.1*, *pax2a* (Figure 32).

Since biallelic GLIS3 mutations are associated with thyroid dysgenesis, we believe these data contribute to increase our understanding on the genetic bases of CH in humans.

However the limitation of the morpholino injection hampers us to follow the progression of the CH. For that reason, we are now generating a stable *glis3* mutant line using the CRISPR/Cas9 technology. The availability of juvenile and adult mutants will let a deep comprehension of the *glis3* contribution to the thyroid hormone synthesis and the follicle proliferation in response to activation of the HPT-axis. Finally, this mutant model will be suitable for a high-throughput drug-screening, providing a new potential therapeutical approach, for NDH and CH pathologies.

BIBLIOGRAPHY

1. Maenhaut, C., et al., *Ontogeny, Anatomy, Metabolism and Physiology of the Thyroid*, in *Endotext*, L.J. De Groot, et al., Editors. 2000: South Dartmouth (MA).
2. Nilsson, M. and H. Fagman, *Development of the thyroid gland*. *Development*, 2017. **144**(12): p. 2123-2140.
3. Williams, G.R. and J.H. Bassett, *Deiodinases: the balance of thyroid hormone: local control of thyroid hormone action: role of type 2 deiodinase*. *J Endocrinol*, 2011. **209**(3): p. 261-72.
4. Cheng, S.Y., J.L. Leonard, and P.J. Davis, *Molecular aspects of thyroid hormone actions*. *Endocr Rev*, 2010. **31**(2): p. 139-70.
5. Brent, G.A., *The molecular basis of thyroid hormone action*. *N Engl J Med*, 1994. **331**(13): p. 847-53.
6. Oetting, A. and P.M. Yen, *New insights into thyroid hormone action*. *Best Pract Res Clin Endocrinol Metab*, 2007. **21**(2): p. 193-208.
7. Zhang, J. and M.A. Lazar, *The mechanism of action of thyroid hormones*. *Annu Rev Physiol*, 2000. **62**: p. 439-66.
8. Chiamolera, M.I. and F.E. Wondisford, *Minireview: Thyrotropin-releasing hormone and the thyroid hormone feedback mechanism*. *Endocrinology*, 2009. **150**(3): p. 1091-6.
9. Bianco, A.C., *Minireview: cracking the metabolic code for thyroid hormone signaling*. *Endocrinology*, 2011. **152**(9): p. 3306-11.
10. Szinnai, G., et al., *Sodium/iodide symporter (NIS) gene expression is the limiting step for the onset of thyroid function in the human fetus*. *J Clin Endocrinol Metab*, 2007. **92**(1): p. 70-6.
11. Wendl, T., et al., *Pax2.1 is required for the development of thyroid follicles in zebrafish*. *Development*, 2002. **129**(15): p. 3751-60.
12. Heijlen, M., A.M. Houbrechts, and V.M. Darras, *Zebrafish as a model to study peripheral thyroid hormone metabolism in vertebrate development*. *Gen Comp Endocrinol*, 2013. **188**: p. 289-96.
13. Marelli, F. and L. Persani, *How zebrafish research has helped in understanding thyroid diseases*. *F1000Res*, 2017. **6**: p. 2137.

14. Opitz, R., F. Antonica, and S. Costagliola, *New model systems to illuminate thyroid organogenesis. Part I: an update on the zebrafish toolbox*. Eur Thyroid J, 2013. **2**(4): p. 229-42.
15. Opitz, R., et al., *Transgenic zebrafish illuminate the dynamics of thyroid morphogenesis and its relationship to cardiovascular development*. Dev Biol, 2012. **372**(2): p. 203-16.
16. Fagman, H., et al., *Gene expression profiling at early organogenesis reveals both common and diverse mechanisms in foregut patterning*. Dev Biol, 2011. **359**(2): p. 163-75.
17. Fagman, H. and M. Nilsson, *Morphogenetics of early thyroid development*. J Mol Endocrinol, 2011. **46**(1): p. R33-42.
18. Parlato, R., et al., *An integrated regulatory network controlling survival and migration in thyroid organogenesis*. Dev Biol, 2004. **276**(2): p. 464-75.
19. Lazzaro, D., et al., *The transcription factor TTF-1 is expressed at the onset of thyroid and lung morphogenesis and in restricted regions of the foetal brain*. Development, 1991. **113**(4): p. 1093-104.
20. De Felice, M. and R. Di Lauro, *Thyroid development and its disorders: genetics and molecular mechanisms*. Endocr Rev, 2004. **25**(5): p. 722-46.
21. Kimura, S., J.M. Ward, and P. Minoo, *Thyroid-specific enhancer-binding protein/thyroid transcription factor 1 is not required for the initial specification of the thyroid and lung primordia*. Biochimie, 1999. **81**(4): p. 321-7.
22. Trubiroha, A., et al., *A Rapid CRISPR/Cas-based Mutagenesis Assay in Zebrafish for Identification of Genes Involved in Thyroid Morphogenesis and Function*. Sci Rep, 2018. **8**(1): p. 5647.
23. Friedrichsen, S., et al., *Expression of pituitary hormones in the Pax8^{-/-} mouse model of congenital hypothyroidism*. Endocrinology, 2004. **145**(3): p. 1276-83.
24. Pasca di Magliano, M., R. Di Lauro, and M. Zannini, *Pax8 has a key role in thyroid cell differentiation*. Proc Natl Acad Sci U S A, 2000. **97**(24): p. 13144-9.
25. Mansouri, A., K. Chowdhury, and P. Gruss, *Follicular cells of the thyroid gland require Pax8 gene function*. Nat Genet, 1998. **19**(1): p. 87-90.
26. Porreca, I., et al., *Zebrafish bcl2l is a survival factor in thyroid development*. Dev Biol, 2012. **366**(2): p. 142-52.
27. Bort, R., et al., *Hex homeobox gene-dependent tissue positioning is required for organogenesis of the ventral pancreas*. Development, 2004. **131**(4): p. 797-806.
28. Bort, R., et al., *Hex homeobox gene controls the transition of the endoderm to a pseudostratified, cell emergent epithelium for liver bud development*. Dev Biol, 2006. **290**(1): p. 44-56.
29. Civitareale, D., et al., *A thyroid-specific nuclear protein essential for tissue-specific expression of the thyroglobulin promoter*. EMBO J, 1989. **8**(9): p. 2537-42.
30. De Felice, M., et al., *A mouse model for hereditary thyroid dysgenesis and cleft palate*. Nat Genet, 1998. **19**(4): p. 395-8.
31. Nakada, C., et al., *Forkhead transcription factor foxe1 regulates chondrogenesis in zebrafish*. J Exp Zool B Mol Dev Evol, 2009. **312**(8): p. 827-40.
32. Gualdi, R., et al., *Hepatic specification of the gut endoderm in vitro: cell signaling and transcriptional control*. Genes Dev, 1996. **10**(13): p. 1670-82.
33. Jung, J., et al., *Initiation of mammalian liver development from endoderm by fibroblast growth factors*. Science, 1999. **284**(5422): p. 1998-2003.

34. Kumar, M., et al., *Signals from lateral plate mesoderm instruct endoderm toward a pancreatic fate*. Dev Biol, 2003. **259**(1): p. 109-22.
35. Manfroid, I., et al., *Reciprocal endoderm-mesoderm interactions mediated by fgf24 and fgf10 govern pancreas development*. Development, 2007. **134**(22): p. 4011-21.
36. Serls, A.E., et al., *Different thresholds of fibroblast growth factors pattern the ventral foregut into liver and lung*. Development, 2005. **132**(1): p. 35-47.
37. Fernandez, L.P., A. Lopez-Marquez, and P. Santisteban, *Thyroid transcription factors in development, differentiation and disease*. Nat Rev Endocrinol, 2015. **11**(1): p. 29-42.
38. Feldman, B., et al., *Zebrafish organizer development and germ-layer formation require nodal-related signals*. Nature, 1998. **395**(6698): p. 181-5.
39. Zhou, X., et al., *Nodal is a novel TGF-beta-like gene expressed in the mouse node during gastrulation*. Nature, 1993. **361**(6412): p. 543-7.
40. Whitman, M., *Nodal signaling in early vertebrate embryos: themes and variations*. Dev Cell, 2001. **1**(5): p. 605-17.
41. Alexander, J., et al., *casanova plays an early and essential role in endoderm formation in zebrafish*. Dev Biol, 1999. **215**(2): p. 343-57.
42. Elsalini, O.A., et al., *Zebrafish hhex, nk2.1a, and pax2.1 regulate thyroid growth and differentiation downstream of Nodal-dependent transcription factors*. Dev Biol, 2003. **263**(1): p. 67-80.
43. Kikuchi, Y., et al., *The zebrafish bonnie and clyde gene encodes a Mix family homeodomain protein that regulates the generation of endodermal precursors*. Genes Dev, 2000. **14**(10): p. 1279-89.
44. Reiter, J.F., Y. Kikuchi, and D.Y. Stainier, *Multiple roles for Gata5 in zebrafish endoderm formation*. Development, 2001. **128**(1): p. 125-35.
45. Artavanis-Tsakonas, S., M.D. Rand, and R.J. Lake, *Notch signaling: cell fate control and signal integration in development*. Science, 1999. **284**(5415): p. 770-6.
46. Lai, E.C., *Notch signaling: control of cell communication and cell fate*. Development, 2004. **131**(5): p. 965-73.
47. Porazzi, P., et al., *Disruptions of global and JAGGED1-mediated notch signaling affect thyroid morphogenesis in the zebrafish*. Endocrinology, 2012. **153**(11): p. 5645-58.
48. Piccoli, D.A. and N.B. Spinner, *Alagille syndrome and the Jagged1 gene*. Semin Liver Dis, 2001. **21**(4): p. 525-34.
49. de Filippis, T., et al., *JAG1 Loss-Of-Function Variations as a Novel Predisposing Event in the Pathogenesis of Congenital Thyroid Defects*. J Clin Endocrinol Metab, 2016. **101**(3): p. 861-70.
50. Tsukui, T., et al., *Multiple left-right asymmetry defects in Shh(-/-) mutant mice unveil a convergence of the shh and retinoic acid pathways in the control of Lefty-1*. Proc Natl Acad Sci U S A, 1999. **96**(20): p. 11376-81.
51. Muzza, M., et al., *Absence of sonic hedgehog (Shh) germline mutations in patients with thyroid dysgenesis*. Clin Endocrinol (Oxf), 2008. **69**(5): p. 828-9.
52. Moore-Scott, B.A. and N.R. Manley, *Differential expression of Sonic hedgehog along the anterior-posterior axis regulates patterning of pharyngeal pouch endoderm and pharyngeal endoderm-derived organs*. Dev Biol, 2005. **278**(2): p. 323-35.

53. Varjosalo, M. and J. Taipale, *Hedgehog: functions and mechanisms*. Genes Dev, 2008. **22**(2): p. 2454-2472.
54. Fagman, H., et al., *Genetic deletion of sonic hedgehog causes hemiagenesis and ectopic development of the thyroid in mouse*. Am J Pathol, 2004. **164**(5): p. 1865-72.
55. Fagman, H., et al., *The 22q11 deletion syndrome candidate gene Tbx1 determines thyroid size and positioning*. Hum Mol Genet, 2007. **16**(3): p. 276-85.
56. Alt, B., et al., *Analysis of origin and growth of the thyroid gland in zebrafish*. Dev Dyn, 2006. **235**(7): p. 1872-83.
57. Persani, L., *Congenital Hypothyroidism with Gland in situ is More Frequent than Previously Thought*. Front Endocrinol (Lausanne), 2012. **3**: p. 18.
58. Park, S.M. and V.K. Chatterjee, *Genetics of congenital hypothyroidism*. J Med Genet, 2005. **42**(5): p. 379-89.
59. Rastogi, M.V. and S.H. LaFranchi, *Congenital hypothyroidism*. Orphanet J Rare Dis, 2010. **5**: p. 17.
60. Wendl, T., et al., *Early developmental specification of the thyroid gland depends on hox-expressing surrounding tissue and on FGF signals*. Development, 2007. **134**(15): p. 2871-9.
61. Lichti-Kaiser, K., G. ZeRuth, and A.M. Jetten, *Transcription Factor Gli-Similar 3 (Glis3): Implications for the Development of Congenital Hypothyroidism*. J Endocrinol Diabetes Obes, 2014. **2**(2): p. 1024.
62. Persani, L., et al., *Genetics and management of congenital hypothyroidism*. Best Pract Res Clin Endocrinol Metab, 2018. **32**(4): p. 387-396.
63. de Filippis, T., et al., *A frequent oligogenic involvement in congenital hypothyroidism*. Hum Mol Genet, 2017. **26**(13): p. 2507-2514.
64. Kim, Y.S., et al., *GLIS3, a novel member of the GLIS subfamily of Kruppel-like zinc finger proteins with repressor and activation functions*. Nucleic Acids Res, 2003. **31**(19): p. 5513-25.
65. Senee, V., et al., *Mutations in GLIS3 are responsible for a rare syndrome with neonatal diabetes mellitus and congenital hypothyroidism*. Nat Genet, 2006. **38**(6): p. 682-7.
66. ZeRuth, G.T., et al., *HECT E3 Ubiquitin Ligase Itch Functions as a Novel Negative Regulator of Gli-Similar 3 (Glis3) Transcriptional Activity*. PLoS One, 2015. **10**(7): p. e0131303.
67. Chou, C.K., et al., *The Potential Role of Kruppel-Like Zinc-Finger Protein Glis3 in Genetic Diseases and Cancers*. Arch Immunol Ther Exp (Warsz), 2017. **65**(5): p. 381-389.
68. Dimitri, P., et al., *Expanding the Clinical Spectrum Associated With GLIS3 Mutations*. J Clin Endocrinol Metab, 2015. **100**(10): p. E1362-9.
69. Jetten, A.M., *GLIS1-3 transcription factors: critical roles in the regulation of multiple physiological processes and diseases*. Cell Mol Life Sci, 2018.
70. Lichti-Kaiser, K., et al., *Gli-similar proteins: their mechanisms of action, physiological functions, and roles in disease*. Vitam Horm, 2012. **88**: p. 141-71.
71. ZeRuth, G.T., X.P. Yang, and A.M. Jetten, *Modulation of the transactivation function and stability of Kruppel-like zinc finger protein Gli-similar 3 (Glis3) by Suppressor of Fused*. J Biol Chem, 2011. **286**(25): p. 22077-89.

72. Han, Y., Q. Shi, and J. Jiang, *Multisite interaction with Sufu regulates Ci/Gli activity through distinct mechanisms in Hh signal transduction*. Proc Natl Acad Sci U S A, 2015. **112**(20): p. 6383-8.
73. Yang, Y., et al., *The Kruppel-like zinc finger protein Glis3 directly and indirectly activates insulin gene transcription*. Nucleic Acids Res, 2009. **37**(8): p. 2529-38.
74. Kang, H.S., et al., *Transcription factor Glis3, a novel critical player in the regulation of pancreatic beta-cell development and insulin gene expression*. Mol Cell Biol, 2009. **29**(24): p. 6366-79.
75. Hansen, C.G., T. Moroishi, and K.L. Guan, *YAP and TAZ: a nexus for Hippo signaling and beyond*. Trends Cell Biol, 2015. **25**(9): p. 499-513.
76. Hossain, Z., et al., *Glomerulocystic kidney disease in mice with a targeted inactivation of Wwtr1*. Proc Natl Acad Sci U S A, 2007. **104**(5): p. 1631-6.
77. Kang, H.S., et al., *Glis3 is associated with primary cilia and Wwtr1/TAZ and implicated in polycystic kidney disease*. Mol Cell Biol, 2009. **29**(10): p. 2556-69.
78. Dimitri, P., et al., *Novel GLIS3 mutations demonstrate an extended multisystem phenotype*. Eur J Endocrinol, 2011. **164**(3): p. 437-43.
79. Kang, H.S., et al., *GLIS3 is indispensable for TSH/TSHR-dependent thyroid hormone biosynthesis and follicular cell proliferation*. J Clin Invest, 2017. **127**(12): p. 4326-4337.
80. Dimitri, P., *The role of GLIS3 in thyroid disease as part of a multisystem disorder*. Best Pract Res Clin Endocrinol Metab, 2017. **31**(2): p. 175-182.
81. Fu, C., et al., *Mutation screening of the GLIS3 gene in a cohort of 592 Chinese patients with congenital hypothyroidism*. Clin Chim Acta, 2018. **476**: p. 38-43.
82. Watanabe, N., et al., *A murine model of neonatal diabetes mellitus in Glis3-deficient mice*. FEBS Lett, 2009. **583**(12): p. 2108-13.
83. Kang, H.S., et al., *The Spatiotemporal Pattern of Glis3 Expression Indicates a Regulatory Function in Bipotent and Endocrine Progenitors during Early Pancreatic Development and in Beta, PP and Ductal Cells*. PLoS One, 2016. **11**(6): p. e0157138.
84. Yang, Y., B.H. Chang, and L. Chan, *Sustained expression of the transcription factor GLIS3 is required for normal beta cell function in adults*. EMBO Mol Med, 2013. **5**(1): p. 92-104.
85. Lieschke, G.J. and P.D. Currie, *Animal models of human disease: zebrafish swim into view*. Nat Rev Genet, 2007. **8**(5): p. 353-67.
86. Nasevicius, A. and S.C. Ekker, *Effective targeted gene 'knockdown' in zebrafish*. Nat Genet, 2000. **26**(2): p. 216-20.
87. Kimmel, C.B., et al., *Stages of embryonic development of the zebrafish*. Dev Dyn, 1995. **203**(3): p. 253-310.
88. Opitz, R., et al., *TSH receptor function is required for normal thyroid differentiation in zebrafish*. Mol Endocrinol, 2011. **25**(9): p. 1579-99.
89. diIorio, P., et al., *TALE-family homeodomain proteins regulate endodermal sonic hedgehog expression and pattern the anterior endoderm*. Dev Biol, 2007. **304**(1): p. 221-31.
90. Pappalardo, A., et al., *Thyroid development in zebrafish lacking Taz*. Mech Dev, 2015. **138 Pt 3**: p. 268-78.
91. Thisse, C. and B. Thisse, *High-resolution in situ hybridization to whole-mount zebrafish embryos*. Nat Protoc, 2008. **3**(1): p. 59-69.

92. Westerfield, M., *The zebrafish book*, ed. O.U.o.O.p. Eugene. 1993.
93. O'Hare, E.A., et al., *Assignment of Functional Relevance to Genes at Type 2 Diabetes-Associated Loci Through Investigation of beta-Cell Mass Deficits*. *Mol Endocrinol*, 2016. **30**(4): p. 429-45.
94. Zhang, C., P. Ojiaku, and G.J. Cole, *Forebrain and hindbrain development in zebrafish is sensitive to ethanol exposure involving agrin, Fgf, and sonic hedgehog function*. *Birth Defects Res A Clin Mol Teratol*, 2013. **97**(1): p. 8-27.
95. Incardona, J.P., et al., *The teratogenic Veratrum alkaloid cyclopamine inhibits sonic hedgehog signal transduction*. *Development*, 1998. **125**(18): p. 3553-62.
96. Chen, J.K., et al., *Inhibition of Hedgehog signaling by direct binding of cyclopamine to Smoothened*. *Genes Dev*, 2002. **16**(21): p. 2743-8.
97. Rurale, G., Persani L., Marelli F., *GLIS3 and Thyroid: A Pleiotropic Candidate Gene for Congenital Hypothyroidism*. *Front Endocrinol (Lausanne)*, 2018. **Vol 9**.
98. Porazzi, P., et al., *Thyroid gland development and function in the zebrafish model*. *Mol Cell Endocrinol*, 2009. **312**(1-2): p. 14-23.
99. Di Palma, T., et al., *TAZ is a coactivator for Pax8 and TTF-1, two transcription factors involved in thyroid differentiation*. *Exp Cell Res*, 2009. **315**(2): p. 162-75.
100. Zhang, J., et al., *The transcriptional coactivator Taz regulates proximodistal patterning of the pronephric tubule in zebrafish*. *Mech Dev*, 2015. **138 Pt 3**: p. 328-35.
101. Yang, Y., et al., *Differential Gene Dosage Effects of Diabetes-Associated Gene GLIS3 in Pancreatic beta Cell Differentiation and Function*. *Endocrinology*, 2017. **158**(1): p. 9-20.
102. Antonica, F., et al., *Generation of functional thyroid from embryonic stem cells*. *Nature*, 2012. **491**(7422): p. 66-71.